THE REFRACTIVE INDEX AND THE LORENTZ-LORENZ FUNCTION OF FLUID ARGON

Thesis by

Richard King Teague

In Partial Fullfillment of the Requirements

For the Degree of

Doctor of Philosophy

California Institute of Technology

Pasadena, California

1968

(Submitted May 31, 1967)

ACKNOWLEDGMENT

I want to express my appreciation to Professor C. J. Pings for his support and encouragement in this work.

I would also like to express my gratitude to the Chemical Engineering shop personnel for their work in the design and construction of the equipment.

During my graduate studies I have received support from Institute Scholarships, from a Union Carbide Corporation Fellowship, and from the Research Assistantships funds of the Directorate of Chemical Sciences of the Air Force Office of Scientific Research.

Thanks to my wife, Rolfe, for the many ways that she has helped me.

ABSTRACT

The refractive index, for λ_{Na} = 5893 Å, of dense fluid argon was measured by the determination of the angle of minimum deviation. The study covered states from 133 to 173°K for pressures 20 to 100 atm. The density data of J. Levelt were used to calculate values of the Lorentz-Lorenz function for these states.

A prism cell with 1/4" diameter sapphire windows in a cryostat was used to contain the sample. The cell temperature was measured to ± 0.015°K and controlled to ± 0.001°K. The pressure was measured with a gage calibrated against a dead weight tester to ± 0.06%.

In a detailed study of the critical region the Lorentz-Lorenz function was used to find the difference between coexisting gas - liquid densities, and the critical coefficient resulting from this work is β = 0.361. The critical temperature was varied to find the best fit of the experimental data to a linear equation for the critical coefficient; the value, T_C = 150.704°K, is significantly different from the accepted value, 150.86°K. Values of n_C = 1.0859 and P_C = 48.18 atm. were also determined. The measurements on the coexistence curve outside the critical region yielded an average gas value of $(L-L)_G$ = 4.152 cc/mole. The average liquid value is 4.213 cc/mole. There are no indications of an anomalous value at the critical point. The values of L-L on the eight isotherms between 133 and 173°K show a sharp peak near the critical point, 2.1% maximum, but this is within the experimental uncertainty.

TABLE OF CONTENTS

LIST OF FIGURES

LIST OF TABLES

I. INTRODUCTION

Much has been written in recent years on the theoretical and experimental attempts to understand the complicated states of matter known as fluids, liquids, and dense gases. The present experimental investigation of the refractive index of fluid argon is an additional investigation in this area. The refractive index itself is an intensive property which has many uses, but when used in the Lorentz-Lorenz function it provides a tool for investigating the molecular structure of fluids.

The refraction of light at the interface of two transparent media is an example of coherent or Rayleigh scattering. The oscillating electric field of the light wave causes the dipoles in the medium, induced or permanent, to emit radiation of the same frequency but out of phase with the incident light. The ratio of the velocity of the incident wave to the velocity of the wave resulting from the phase combination is called the relative refractive index. When the first medium is a vacuum where the velocity of light is c, then the refractive index is $n = c/v$. This relation also comes directly from Maxwell's equations which show that $v = c/\sqrt{\epsilon \mu}$ where ϵ is the dielectric constant and μ the magnetic permeability.

The major interest in the study of light refraction is the dipoles that produce the secondary radiation. The suitability of argon for this study results not only from the simplicity of its treatment in the liquid state theories but also from the simplicity of the dipoles that it exhibits. The spherical symmetry of the argon atom, or molecule, limits the dipoles to induced dipoles. In general the polarizability of a molecule is

given by

$$\vec{p} = \hat{a}_0 \cdot \vec{E} \tag{1}$$

Here $\vec{p}$ is the dipole moment vector, $\vec{E}$ the electric field vector, and $\hat{a}$ the polarizability tensor. It is possible to formulate an explicit relation for the polarizability using quantum mechanics, but as yet the calculations to produce accurate results can not be carried out.

The calculation of the polarizability in quantum mechanics shows that $\hat{a}_0$ should depend only on the frequency of radiation. For non-polar molecules and for all molecules acted on by a light wave the only polarizability of importance is electronic polarizability. Since the polarizability depends on the frequency, a correction must be made in order to use the theoretical developments or experimental measurements of the static dielectric constant in connection with the refractive index. This correction is called the dispersion correction, and experimental measurements show that the polarizability has a 1.8% increase between zero frequency and the frequency of visible light.

In order to investigate the refractive index of dense fluids the polarizability of an atom in a many body environment is needed. At present only a qualitative picture of the density dependence of the polarizability is available from theoretical considerations. When starting at low density, on increasing the density the molecule is effected by the attractive forces of the electronic field of the neighboring molecules, and its electrons are spread out, and the polarizability is increased. On further increasing the density the molecules become closely packed and experience repulsive forces. This repulsion causes a contraction of the electron shells and, thereby, a decrease in

polarizability. A quantum mechanical calculation has been carried out for helium and the result used directly with argon for lack of better information.[1]

In most instances the usefulness of the refractive index is its ability to indicate, indirectly, something about the state or structure of the material under consideration. In order to do this it is necessary to find the polarizability and electric field which produce the dipole in the many body environment. The dipole moment of molecule i is then[1]

$$\vec{p}_i = \hat{a}_i \cdot (D - \sum_{k \neq i} T_{ik} \cdot \vec{p}_k) \qquad (2)$$

$\hat{a}_i$ - polarizability tensor of i

$\vec{D}$ - electric displacement vector in the medium

$\hat{T}_{ik} = \vec{\nabla}_i \vec{\nabla}_k (1/r_{ik}) = r_{ik}^{-3} (\hat{U} - (3\vec{r}_{ik}\vec{r}_{ik}/r_{ik}^2)$

$\vec{p}_k$ - dipole moment of molecule k

This equation expresses the fact that the electric field producing the dipole in i is made up of D, the electric displacement vector due to the external field, and the electric field at i produced by the induced dipoles of the surrounding molecules, k. This equation is valid for non-polar, spherical molecules (isotropic polarizability) in a uniform electric field. It only accounts for the dipole part of the multiple interactions. As written it applies to a static electric field, but it can also be formulated for an electromagnetic field of optical frequency as shown by Yvon[2], Münster[3], and Mazur[4]. In this case the electric field is $\vec{E}_0 e^{i\omega t}$, and the dipole moment is $\vec{p}_i e^{i\omega t}$. This approach is mathematically more complicated and can be

generalized from the static field case.

Yvon[2] and Kirkwood[5] saw that in order to obtain macroscopic results it was necessary to find the average moment $\overline{p_i}$. They carried through the solution for the average field contributed by the surrounding molecules, $\overline{\sum_{k \neq i} \hat{T}_{ik} \cdot \vec{p}_k}$. They both solved the problem for constant polarizability $\hat{a}_i$, but Mazur[1] extended it to account for the variation of polarizability with density based on Jansen's[6] work. Kirkwood[5] showed that when the statistical fluctuations away from the mean value are zero, the original Lorentz-Lorenz relation is rigorously valid, using the average polarizability.

$$\left(\frac{n^2 - 1}{n^2 + 2}\right) \frac{1}{\rho} = \frac{4}{3} \pi \bar{a} \tag{3a}$$

$$\left(\frac{\epsilon - 1}{\epsilon + 2}\right) \frac{1}{\rho} = \frac{4}{3} \pi \bar{a} \tag{3b}$$

Equation (3a) is the Lorentz-Lorenz equation, and (3b) is the older Clausius-Mossotti equation for the static dielectric constant.

Equation (3a) was first derived by H. A. Lorentz for a continuum. He considered a continuum surrounding a small sphere that contained molecules in a cubic lattice. L. Lorenz derived a similar relation about the same time using the solid elastic theory of light. One significant aspect of equation (3) is the assertion that the quantity $\left(\frac{n^2 - 1}{n^2 + 2}\right) \rho^{-1}$ is independent of the thermodynamic state. Most of the analysis of the experimental data is devoted to an investigation of equations (3), and the following equation is added only to show the direction that an extension

of the theory would follow.

The more complete equation was first developed by Yvon[2].

$$\left(\frac{n^2-1}{n^2-2}\right)\frac{1}{\rho} = \frac{4}{3}\pi a_0\left[1 + a_0^2\, 16\pi\rho\int_0^\infty \frac{g^{(2)}(r_{12})}{r_{12}^4}\,dr_{12} + \right.$$

$$\left. a_0^2\,\rho^2\iint r_{12}^{-3}\, r_{23}^{-3}(3\cos^2\gamma - 1)\left[g^{(3)}(\vec{r}_1, \vec{r}_2, \vec{r}_3) - \right.\right. \qquad (4)$$

$$\left.\left. g^{(2)}(\vec{r}_1, \vec{r}_2)\, g^{(2)}(\vec{r}_2, \vec{r}_3)\right]\, d\vec{r}_1 d\vec{r}_2\right]$$

In this equation ρ is the number density; $g^{(2)}(r_{12})$ is the pair radial distribution function; $g^{(2)}(\vec{r}_1, \vec{r}_2)$ the probability of finding any molecule 1 in $d\vec{r}_1$ around $\vec{r}_1$ and any molecule 2 in $d\vec{r}_2$ around $\vec{r}_2$; γ is the angle between 2 and 3. The factor $16\,a_0^2$ appears in this equation instead of the usual $8\,a^2$ to account for the density dependence of the scalar polarizability of an isolated molecule. In order to make use of equation (4) the radial distribution function is needed. It can be obtained from either x-ray defraction data or estimated from the potential function for argon. Some values for g(r) are available from the work of Mikolaj[7], but this aspect will not be pursued.

There have been several attempts[1, 4, 5, 8] to use equation (4) to calculate directly the density behavior of L - L. Nearly all of these calculations used an intermolecular potential function to find the radial distribution function. The earlier calculations of Kirkwood[5] and De Boer[8] showed the correct qualitative behavior, but the density dependence was only half the experimental value. Later Mazur[1] showed that the density dependence of the polarizability contributed an additional half. L - L refers to the left side of Eqs. (3) and (4).

There are a number of published measurements of both the dielectric constant and the refractive index for argon. Most of these are at room temperature and near atmospheric pressure. Michels and Botzen[9] measured n at 25°C for pressures up to 2300 atm. Orcutt and Cole[10] presented very precise results for the dielectric constant at 50, 100, and 150°C for pressures 2 to 100 atm. Very few measurements have been made on liquid argon at low temperatures. Amey and Cole[11] measured the dielectric constant at the melting and normal boiling points, 84 and 87°K, for argon, and Smith[12] reported the refractive index of liquid argon near the triple point 84°K.

At this time a complete investigation of the refractive index of the dense fluid region for argon has not been published. The present study includes states from near the boiling point to above the critical point. This will fill in the unstudied region and make available a complete picture of the dielectric properties of argon from the solid region to the higher temperature gas region.

Of major interest in this area is the ability of equation (3) to describe the behavior of materials. The expanded theory says that L - L is not a constant characteristic of each material and that the deviations are density dependent. Therefore, the L - L values are plotted versus density for an isotherm. The data are separated by isotherms since although the theory shows an independence of temperature, this has not been established experimentally. If this same procedure is followed along the vapor pressure-temperature curve, additional considerations are introduced. For these states the density and temperature must vary together. Therefore, a plot of L - L

versus ρ is not independent of temperature. At each state though, the corresponding gas and liquid values of L - L represent a change in the density at constant temperature. There have been some theoretical estimations of the change in L - L that would occur during isothermal compression, but no definite answer has yet been put forth.

In any case as the temperature approaches the critical temperature, the gas and liquid densities approach the same value. From this it could be inferred that L - L values should behave the same way. But, the fact that this is the critical region means additional problems. It is well known that at the critical point opalescence occurs, and this indicates clusters or density inhomogeneities comparable to the wave length of light, 5000 Å. This molecular ordering has a much longer range than normally found in liquids, 4 to 7 Å. At the critical point one can not measure the bulk phase refractive index due to scattering of the light. There would seem to be some sort of transition region, a range of temperatures during which the range of molecular order would increase to the cluster size of the critical opalescence. The L - L relation given in (3) clearly should not hold since it assumes complete disorder.

The fluctuations of local density away from the bulk density are accentuated near the critical point, and $d\rho/dP$ becomes very large in this region. The large value of this derivative causes a large variation of density with the height in the cell, and this leads directly to questioning PVT measurements performed in this region. Experimental measurements of light scattering and variation of density with height both yield the same magnitude for the clusters or density fluctuations.

Schmidt[13] shows that for CO_2 at the critical pressure and within $\pm 0.007^{\circ}K$ of the critical temperature the density gradient is approximately 1% per 1 mm. Cataldi's[14] light scattering measurements on ethylene show that $\pm 0.25^{\circ}$ from the critical temperature clusters exist of 600 molecular diameters.

The lack of experimental measurements on argon for this region means that the above discussion can be used only to indicate qualitatively the behavior expected. The uncertainties in density and in the theoretical significance of the L - L function in an inhomogeneous system mean that a measurement of L - L in this region is at best uncertain and at worst invalid. Many of these same considerations must be applied to states in the one phase region near the critical point.

Since this investigation dealt only with measurements of the index of refraction, densities obtained from an independent determination are necessary to calculate the L - L function. The best available density data are those of J. M. H. Levelt[15] measured at Amsterdam in 1958; the accuracy of these results is discussed below with the experimental results. She gave the densities for the gas and the liquid along the gas-liquid coexistence curve from $120^{\circ}K$ to $150^{\circ}K$. She also presented data for the density of fluid argon from $130^{\circ}K$ to room temperature. In order to make full use of the accuracy of her work it was decided to correlate the states studied by refractive index to the states for which Levelt presented density data.

The refractive index of coexisting gas and liquid argon was measured using the method of the angle of minimum deviation for states from $85^{\circ}K$ to $150^{\circ}K$. Special emphasis was placed on the states

near the critical point, 150.704°K. Eight isotherms in the fluid region from 133°K to 173°K were studied for pressures to 100 atm. These isotherms are the same as studied by Levelt -140°, -135°, -125°, -120°, -110°, and -100°C. The density values of Levelt were then used to calculate the L - L function for each state.

One additional theory was investigated with the experimental data. This is an attempt to determine the exponent in the equation[16]

$$(\rho_L - \rho_G) = B_0(T_C - T)^{\beta} \tag{5}$$

Here ρ_L is the density of the liquid, and ρ_G the density of the gas in equilibrium along the coexistence curve. T_C is the critical temperature. This equation expresses the experimental fact that the densities of the two phases become equal at the critical point, and the equation attempts to find the functional form for the approach to the critical point. The theory actually predicts a functional form[17]

$$\beta = \lim_{T \to T_C} [\ln(\rho_L - \rho_G)/\ln(T_C - T)] \tag{6}$$

As discussed by Uhlenbeck[18] and Fisher[19], the value of β from the van der Waals theory is 1/2. The van der Waals theory uses long range attractive forces between the molecules, a range proven to be incorrect. The Ising lattice model which uses short range forces yields a value of β in the range 0.303 to 0.312. Experimental PVT determinations of β for such substances as He, Xe, and CO_2 yield values from 0.33 to 0.36.

Refractive index measurements in the region of the critical temperature can provide a further experimental determination of β. In order to use the refractive index measurements the Lorentz-Lorenz

function must apply in this region. From (3) follows (7)

$$\frac{n^2 - 1}{n^2 + 2} = \frac{4}{3}\pi \bar{a}\ \rho \qquad (7)$$

and n gives a direct measure of ρ. Then in order to use (5) or (6) it must be assumed or proved that $\bar{a}_L = \bar{a}_G$ at each temperature. The last assumption is questionable, but it is used here to calculate β for the argon system.

A more complete functional form for $\rho_L - \rho_G$ would be

$$\rho_L - \rho_G = B_0(T_C - T)^{\beta}[1 + B_1(T_C - T) + B_2(T_C - T)^2 + \ldots], \qquad (8)$$

and these additional terms would be necessary as $T_C - T$ becomes larger. An attempt was also made to investigate this equation. In addition, since the critical temperature is read from a large scale plot of the experimental data, this is subject to uncertainty. Therefore, it was desired to determine how small variations in T_C effected the fit of equations (5) and (8) and the value of β.

II. EXPERIMENTAL DETAILS

A. Optics

The basic experimental technique is to fill a prismatic cell with argon and to measure the angle of minimum deviation D along with the temperature and pressure. From the angle D the refractive index n can be determined from the following formula[20]

$$n = \sin \tfrac{1}{2}(A+D) \;/\; \sin \tfrac{1}{2} A \qquad (9)$$

A is the angle between the prism faces. The cell was made from 70 - 30 copper-nickel alloy rod 5/8" in diameter and 0.650" long. Two faces were cut at 45° as shown in Figure 1, and two sapphire optical flats 0.254" in diameter by 0.090" thick were set into flanges. The angle between the faces is approximately 45°. The sample chamber is 0.214" in diameter by 0.350" in length. The sapphire windows were brazed into the cell by Eitel-McCullough Inc. This manufacturer quotes a pressure limit of 10,000 psi on this assembly; 1,500 psi was the experimental limit used. A 1/16" diameter stainless steel tube was brazed in when the windows were attached. The cell was completely sealed in this operation, and no leakage has occurred. This design avoids the leakage problem of the older cell, which employed low temperature, high pressure, mechanical seals. The new cell was positioned in the cryostat as shown in Figure 2. The cryostat is the same as described by Abbiss[21]. The cell is supported and positioned by a 1/16" diameter Bakelite rod which rests on the radiation shield.

The cryostat was positioned at the center of a Gaertner spectrometer model L114. It was not feasible to rotate the cryostat in the

determination of the angle of minimum deviation so the spectrometer was rotated instead. For the first runs up through B-3 the spectrometer was mounted on a 7" diameter thrust bearing. Later the spectrometer was disassembled, and the two telescope arms were mounted to rotate around a central housing. This mounting which used a pair of matched super-precision bearings for each telescope shaft provides maximum concentricity for rotation of the two telescopes. This housing was bolted directly to a surface plate. The cryostat support was made from 4" x 4" H-beams and also bolted to the surface plate. This arrangement improved the rigidity of the apparatus, but most importantly it improved the ability to maintain the alignment between the cell and the spectrometer. The only part of the spectrometer changed was the base mounting. All the original scales and the telescope mountings were retained. The new arrangement improved the ability to position the cell in the plane of rotation of the telescopes. This new assembly is shown in Figure 3. A sodium vapor lamp, wave length 5893 Å, illuminating an adjustable slit on the collimating telescope was used as a light source for all measurements.

The procedure to set up and operate the spectrometer given by Houston[22] was used in this work. The telescopes were adjusted so that the axes were co-planar and perpendicular to the axis of rotation of the spectrometer. Before the cell was enclosed in the cryostat it was determined that the lines normal to the cell windows were in the same plane. The prism angle, A was determined from the angle of minimum deviation for water, $A = 44^{\circ}18.57' \pm 0.40'$. Details of this determination are given in Appendix A. As discussed in Appendix A,

the uncertainty in D at a 95% confidence level is ± 0.26'.

After the cryostat containing the cell was positioned at the axis of the spectrometer, the Gauss eyepiece in the viewing telescope was used to align the cell in the plane of rotation of the telescopes. This must be done so that the prism faces, cell windows, are perpendicular to the axis of the telescope and parallel to the axis of rotation. Then the angle measured by the telescope is in the same plane as the angle of minimum deviation. This alignment was achieved to 10', and this introduced an error in n of less than 0.001%. No error is introduced into the angle of D measured by this technique even if the cell is not at the axis of rotation. This assumes that the light after refraction is focused at the cross hairs of the viewing telescope.

Since the cell was surrounded by a vacuum during the measurement, the refractive index measured is the true refractive index and not relative to air. The error introduced by the cryostat windows between the surrounding air and the vacuum was negligible. Although they are not optical flats, the density of air is very small.

B. Temperature

The cryostat used is shown in Figure 2 and was described by Abbiss[21]. The liquid nitrogen reservoir was kept filled to a 1" depth by a differential expansion level controller. This level maintained a uniform heat sink and kept condensation from the outside walls of the cryostat. The jacket and inner chamber were pumped to a high vacuum with a diffusion pump. It was found that a vacuum greater than 1×10^{-4} mm Hg was sufficient for good temperature control.

The volume inside the controlled temperature radiation shield was evacuated with either a mechanical pump or a diffusion pump. For all the measurements except those near the critical point the vacuum of 3 or 4 x 10^{-3} mm. Hg produced by a mechanical pump was used. This increased the heat loss from the cell and gave better temperature control.

The temperature control scheme was much the same as described by Honeywell[23, 24] and Abbiss[21]. The control point for the copper-constantan thermocouple attached to the radiation shield was set 2 or 3 degrees below the temperature at which the cell was to be controlled. The difference in e.m.f. between the set point and the thermocouple was fed consecutively to an amplifier D.C. power supply. This power supply supplied current to the heater wire attached to the radiation shield. The vacuum surrounding the cell and temperature difference between the cell and shield could be adjusted to suit the thermodynamic state being investigated.

The heater on the shield was made from 45" of 0.010" copper-nickel wire of about 12.5 Ω. Approximately 0.2 amperes were required to maintain temperature control for the range of temperatures studied, 130° to 175°K. As in all applications where an electric heater is surrounded by a vacuum, care was taken to insure good thermal contact to the shield. The heater wire was placed over cigarette paper and secured with General Electric Adhesive and Insulating Varnish #7031. The connection to the 0.010" copper wire lead was made in contact with the shield. The lead wires were thermally anchored to the liquid nitrogen reservoir before passing out of the vacuum chamber through a

lucite plug in an Edwards vacuum fitting.

The temperature of the sample cell was measured and controlled from a platinum resistance thermometer fitted at the back edge of the cell. The current through the thermometer was determined from the potential drop across a 10Ω standard resistor. The potential corresponding to the desired resistance was set on a Leeds and Northrup Wenner potentiometer. The difference in potential between the thermometer and the Wenner was fed to the D. C. amplifier-controller system that duplicated the shield control system.

This thermometer is No. 4 in the series discussed by Knobler[25] and Honeywell[24]. It has an ice point resistance of 100.04718Ω (273.15°K) and was calibrated over the range 75° to 300°K. The thermometer calibration used degrees K (NBS 1955) for which the ice point of water is 273.15°K = 0°C.

The thermometer calibration as prepared by Dr. Knobler is considered accurate to ± 0.005°K. This accuracy was coupled with the uncertainty in the potential measurement. A small additional uncertainty was introduced by the comparison of the Wenner to the Leeds and Northrup K-3 potentiometer, used to measure the potential drop across the 10Ω standard resistance. A total absolute uncertainty of 0.015°K is claimed for all temperatures measured. The stability of control achieved by the control system for all measurements except near the critical point was at least an order of magnitude better than the absolute uncertainty.

The thermometer was embedded in a groove at the back edge of the cell and was held in place by Woods metal. Copper wire, 0.002"

was used for the four thermometer leads. These were anchored to the cell, coiled above the cell, and anchored to the top of the radiation shield chamber. This arrangement was used to minimize the heat flow along the wires. The maximum gradient along the wires was the difference between the cell and radiation shield. An aluminum foil radiation shield was placed over the thermometer to eliminate radiation and convection losses from the ends that extended past the edge of the cell.

The heater on the cell was made from 6 5/16" of 0.003" copper-nickel wire with a resistance of approximately 18Ω. The wire was arranged on the cell to achieve uniform heat input and cemented in place with G. E. varnish. The lead in wire was the same as used for the shield, 0.010 Cu. A current of 0.010 to 0.015 amps. was sufficient to control the cell temperature under most operating conditions.

The lead in wires for the cell heater were coiled above the cell and anchored to the top of the shield chamber. As shown in Figure 2, the sample inlet line was coiled above the cell inside the radiation shield chamber. This was done to minimize heat conduction along the inlet line to the cell. On the inlet line above the shield chamber a 10Ω electrical heater 0.165" in diameter was placed. This could be used to control the temperature gradient in the coil above the cell. Thermocouples were placed at the mid point of the coiled inlet line and just above the heater on the inlet line. Under normal operation the heater on the inlet line was not used, and the temperature of the mid point of the coil above the cell was approximately the same as the shield temperature. All the wires from inside the shield chamber were

brought out of the vacuum chamber through a lucite plug in an Edwards fitting.

In order to achieve linear response at the correct control current from the D. C. power supply, external power dissipation resistors were added to both the shield heater and the cell heater circuits. A series of resistors and switches provided for adjustment of the resistance to the control setting.

C. Pressure

The pressure of the argon gas in the sample cell was measured with a Texas Instruments Precision Pressure Gage connected directly into the sample line. The gage indicates the pressure from the deflection of a Bourdon tube. The Bourdon tube does not perform any mechanical work except to rotate a small mirror attached to the end. The pressure gage was calibrated against a Hart Balance dead weight tester described by Honeywell[24]. The details of the calibration and the experimental data are given in Appendix B. As shown there, the limits of accuracy placed on the pressure measurements at a 95% confidence level are ± 0.06%.

With the pressure gage hooked directly into the argon sample line a continuous indication of the pressure was available. The argon pressure was generated by condensing argon from the supply cylinder into a pressure bomb at liquid nitrogen temperature. After warming to room temperature, the gas was added to the system through a needle valve. In general no fixed pressure was sought. Gas was added in increments while the temperature was held constant. Pressure

stability of 0.01% or greater was achieved for all measurements except near the critical point.

The gage pressure recorded was converted to absolute pressure by adding the barometric pressure measured with a Princo Fortin barometer. All pressures were then reported in atmospheres.

D. Argon Sample

The argon used in the experiments was obtained from the Linde Corporation or from J.T. Baker Chemical Co. who distribute Linde gases. Batch analysis for the gas purchased showed less than 20 ppm. impurities. Before the introduction of argon, the sample lines were evacuated with a mechanical pump and then purged by alternately filling to atmospheric pressure and evacuating. After purging, the sample lines were maintained under pressure or pumped with the vacuum pump. For runs 16 to 26 the sample gas was evacuated from the system after each run, and the system was refilled from the supply tank. All the sample lines in direct use were made from 1/16 or 1/8" stainless steel tubing joined with Swagelok fittings.

Analysis of the argon by gas chromatography was performed after run 71 and showed less than 20 ppm. air. Several attempts were made during the later runs to analyze the argon gas with a mass-spectrometer. These proved unsuccessful due to residual gases absorbed on the glass of the sample bulb.

E. Experimental Operation

Coexisting Gas - Liquid States

The experimental feature that distinguished these measurements from those in the one phase region was lack of pressure measurements. In this case the temperature was the independent variable, and the state was changed by changing the temperature.

After the radiation shield was placed on control 2 or 3 degrees below the temperature of the state to be measured, the cell was evacuated. Now the spectrometer instrument zero was recorded. This is the position of the telescopes when the light passed through the empty cell. The cell was then filled with argon until the gas-liquid interface was visible at the center. The temperature of the cell as measured by the platinum resistance thermometer was then controlled to the set potential of the Wenner potentiometer. The angle of minimum deviation for both the gas and the liquid was recorded. Both telescopes were rotated around the cell and adjusted until the minimum deviation of the light beam fell on the cross hairs of the viewing telescope. Other special details of the spectrometer operation are given in Appendix A. To measure a new state both the temperature of the cell and the radiation shield were changed. Measurements in this manner were carried out from 85°K, near the freezing point, to 150.697°K.

These experimental measurements are recorded in the appendix Table C-1 under runs 71, 3, 4, 6, B-2, and 26. Run 71 was made with the original cell and has been published by Abbiss[21]. The remaining runs were performed with the new cell for which A = 44.3094° ± 0.0067°. The estimate of uncertainty in temperature as recorded is

$\pm 0.015^{\circ}K$. The uncertainty in n, ± 0.0001, results from $D \pm 0.005^{\circ}$ and $A \pm 0.0067^{\circ}$. The * denotes points not considered reliable because of possible incorrect procedure noted when the points were taken.

Near the critical temperature the stability of the system decreased, and the measurements became much more difficult. Since at the critical temperature the compressibility becomes infinite, as one approaches this state, large changes of phase are caused by small temperature fluctuations. These changes of phase cause greater temperature instability.

In order to achieve temperature control in this region it was necessary to operate with a higher vacuum in the shield chamber. This decreased the heat loss, and therefore, the heat input could be decreased. The smaller heat loss caused the cell to respond more slowly.

Another technique was to decrease the temperature difference between the cell and the shield. At the same time the heater on the inlet line above the shield chamber was used to decrease the temperature gradient along the coiled inlet line. The heater on the inlet line and the shield heater were connected in parallel to the same control circuit. The current was proportioned between them to achieve optimum control.

A much longer period of time must be allowed for equilibrium in the region near the critical temperature. Over a period of an hour when the temperature was recorded as constant to $\pm 0.001^{\circ}K$, the amount of liquid or gas slowly decreased. For the final measurements recorded, the relative amounts of the two phases did not change. In spite of this a temperature control to $\pm 0.0025^{\circ}K$ is all that can be

claimed in this region. At times it was possible to boil argon from the cell and recondense it in the coiled line above. An absence of this condition is also necessary for correct temperature measurement.

The measurements in the critical region were recorded in the appendix under runs 6 and 26. Run 26 is the only set of measurements in the critical region considered reliable. By this time it had become apparent that for reliable results great care had to be taken with temperature stability and true equilibrium conditions. These measurements consist of a series of runs over several days. The sample was changed each day and the spectrometer rezeroed. At the same time the potentiometers were checked with a new standard cell and compared with each other. The reproducibility over several days and the absence of boiling or change in the relative amounts of each phase led to the conclusion that these are the most correct values in this region.

Schmidt[13] indicated from his work on density gradients that a gradient of 1% per mm. existed 0.007 degrees from the critical point. He used an optical method, the refractive index, to specify the density. He noted that the image of the light source seen in the viewing telescope of the spectrometer became broad and indistinct very near the critical point. He then focused on small regions defined by a horizontal slit. This allowed him to measure the refractive index versus height.

In the present cell, the total sample height was 6 mm., thus the liquid and gas samples were both 3 mm. The point recorded at 150.697°K is about 0.01°K below the critical temperature, thus the density gradient could be as high as 1% over each phase. The light

passing through the liquid gave a sharp image, but the gas showed a very slight broadening. The measurements at 150.683 and 150.692°K showed some broadening of the light image due to density gradients. The value of 150.692°K looks inconsistent with the other values measured and was generally excluded from the analysis. The points at 150.657 and 150.675°K had a broad light line due partially to poor temperature control. Two measurements at 150.429 and 150.556°K presented values for the liquid only since the cell was too full of liquid to give sufficient intensity to the light passing through the gas.

In general a sharp, distinct light image was used as the criteria for a homogeneous sample. This covered density gradients caused by both temperature and pressure, or gravity. The optical observations corresponded well with the temperature control. For gas-liquid measurements not in the critical region, a temperature stability of 0.0002°K was maintained over the 10 minutes required to record the data at each temperature. No density inhomogeneities were observed for these measurements.

In the investigation of the critical region from equation (5), the difference of the value of $\frac{n^2 - 1}{n^2 + 2}$ for the gas and the liquid states was needed. Since both of these quantities were measured at the same time, the error in the difference is only half the normal error associated with two measurements. The same reasoning applies to the temperature measurements except that the extrapolation of T to T_C must be considered.

When run 26 was performed, the pressure gage had been

completely calibrated, and it was possible to measure the vapor pressure of argon during this set of measurements. The readings were recorded directly with the gage and converted to absolute pressure using the barometric pressure. The position of the cell is approximately 4 inches higher than the mean height of the spiral in the pressure gage. This is for the new apparatus assembly that was used for runs 16-26. It must also be considered that there was 1 inch of the inlet line to the cell which was at the lower temperature of the cell. These two effects essentially cancel, and no correction is needed to obtain the correct vapor pressure.

Single Phase Fluid States

As noted before, an additional measurement of the sample pressure was necessary in this region. The temperature control and spectrometer zero were set up as before. Then argon was fed into the system from the high pressure bomb. The temperature increase due to the compression of warm argon gas will upset the cell temperature control, but this was soon corrected automatically. After the temperature control was restored, the angle of minimum deviation was measured. The gage reading and the barometric pressure then specified the state at that temperature.

In this investigation specific isotherms corresponding to the isotherms of Levelt's[15] PVT measurements were studied. The pressure range studied was from 15 to 100 atmospheres in arbitrary steps. In order to specify an exact temperature the current through the resistance thermometer and the 10Ω standard resistor was measured with the K-3 potentiometer. Then the potential on the Wenner was

set to give the correct resistance for that temperature. The current in the thermometer was measured before each angle determination and the Wenner adjusted if necessary.

Nine isotherms between 133 and 173°K were studied. The experimental data are reported in Appendix C, Table C-2. On all isotherms two runs were made although not exactly at the same temperature in all cases. On runs 7 to 11 the Hart pressure balance was used along with the Texas Instrument gage. The measurements with the pressure balance were used as part of the pressure gage calibration. All pressures recorded were calculated from the pressure gage readings after the complete calibration.

For the earlier runs, up to B-3, the pressure gage and the prism cell were at the same height. But since approximately 1 inch of the height above the cell was at low temperature, the hydrostatic heads did not cancel. The worst case was at -140°C near the liquid-vapor coexistence curve where the error in P is less than 0.01%. But in this region the liquid is very incompressible, and the error in density calculated is insignificant. Near the critical point where the fluid is very compressible, the error in P is only 0.003%. For runs 16 to 26 the new assembly as described in the discussion of the two phase measurements made this error essentially zero.

All measurements on the isotherms were made using the new cell, and the values of n are considered accurate to ± 0.0001. The pressure is accurate to ± 0.06% and the temperature to ± 0.015°K. The temperature reproducibility on any isotherm should be greater then 0.015°K.

Two runs 7 and 8 are not included in the final results. In plotting the results these isotherms crossed other isotherms, and two attempts to reproduce the data failed. The later runs at these temperatures gave results consistent with the other isotherms.

For the low temperature, low pressure states the angle of minimum deviation was small and therefore, relatively inaccurate. They were also at the lower end or outside the pressure calibration which increased the error, but they were added for completeness. For the higher density, low temperature states the compressibility is very small, and the angle of minimum deviation does not vary significantly over the pressure range. For this reason the steps in pressure were rather large. For isotherms near the critical temperature the compressibility is very large, and incremental increases of pressure were adjusted accordingly. The isotherm at 150.665°K, which Levelt gave as -122.5°C, is much closer to the critical temperature as measured by this system than would appear from Levelt's measurements. Therefore, most of the difficulties encountered in the critical region were presented here. All the measurements presented were obtained with a sharp, distinct light image. Both temperature and pressure stability was maintained over the 5 to 10 minutes necessary to record the measurement.

The isotherm at 151.665°K was actually measured by mistake. There are no densities for this isotherm, and in this region the high compressibility makes interpolation inaccurate. It was included in the raw data for possible use when more density data become available.

III. EXPERIMENTAL RESULTS

The experimental angles of minimum deviation recorded in Tables C-1 and C-2 were converted into the refractive index using equation (9)[20].

$$n = \sin\tfrac{1}{2}(A+D) \,/\, \sin\tfrac{1}{2}A \qquad (9)$$

These are also tabulated in Tables C-1 and C-2. A plot of these experimental values of n and P is given in Figure 4. On the gas-liquid coexistence curve only representative values are included; inclusion of all the experimental points would make the graph indistinct. Along the isotherms all the experimental points are included except at the low pressure end where the plotting symbols would overlap. For those isotherms where the repeat runs were not exactly at the temperature of the original run, the values of n were corrected to the temperature of the original run. No error bands are included on this graph.

In equation (9) only the prism angle A and the angle D are needed to calculate n. The determination of A is covered in Appendix A; this same section also discusses the accuracy with which D can be measured. From the uncertainty in A, $\pm\ 0.0067^{\circ}$, and D, $\pm\ 0.005^{\circ}$, the fractional error in n is calculated from the equation

$$d\ln n = \frac{+\ \sin\frac{1}{2}D}{2\ \sin\frac{1}{2}(A+D)\ \sin\frac{1}{2}A}\, dA + \frac{1}{2}\cot\tfrac{1}{2}(A+D)\, dD \qquad . \quad (10)$$

The fractional error for each data point is calculated at the same time as the refractive index using the I. B. M. computer. The error ranges from a minimum of 0.0093% at $D = 0.250^{\circ}$ to 0.00102% at $D = 8.72^{\circ}$.

All of these are listed at 0.01% for all the data recorded.

A. Critical Region

Once the refractive index is obtained, further analysis can be carried out. The data in the critical region will be discussed first since information about this region is necessary for the complete analysis of the remaining gas-liquid coexistence states. The data on the coexistence curve from 149.8°K up were plotted on a large scale graph, and a flexible spline was used to draw the curve. From this the critical point, the maximum in the curve or the point where the slope is infinite, was read. This is shown in Figure 5. In this figure the absolute uncertainty in T ± 0.015°K is shown by error bands. The uncertainty in n is smaller than the plotting symbol and is not shown. The critical temperature determined from the graph is $T_C = 150.709°K$. At this point the rectilinear diameter is used to find the critical refractive index. The idea of the rectilinear diameter, the average of the gas and the liquid coexisting densities, has been used for some time and is known as the Law of Cailletet and Mathias[26]. Mathias[27] and many others have used it in working with densities. Partington[28] discussed this concept extensively and showed that contrary to Cailletet and Mathias the rectilinear diameter is not independent of the temperature and is not equal to the critical density. An equation of the form

$$\frac{1}{2}(\rho_L + \rho_G) = \Psi_0 + \Psi_1 (T_C - T) \qquad (11)$$

will usually fit the data near the critical temperature, and over a

large range of temperatures it may be necessary to add a term $\Psi_2 (T_C - T)^2$. In order to use equation (11) for the refractive index, it is necessary to assume the validity of the Lorentz-Lorenz function and use equation (7). It is necessary to assume that the polarizability is the same for both gas and liquid and independent of temperature. Both of these assumptions are questionable or incorrect. Nevertheless, the substitution of $\frac{n^2 - 1}{n^2 + 2}$ for ρ in equation (11) yields a very good linear fit.

Since for n approximately equal to 1, the quantity $\frac{n^2 - 1}{n^2 + 2}$ can be replaced by $\frac{2}{3}(n - 1)$, and the rectilinear diameter equation is also applied to n. The value of n_C from the rectilinear diameter for n or $\frac{n^2 - 1}{n^2 + 2}$ is the same, $n_C = 1.08587$. This coincidence at the critical point together with the fact that the rectilinear diameter is as linear for n as for $\frac{n^2 - 1}{n^2 + 2}$ and both possibly more linear than ρ justifies its use. This could even be used as a justification for saying that the rectilinear diameter applies for many properties of coexisting gases-liquids. This idea will be used in other data smoothing. The line fitted by least squares to the value $\frac{1}{2}(n_L + n_G)$ is shown in Figure 5. The band of 95% confidence is shown by the dashed lines in the figure.

With the critical temperature estimated it is possible to use equation (5) or (6) to solve for the critical coefficient β. Again it is necessary to assume the validity of equation (7) as in the case of the rectilinear diameter. The data for $\left(\frac{n^2 - 1}{n^2 + 2}\right)_L - \left(\frac{n^2 - 1}{n^2 + 2}\right)_G$ are presented in Table 1 together with $T_C - T$. In the table Φ was substituted for $\frac{n^2 - 1}{n^2 + 2}$ for brevity. Since the actual determination of β consisted of a least squares fit of the linear equation

$$\ln(\Phi_L - \Phi_G) = \theta + \beta \ln(T_C - T) \quad , \tag{12}$$

$\ln(\Phi_L - \Phi_G)$ and $\ln(T_C - T)$ are also given. The value of β from this fit is approximately 0.375, and it was noticed that the value changed when different temperature ranges were used. It also appeared that the values of $\ln(\Phi_L - \Phi_G)$ curved downward from a straight line as the critical temperature was approached.

The values of $\Phi_L - \Phi_G$ and $T_C - T$, $T_C = 150.709^{\circ}K$, are plotted on a log-log scale in Figure 6. The line in the plot is a straight line of slope 0.375. The estimate of relative error in $T_C - T$ is $\pm 0.005^{\circ}K$, and this is added at the lower end. For the higher values of $T_C - T$ the error band is the same size as the plotting symbol. The error in $\Phi_L - \Phi_G$ is also too small to show on the graph. The band of 95% confidence would be just at the edge of the plotting symbols, and therefore, it is not shown.

This information seemed to indicate that the higher order terms as presented in equation (8) are indeed significant. But the only avail-

able computer sub-routine was for linear regression and, therefore, not suitable for use with an equation such as (8). Since the value of β is really the slope in the limit $T \to T_C$ as presented in equation (6), an equation which yields the same limit is

$$\ln(\Phi_L - \Phi_G) = \theta + \beta \ln(T_C - T) + \theta_1 (T_C - T) + \theta_2 (T_C - T)^2. \qquad (13)$$

This equation can be used with linear regression analysis, and the results are presented in Table 2. It was found that terms as high as $\theta_2 (T_C - T)^2$ did yield a significant improvement in the fit. The standard deviation of the fitted equation from the experimental data as given in Table 2 decreased as the additional terms were added. The coefficients and their standard error are presented.

It is found that the value of β increased as the additional terms were added. Although there is no experimental or theoretical evidence to dispute the value of β from this approach, this value of β is not similar to other experimental and theoretical investigations that used only equations (5), (6), or (12). At the suggestion of Professor Michael Fisher, it was decided to determine what effect the value choosen for the critical temperatures has on the coefficients and fit of equation (13). For this, increments of $0.001^{\circ}K$ were added and subtracted to the value of $T_C = 150.709^{\circ}K$. These increments of temperature did not seem unreasonable although it was felt that the critical temperature indicated by the large scale plot of n versus T was reliable to $\pm 0.005^{\circ}K$ since this is a relative and not an absolute quantity. The values of the coefficients and the standard deviation for the fit which result from this shifting of T_C are presented in

Table 3.

The result of this manipulation seems somewhat remarkable. Professor Fisher predicted that if the proper value of T_C was used, the value of β would be in line with other measurements, and the higher order terms would not be needed to obtain a good fit. This is exactly what happened. The standard deviation of the fitted equation from the experimental points passes through a minimum at $\Delta T = -0.005^{\circ}K$, and the value of β is 0.361. The standard error of β also is a minimum here, $\pm$ 0.0015. In Table 3 the coefficients of the higher order terms are not recorded when they no longer make a significant contribution to the fit. As presented in the table, the higher order terms no longer contribute to the fit, and all the predictions are satisfied.

The results of this shift are plotted in Figure 7. The value of $T_C - T$ is now computed with $T_C = 150.704^{\circ}K$. The line on the graph was determined by least squares fitting with equation (12). The slope is $\beta = 0.361$. The relative error in $T_C - T$ is again assumed approximately equal $\pm$ 0.005°K and is shown as in Figure 6. The error in $\Phi_L - \Phi_G$ is too small to be seen, and the band of 95% confidence is just at the edge of the plotting symbols.

The result of the preceding analysis indicates that the critical temperature for argon should be 150.704°K. The confidence in this value is based on the experimental technique and the fact that the measurements in this region were repeated three times with different samples and different settings as discussed in the section on Experimental Details and Appendix C. This value does not agree with that obtained by Levelt, $T_C = 150.86^{\circ}K$, in her PVT measurements, but

her work is not specifically designed to determine this value. She only presented four values within 1° of the critical temperature, and these values of the gas or liquid coexistence density result from an extrapolation which she said is accurate to $\pm 0.05^{\circ}K$. Another consideration must be the density gradients produced by gravity. Her cell was at least 3" (7.6 cm.) in height, and although she used a correction for the effect of gravity on her isotherms, extrapolations near the critical point would be uncertain.

Another determination of the critical point is presented by Crommelin[29, 30] and Mathias, Onnes, and Crommelin[27]. In the first of these articles the vapor pressure, critical temperature, and critical pressure were determined independently of density measurements. The critical temperature was observed directly as the temperature at which the meniscus disappeared at the mid-point of the sample cell. This optically observed critical point should be directly comparable to the one found in the refractive index experiment. The value he published is $150.72^{\circ}K$. In the second two articles densities along the coexistence curve were given.

Another verification for the critical point is related to the critical pressure. Levelt gives a critical pressure of 48.34 atm., and Crommelin gives 47.996 atm. A determination of the vapor pressure of argon by Clark[31] agrees well with that of Crommelin and gives a critical pressure of 48.00 atm. When the vapor pressures recorded in the refractive index measurements were plotted, a critical pressure of 48.18 atm. is estimated at the critical temperature, $150.704^{\circ}K$. Levelt presented values of the vapor pressure applicable

in the region 150.0 to 150.8°K, and these are 0.13 atm. lower than the ones presented here. Clark does not present any values in this region.

A summary of the critical values obtained in this investigation is

$$T_C = 150.704^\circ K$$

$$p_C = 48.18 \text{ atm.}$$

$$n_C = 1.08587$$

These were the result of the most numerous states measured near the critical point, and therefore, they will be used with confidence.

B. Gas-Liquid Coexistence States

With information from the critical state, the remaining gas-liquid coexistence measurements can be investigated. The data of Table C-1 were used to calculate the Lorentz-Lorenz value of equation (3), $\left(\frac{n^2 - 1}{n^2 + 2}\right)\rho^{-1}$. The data presented by Levelt for coexisting gas-liquid densities were used in this relation. For each temperature the density was obtained by interpolation in a computer program that used the Aitken iterative method. Below 150°K a second order interpolation was used, and above 150°K a linear interpolation was used. The critical temperature and density presented by Levelt were used in this part of the analysis. All the interpolated densities were plotted to insure smooth continuous values. For temperatures below Levelt's work the densities of Mathias[27] were used on a large scale plot for density information. Some of these data were published[21] and are

included here for completeness. For temperatures below 120°K the data are reproduced as published but for higher temperatures new values of L - L using interpolated densities are reported.

The final values of n and L - L are given in Table 4. The error in T is discussed in the section on experimental details; the error in D and n is covered in the Appendix A. In the calculation of the error in the L - L values only the error of ± 0.01% in n is used to find the fractional error contribution of n to L - L. The following equation gives this value

$$\Delta\left(\frac{n^2-1}{n^2+2}\right)\Big/\left(\frac{n^2-1}{n^2+2}\right) = 6n^2\left(\frac{\Delta n}{n}\right)\frac{1}{n^4+n^2-2} \qquad (14)$$

From this equation it is obvious why the spectrometric method of refractive index measurements is not good at low densities. Although this method gives values of n to ± 0.01%, at low densities n is very nearly 1, and the denominator of the right hand side of (14) becomes very small. This increased uncertainty is shown in Table 4.

The uncertainty in T, ± 0.015°K, for the refractive index measurements and the uncertainty in T for the density measurements, ± 0.02°K, were both used in finding the contribution of $\Delta\rho/\rho$ to the error in L - L. The experimental values of ρ and T from Levelt's thesis were used in a computer program that calculated $\Delta\rho/\Delta T$ and used this as an approximation of $d\rho/dT$ at the mid-point of the temperature interval. The value of $d\rho/dT$ for each experimental value of n was then found by interpolation. The value of $\Delta\rho$ was calculated using $\Delta T = 0.035$°K for all points even though Levelt reports that near the

critical temperature her $\Delta T \pm 0.05^{\circ}K$. As noted previously, the error in ρ becomes very large near the critical point and goes to infinity at ρ_c.

The total error listed in Table 4 is the sum of the fractional errors resulting from n and ρ. The error for the lowest density gas values is $\pm$ 2.5% at 112°, and this decreases to a minimum of 0.48% at 145°. The error then increases to approximately 2.7% for the state nearest the critical temperature. A more realistic value for ΔT near the critical point is $\pm 0.065^{\circ}$, and the error in L - L for this is $\pm$ 4.8%. The error in L - L for the coexisting liquid states is 2.1% near the critical point and decreases to 0.04% at 120°. The data of Table 4 with error bands are presented in Figure 8. For many of the liquid states the error band is smaller than the plotting symbol and, therefore, not shown.

As shown in Figure 8 there is a large gap in density between the gas and liquid states at the critical point. This results from the fact that Levelt's critical temperature is not the same as the one found in this investigation. There are a number of aspects that can be considered on this point, but a simple approach says that there are states where Levelt measured density for which no refractive index can be measured. This problem leads to several curious results. The values of L - L for the gas near the critical temperature become very large almost asymptotically, but the values of L - L for the coexisting liquid become smaller. Then there would appear to be a very large discontinuity in L - L at the critical point. However, if the two sets of measurements are adjusted to the same critical point, the gas and

liquid L - L values meet at the critical density and pass continuously from one phase to the other. If the reverse situation occurred and the critical point for the refractive index was at a higher temperature than for the density, the liquid values of L - L would become larger and the gas values smaller.

From this, it is obvious that the present data can not make a definite statement about L - L in the critical region. It is easier to think of L - L as being continuous in the critical point passing from the gas value to the liquid value since there does not appear to be a discontinuity in either n or ρ. It should be remembered that all the measurements presented here are outside the region where critical opalescence occurs.

There are some published values of n or the dielectric constant in this region that can be used for comparison with the present data. Jones and Smith[12] gave values of n from 83 to 95°K at 5893 Å, the Na line used in the present work. The values agree very well, at 85° from the graph presented by Jones n = 1.2312; this compares with the present values at 85.5 of 1.2312. Amey and Cole[11] reported values of ϵ, the dielectric constant, for liquid argon at the melting point 83.85°K and at the boiling point 87.27°K. Before these can be compared directly with the refractive index, the correction for dispersion must be considered. The experimental value for the dispersion in the gas was reported by Cuthbertson[32]. Abbiss and Knobler[21] made some measurements on liquid argon and reported the same 1.8% increase of the optical polarizability from the static polarizability. A straight line through the results of Amey and Cole gives a value of

$(\epsilon - 1) / (\epsilon - 2) = 0.144$ at 85.5°K. When the 1.8% correction is added, the value is 0.1466, and this compares well with the value for $\frac{n^2 - 1}{n^2 + 2} = 0.1467$. Amey and Cole[11] comment that their value at 83.85 agrees with that of Jones[12] at this temperature. Amey's values of the Clausius-Mossotti function, the dielectric constant analogue of the Lorentz-Lorenz function, agree fairly well even though different sources were used for density values. Corrected for dispersion their value for the low temperature liquid is 4.175 ± 0.005 cc/mole, and the value from this work is 4.190 cc/mole.

Figure 8 shows clearly the much greater scatter found at low density where the experimental uncertainty is high. Much less scatter for the high density liquid states is shown. It is difficult to get a clear picture of the dependence of L - L on density for coexisting gas-liquid states from this figure because of the uncertainties in the region of the critical point. As already indicated, there is some question about Levelt's density near the critical point, and as will be shown later her values above 149.6°K are considered as incorrect by this investigation. Since the interpolated densities take Levelt's work as it was reported, the value of L - L for temperatures between 149.6 and 150.7 are not considered correct. It is desirable, nevertheless, to make some statement about the values of L - L in the remaining region. The average value of L - L for all gas states up to 149.6 is 4.158 cc/mole. If the values below 125°K which have a very high uncertainty and scatter are excluded, the value is 4.152 cc/mole. The average value

for all measurements, gas and liquid, is 4.188 cc/mole.

This difference between the gas and the liquid values of L - L is very interesting. There is an increase of 1.5% in L - L for the liquid compared with the gas. The difference is almost within the experimental uncertainty of the gas values, but it is not within the uncertainty of the liquid values. The same statement applies to the scatter of the gas and liquid values. Therefore, there would appear to be a definite change in L - L on isothermal condensation. There is a slight dependence on density of the liquid L - L values, but this is within the experimental uncertainty and scatter.

A feature of these results that is not very encouraging from the theoretical point of view is that the value of L - L for the gas phase in this region is considerably less than the accepted room temperature gas value L - L = 4.21 cc/mole. This room temperature value results from both dielectric constant measurements and refractive index measurements. If the theoreticians have their way, and the Lorentz-Lorenz theory is not temperature dependent, then a serious problem exists. No attempt to predict a zero density value of L - L from these measurements is made since no measurements at very low densities are available, and the experimental method is inherently unsuitable for this work.

It is desirable to attempt to smooth the value of n along the gas-liquid coexistence curve in order to obtain a best estimate at each temperature. An arbitrary linear polynomial proved unsatisfactory when applied to densities, and it was noted that if the equation (11) for the rectilinear diameter was added to or subtracted from the equation

(5) for the critical coefficient, an equation in ρ_L or ρ_G and $T_C - T$ results. Since both of these equations apply to $\frac{n^2-1}{n^2+2}$ even in excess of the validity due to the Lorentz-Lorenz theory, this quantity was fitted by least squares to the equation.

$$\left(\frac{n^2-1}{n^2+2}\right)_L = \Psi_0 + \Psi_1 (T_C - T) + \Psi_2 (T_C - T)^2 + \Psi_3 (T_C - T)^{\beta}. \quad (15)$$

The value of T_C used is the same as obtained in the earlier analysis, 150.704°K, and the value of β is 0.361. The extra term $\Psi_2 (T_C - T)^2$ was added to improve the fit for temperatures far from the critical point. Only those points for which both gas and liquid values were available were included in the fit. The range of temperature covered is from 105° to 150.697°K. Some points were rejected at a 95% confidence level but only those points for which both gas and liquid values were outside the 95% confidence limit. The extrapolated value for the critical point was included in the fit to improve the curve when $T_C - T = 0$. The equations resulting from this fit are

$$\begin{aligned}
\left(\frac{n^2-1}{n^2+2}\right)_G &= 5.6364 \times 10^{-2} + 2.9175 \times 10^{-4}(T_C - T) + \\
&\quad 1.1557 \times 10^{-6}(T_C - T)^2 - 1.747 \times 10^{-2}(T_C - T)^{0.361} \\
\left(\frac{n^2-1}{n^2+2}\right)_L &= 5.6253 \times 10^{-2} + 1.8425 \times 10^{-4}(T_C - T) - \\
&\quad 1.8579 \times 10^{-7}(T_C - T)^2 + 1.7515 \times 10^{-2}(T_C - T)^{0.361}
\end{aligned} \quad (16)$$

The standard deviation for the fit is 2.0×10^{-4} for both equations, and the 95% confidence interval at the critical point is ± 0.71%. This fit is not too bad considering that the errors in n are magnified in $\frac{n^2 - 1}{n^2 + 2}$.

With these equations it is possible to calculate the value of L - L at each of the experimental densities presented by Levelt. In order to compensate for the fact that Levelt's critical temperature does not agree with the one measured in this study, each experimental value of $\rho(T)$ is considered at 150.86 -T. This gives each value of ρ at a specified increment of temperature away from the critical temperature determined in the density experiment. Then solving equation (15) for $\left(\frac{n^2 - 1}{n^2 + 2}\right)(T)$ at the same temperature increment of 150.704 -T, the problem of the difference in the critical temperature was eliminated.

This shifting of the data places the n versus T curve in coincidence with the ρ versus T curve. Since obviously there can not be two critical temperatures, this procedure says that one thermometer, Levelt's, was calibrated incorrectly, and all of her temperatures should be shifted down by $0.156^{\circ}K$. The values of L - L resulting from this calculation are presented in Table 5 and Figure 9. Since now the values of $\frac{n^2 - 1}{n^2 + 2}$ are calculated from a smooth monotonic function, the values of L - L should be smooth if Levelt's density values are self-consistent. The value of L - L at the critical point was calculated from

the extrapolated value of ρ given by Levelt and the extrapolated value of $\frac{n^2 - 1}{n^2 + 2}$ given by the present work.

The values of L - L in Figure 9 are not smooth especially for the two values nearest the critical point in both gas and liquid. The inconsistency of these points near the critical temperature reinforces the idea that Levelt's measurements in this region are in error. The L - L values are a very critical test of data consistency and show that what looks like smooth values of ρ are not smooth. This is the reason that the averages of the results of L - L are not extended past 149.6°T, the last consistent value of Levelt. It should be noted that these inconsistencies are not due to differences between the two thermometer calibrations. The average values of L - L in Table 5 are: gas - 4.098 cc/mole, liquid - 4.234 cc/mole. The gas value is lower than in the previous case and the liquid values higher. This is due to the temperature shift of 0.156°K. This change of temperature presents a slightly unrealistic picture since it is believed that only the data near the critical point are in error, and therefore, all the data should not be shifted in temperature. These values of L - L present an even greater discrepancy between the low temperature gas values and the room temperature gas values. The value of L - L at the critical point is 4.202 cc/mole, and this falls between the gas and the liquid values. But from Figure 9 it is not apparent that the gas and the liquid values of L - L will converge to the critical state value.

If these same equations (16) are used to calculate

$\frac{n^2-1}{n^2+2}$ at Levelt's original temperatures, the value for the gas phase L - L increases, and the liquid phase values decrease. This was calculated by assuming that the T_C for Levelt's data is 150.704°K. With this assumption no temperature shift occurs with the use of equations (16). This should present a more realistic picture of the smoothed values of L - L. The average value for the gas phase is $(L-L)_G$ = 4.144 cc/mole, and the average liquid phase value is $(L-L)_L$ = 4.214 cc/mole. These are in much better agreement with the original values given in Table 4. In this case it looks as though the gas and liquid values will converge at the critical point. The two density points nearest the critical temperature are omitted from the average. These values show a slightly larger $\Delta L - L$ for isothermal condensation, 1.65%, and the difference between the room temperature gas value and the low temperature gas value is the same amount, 1.65%.

The last step in the analysis of the coexisting gas-liquid states is to present the best estimate or smoothed values of n on the coexistence curve. The best functional form for this smoothing appears to be an equation such as (15) where n is used instead of $\frac{n^2-1}{n^2+2}$. The justification for the use of n with the rectilinear diameter equation is discussed in the first section. It appears possible to solve equation (12) for n and thus obtain a new value of β. Instead it was decided to see what happens if n is substituted directly for

$\frac{n^2 - 1}{n^2 + 2}$ in equation (12). The same analysis was applied as before, and T_C was varied to find the minimum in the standard deviation of the fit. This minimum occurred at $T_C = 150.704$, and the value of β was again 0.361. This follows directly from the fact that n obeys the rectilinear diameter, and $n^2 + 2$ can be considered as nearly constant at 3. The equations resulting from a least square fit of n are

$$n_G = 1.08603 + 5.63 \times 10^{-4}(T_C - T) - 2.7236 \times 10^{-2}(T_C - T)^{0.361}$$

$$n_L = 1.08565 + 3.38 \times 10^{-4}(T_C - T) + 2.7393 \times 10^{-2}(T_C - T)^{0.361} \qquad (17)$$

The data from 105 to 150.697°K were fitted with these equations. The standard deviation of the fit is 0.0005, and the 95% confidence interval is ± 0.10% at the critical point. Points eliminated from the fit are the same as those rejected from equation (16) since $\frac{n^2 - 1}{n^2 + 2}$ magnifies the errors and applies a stricter test for consistency. The equations (17) were used to calculate smoothed values of n along the coexistence curve at integer temperatures from 120 to 150°K, and three additional values were added near the critical point. This table of values is given in Table 6.

C. One Phase Isotherms

The data on the isotherms presented in Table C-1 were used to calculate the Lorentz-Lorenz function for all states. There does not appear to be any preliminary smoothing technique that can be applied to n alone. Therefore, L - L values were calculated for all the data points. The original intention was to run at the exact isotherms for which Levelt presents polynomials of $PV = A + B\rho + \ldots$. This causes the minimum error in temperature interpolation. Since the isotherms are not exactly the same, the value of $(\partial \rho / \partial T)_P$ was calculated and used for small range interpolation.

At each experimental value of P, Levelt's polynomial was solved for ρ in a computer program that used Muller's method. For the $-120^{\circ}C$ isotherm the values of ρ obtained from the computer program were plotted with Levelt's original experimental measurements to check for consistency. The calculated data agreed with experimental data, well within the 95% confidence interval, $\pm 3.2 \times 10^{-4}$ amagats or $\pm 0.2\%$ at 54 atm.

The correction in density for the difference between the refractive index isotherm and the density isotherm was obtained from $(\partial \rho / \partial T)_P \Delta T$. The values of $(\partial \rho / \partial T)_P$ were obtained from the equation

$$\left(\frac{\partial \rho}{\partial T}\right)_P = -\rho\left[\mu C_P \frac{\rho + 1}{T}\right] \qquad (18)$$

The computer interpolation routine was used to find $\mu C \rho$ for each value of ρ. Values of μ, the Joule Thompson coefficient, and C_P, the heat capacity, at intervals of ρ were taken from the tables presented by

Levelt. A linear interpolation was used since $(\partial \rho / \partial T)_P$ has a very sharp maximum near the critical point. The interpolated values were plotted together with original data to check for consistency. The maximum shift is -0.061°K for run 21, 173.083°K. With this density correction the value of ρ on the refractive index isotherm was obtained for each P. *For the higher temperature isotherms, 153 to 173°K,* the two runs are not the same temperature, but the difference is considered small enough so that the values of L - L would not be effected. The experimental values of n together with the calculated value of L - L for all the isotherms are presented in Table 7. The values of L - L are plotted against ρ for each isotherm in Figures 10 to 21.

The relative error for each experimental point is also reported in Table 7. The error in L - L due to the uncertainty in n, ± 0.0001, was calculated from equation(14). The error in L - L due to the combined uncertainty in T, ± 0.035°K, was obtained from the previously calculated values of $(\partial \rho / \partial T)_P$. The error due to P was obtained by differentiating the PV polynomial and inverting to get $(\partial \rho / \partial P)_T$. The error Levelt ascribes to her pressure measurements is ± 0.01%, and this was added to the uncertainty in P discussed in Appendix B, ± 0.06%. The error in L - L is large for low densities due to the error in n, and the error in L - L due to n decreases as the density increases. For isotherms near the critical isotherm, the error in ρ due to T and P becomes very large as P approaches the critical pressure. This is just another aspect of the inherent instability of this region.

In Figure 10 the data from runs 14 to 21 are plotted on the same graph since the temperature difference between them, 0.07°K,

should not effect the value of L - L significantly. The total uncertainty estimated from all sources is shown by the error marks on representative points. The line on this graph represents the least squares fit of L - L to a linear polynomial of terms to ρ^3. The dashed lines represent the 95% confidence band. Points outside 95% confidence are excluded from the fit. The excluded points are indicated by a † in the raw data of Table C-2. This graph presents the standard behavior as reported by Michels[33] for CO_2 or Michels and Botzen[9] for argon. At room temperature Michels[9] gives a zero density value of 4.21 cc/mole; the maximum is 4.218 cc/mole at 0.009 moles/cc. While the behavior of L - L presented in Figure 9 is similar to that of Michels, there are significant differences.

No attempts are made to predict a zero density value of L - L, but the value, 4.193 cc/mole, at the lowest density, 0.002 moles/cc. is significantly lower than Michel's. The difference is outside the 95% confidence band for the data, but it is within the estimate of the absolute uncertainty. Figure 9 does show a maximum in L - L of approximately 4.217 cc/mole, but it occurs at 0.012 moles/cc.

In the theoretical calculation of the dependence of L - L De Boer[8] finds the same value for the maximum, but it occurs at 0.015 moles/cc. This calculation did not consider the density dependence of a. When Mazur[1] recalculated using equation (4), which accounts for the density dependence of a, the maximum occurs at 0.0075 moles/cc. This last calculation yields a result that is the closest to the room temperature behavior reported by Michels.

Figure 11 for the 163°K isotherm presents a somewhat different

behavior. Here the lowest density value is slightly lower than for 173°K, 4.185 cc/mole, but the values increase rapidly to a maximum of 4.225 cc/mole at 0.0115 moles/cc. Then the values fall sharply to approximately 4.21 cc/mole at the highest density 0.020 moles/cc. In order to reproduce the sharp maximum in the data with a fitted polynomial, the data were divided into two sections and fitted separately. A polynomial of the form $H_0 + H_1\rho + H_2\rho^3$ is needed to get the sharp maximum.

Figure 12 for 153°K gives a picture much the same as 163°K. Again there is the sharp maximum, and this time it is much larger. The maximum at 0.011 moles/cc is 2.1% greater than the value at low density. For both 163 and 153°K the absolute error near the maximum in L - L is very large. This results from the nearness to the critical isotherm and occurrence of the maximum error near the critical density. For both temperatures the experimental error in L - L is as large as the change in L - L.

Since near the critical point small errors in T or P cause large errors in ρ, the effect of small changes in T was investigated. The change of ρ due to changes in T can be easily calculated from the available values of $(\partial \rho / \partial T)_P$. The values of L - L for 153°K were recalculated for two changes in temperature, $\Delta T = -0.10, -0.05$°K. The results are presented schematically in Figure 22. For $\Delta T = -0.10$°K the maximum becomes a minimum, and for $\Delta T = -0.05$°K the values are nearly constant. The values of L - L for the correct temperature shown in Figure 12, are the top curve in Figure 22. This calculation makes it unwise to predict that the sharp maximum is a

real physical phenomenon. Nevertheless, this behavior is consistently exhibited by all the isotherms investigated.

The 150.665°K isotherm is the first one divided into gas and liquid sections by the coexistence curve. The data for the gas phase are presented in Figure 13 and shows that L - L increases slowly until near the coexistence curve where the values rise very steeply. Being unable to fit the data with a polynomial, the curve was drawn by hand. The liquid phase continues the behavior of isotherms above the critical temperature. As shown in Figure 14, the values of L - L start at 4.248 cc/mole at 0.0168 moles/cc and decrease by 1% at 0.024 moles/cc. This change is much greater than anything the present theory would predict.

Figure 15 for the gas phase at 148°K presents something of a difficulty since the lowest density values of L - L are much lower than any other isotherm. Although there is no apparent reason for this low value, the values do present the same phenomenon of a sharp maximum near the coexistence boundary. In general at 0.002 moles/cc near the lowest density studied, the values of L - L decrease with temperature. The 143, 138, and 133°K isotherms also show a slight decrease with temperature at 0.002 moles/cc. The value for most temperatures is about 4.18 cc/mole, considerably higher than 4.15 cc/mole for 148°K. None of the isotherms in the gas phase presents any values of L - L as low as those for the coexistence curve. On all gas phase isotherms as the density approaches coexistence, the value of L - L is much higher than the coexistence value. This says that there is discontinuity in the gas phase when coexistence is reached. This is rather difficult

to understand. It should be remembered that only one, supposedly self-consistent, density investigation is used for all values of L - L. The three gas phase runs 143, 138, and 133°K, shown in Figures 17 and 19 give a very consistent picture; L - L increases linearly with the density. Although the absolute error is very large, the 95% confidence interval for the linear fit is ± 0.05%. For 143°K the value of L - L is 4.203 cc/mole at 0.005 moles/cc; this is a density very near the coexistence density. At coexistence, T = 142.803°K, ρ = 0.005297 moles/cc, the value is 4.133 cc/mole. No theory offers an answer for this, except an error in one of the experimental values, ρ or n.

Although the very low values for the coexistence curve can not be used to indicate a temperature dependence in L - L, the values for the gas isotherms can. For 173°K, at 0.002 moles/cc, L - L = 4.193; and for 133°K at the same density the value of L - L is 4.178. This difference of 0.36% is well within the estimate of the absolute uncertainty. This difference is significant if the relative error from the 95% confidence interval is used. A temperature dependent L - L is very upsetting to the theoreticians. From equation (4) the only term that could have a temperature dependence is g(r). The whole value of a theory based on g(r) is that it is not temperature dependent, only density dependent.

The very precise measurements of the dielectric constant by Orcutt[10] at 50, 100, and 150°K indicate that the zero density value of L - L is independent of temperature. In this work the densities are measured at the same time as the dielectric constant, and the work extends to very low densities. In this work and a later publication[34],

he presented values for a virial expansion of the Clausius-Mossotti function. He finds that the second virial coefficient is less than that calculated from theory.

The liquid phase isotherms below the critical temperature present a fairly uniform behavior. They do not coincide, but all start at a high value near the coexistence density and than decrease. There is a significant difference between the value on the isotherm at 148°K and the value at coexistence, but since this is near the critical point, it is probably due to experimental error. At 133°K the difference between the two is 0.07% and indicates a fair consistency. For all liquid isotherms the highest density value of L - L is approximately 4.20 cc/mole.

On none of the isotherms investigated does the value of L - L at high density fall below the value at low density. The data of Michel's[9] says that for densities greater than 0.022 moles/cc, the value of L - L is less than the low density limit. At a density of 0.0315 moles/cc his value is approximately 4.167 cc/mole, and his value at 0.0282 moles/cc is L - L = 4.185 compared to L - L = 4.191 for the 133°K isotherm. This agreement is not unreasonable considering all the uncertainty involved.

The final data analysis of the refractive index on the eight isotherms studied is to present a table of values. A smoothed or best estimate of n is desirable. For this all the values of n for each isotherm were fitted by least squares to a polynomial in P. From this, values of n were computed for every 5 atm. In order to obtain an acceptable fit, the 163, 153, and 150.7°K isotherms had to be divided

into sections. The 95% confidence interval for all the fitted curves is ± 0.01 to 0.02% except near the critical point where it is ± 0.10%. These values are presented in Table 8. This fit is considered very compatible with the experimental accuracy of the data.

IV. CONCLUSIONS

The experimental technique described in this investigation has proved adequate for measurements of refractive index over a wide range of temperatures and pressures. The small cell with sapphire windows sealed by brazing is well suited for measurements near the critical point. The absence of leakage and window distortion makes this cell suitable for high pressures and high or low temperatures. The refractive index with the spectrometric system can be measured to ± 0.01%.

The temperature control system designed by Knobler and Honeywell works well in this application. The temperature could be determined and controlled to ± 0.001°K although the absolute accuracy is only ± 0.015°K. The new pressure measuring system is a distinct improvement over the conventional gages although it does not have the accuracy of the dead weight tester. The instantaneous response and ease of operation are distinct advantages in this work. More recent work shows that the ± 0.06% accuracy can be increased two or three fold by using the manual null instead of the servo nulling system.

The results in the critical region on the coexistence curve are the most informative. They provide a thorough and consistent representation of the phenomena in this region. Both the rectilinear diameter and the equation for the critical coefficient apply equally well to the refractive index and the Lorentz-Lorenz function in this region. The value of $T_C = 150.704°K$ which gives the best fit of the experimental data to the equation $\Phi_L - \Phi_G = A(T_C - T)^{\beta}$ is the best value available

from this investigation. The value of $n_C = 1.08587$ is obtained from the rectilinear diameter, and the value of $P_C = 48.18$ atm. is from an extrapolation of the vapor pressure to the critical temperature.

On the coexistence curve the data are not as conclusive. The values of n are consistent and can be fitted to a smooth functional form. They provide reliable data for n_L from 85°K to the critical point, and for n_G the values are from 105°K to T_C. The values of $(L - L)_G$ in this same region are not as consistent. The large error for states below 120°K makes these data unreliable. In the region where the data are good, 125 to 149.6°K, the gas phase L - L is constant and independent of density within the experimental accuracy, average $(L - L)_G = 4.152$ cc/mole.

Because of the lack of reliable density data in the critical region, no definite statement about L - L in this region can be made. From all the analysis the most reliable speculation is that there is not an anomaly in this region. The values of $(L - L)_G$ and $(L - L)_L$ converge at the critical point to a value $(L - L)_C = 4.202$ cc/mole. The values of L - L in the liquid coexistence phase show a slight dependence on density, but the change is within the limits of the experimental accuracy. The average value of $(L - L)_L$ from 85°K to 149.6°K is 4.213 cc/mole. This represents a 1.5% increase compared to the coexisting gas, provided the density measurements are reliable. The general conclusion about the coexisting densities presented by Levelt is that the two data points nearest the critical point are in error. The major difference between L - L for coexisting gas and room temperature gas can not be considered as significant

because of questionable density values.

For the eight isotherms between 133 and 173°K the most significant feature is the sharp maximum in L - L that occurs near the critical density. Although it is shown that this is possibly the result of a temperature discrepancy of 0.05°K, the behavior is regular and shown to some degree by all isotherms.

The other important result obtained from these isotherms is the small but significant temperature dependence of L - L in the low density gas region. There would also appear to be a discrepancy between the gas densities near the coexistence curve and the coexistence gas density since the L - L values are discontinuous here.

The most obvious recommendation is to make density measurements concurrent with the refractive index measurements. A cell which can be sealed at low temperature to provide constant density measurements is a realizable objective. This can give a definite answer for the temperature dependence of L - L. The greatest relative error is in the pressure measurement, and it is recommended that the pressure gage be used in the manual mode of operation. In the critical region the extreme care necessary for thermal equilibrium must be recognized and accounted for.

NOMENCLATURE

A - prism angle

B - arbitraty coefficient

c - speed of light

D - angle of minimum deviation

$\vec{D}$ - electric displacement in a medium

$\vec{E}$ - electric field

$g(r)$, $g^{(2)}(r_{12})$ - pair radial distribution function

$g^{(2)}(\vec{r}_1, \vec{r}_2)$ - probability distribution function

H - arbitrary coefficient

L - L - Lorentz-Lorenz function

n - refractive index

P - pressure

p - dipole moment

r - distance

T - temperature

t - time

$\vec{T}$ - vector operator

$\hat{U}$ - unit tensor

v - velocity of light in a medium

Greek

α - polarizability

β - critical coefficient

γ - angle

ε - dielectric constant

θ - arbitrary coefficient

λ - wave length

μ - magnetic permeability

ρ - density

Ψ - arbitrary coefficient

ω - frequency

Subscripts

C - critical state value

G - gas

i, k - molecules i and k

L - liquid

O - isolated state

Superscripts

$\rightarrow$ - vector

$\hat{}$ - tensor

$\bar{}$ - average

REFERENCES

1. P. Mazur and L. Jansen, Physica 21, 208 (1955).
2. J. Yvon, "Recherches sur la Theorie Cinetique des Liquids," (Herman et Cie., Paris, 1937).
3. A. Münster, "Statistische Thermodynamik kondensierter Phasen," Handbuch der Physik, Vol. 13, 256 (Springes-Verlag, Berlin, 1962).
4. P. Mazur and J. Postma, Physica 25, 251 (1959).
5. J.G. Kirkwood, Journal of Chemical Physics 4, 592 (1936).
6. L. Jansen and P. Mazur, Physica 21, 193 (1955).
7. P.G. Mikolaj, doctoral thesis, California Institute of Technology 1965.
8. J. de Boer, F. van der Maesen, and C.A. ten Seldam, Physica 19, 265 (1953).
9. A. Michels and A. Botzen, Physica 15, 769 (1949).
10. R.H. Orcutt and R.H. Cole, Physica 31, 1779 (1965).
11. R.L. Amey and R.H. Cole, Journal of Chemical Physics 40, 146 (1964).
12. G.O. Jones and B.L. Smith, Philosophical Magazine 5, 355 (1960).
13. E.H.W. Schmidt, Critical Phenomena, 13 (National Bureau of Standards Miscellaneous Publication 273, Washington, D.C., 1966).
14. H. Cataldi and H.G. Drickamer, Journal of Chemical Physics 18, 650 (1950).

15. J. M. H. Levelt, doctoral thesis, Amsterdam, 1958.

16. R. H. Sherman, Critical Phenomena, 7 (National Bureau of Standards Miscellaneous Publication 273, Washington, D. C., 1966).

17. J. S. Rowlinson, Critical Phenomena, 9 (National Bureau of Standards Miscellaneous Publication 273, Washington, D. C., 1966).

18. G. E. Uhlenbeck, Critical Phenomena, 3 (National Bureau of Standards Miscellaneous Publication 273, Washington, D. C., 1966).

19. M. E. Fisher, Critical Phenomena, 21 (National Bureau of Standards Miscellaneous Publication 273, Washington, D. C., 1966).

20. F. A. Jenkins and H. E. White, Fundamentals of Optics, 24 (McGraw-Hill Book Co., New York, 1950).

21 C. P. Abbiss, C. M. Knobler, R. K. Teague, and C. J. Pings, Journal of Chemical Physics 42, 4145 (1965).

22. R. A. Houston, A Treatise on Light, 98, (Longman, Green and Co., London, 1921).

23. W. I. Honeywell, C. M. Knobler, B. L. Smith, and C. J. Pings, Review of Scientific Instruments 34, 1216 (1964).

24. W. I. Honeywell, doctoral thesis, California Institute of Technology, 1964.

25. C. M. Knobler, W. I. Honeywell, and C. J. Pings, Review of Scientific Instruments 34, 1437 (1963).

26. L. Cailletet and E. Mathias, Comptes Rendus 102, 1202 (Academie des Sciences, Paris 1886).

27. E. Mathias, H. Kamerlingh Onnes and C. A. Crommelin, Communications from the Physical Laboratory, University of Leiden, No. 131a, (1912).

28. J. R. Partington, Treatise on Physical Chemistry, Vol. 1, 639 (Longman and Green, London, 1949).

29. C. A. Crommelin, Communications from the Physical Laboratory, University of Leiden, No. 115a, (1910).

30. C. A. Crommelin, Communications from the Physical Laboratory, University of Leiden, No. 118, (1910).

31. A. M. Clark, F. Din and J. Robb; and A. Michels, T. Wassenaar and Th. Zwietering, Physica 17, 876 (1951).

32. C. Cuthbertson and M. Cuthbertson, Royal Society of London, Proceedings A 84, 13 (1910).

33. A. Michels and L. Kleerekoper, Physica 6, 586 (1939).

34. R. H. Orcutt and R. H. Cole, Journal of Chemical Physics 46, 697 (1967).

35. R. M. Waxler and C. E. Weir, Journal of Research, National Bureau of Standards 67A No. 2, 163 (1963).

36. B. L. Smith, Review of Scientific Instruments 34, 19 (1963).

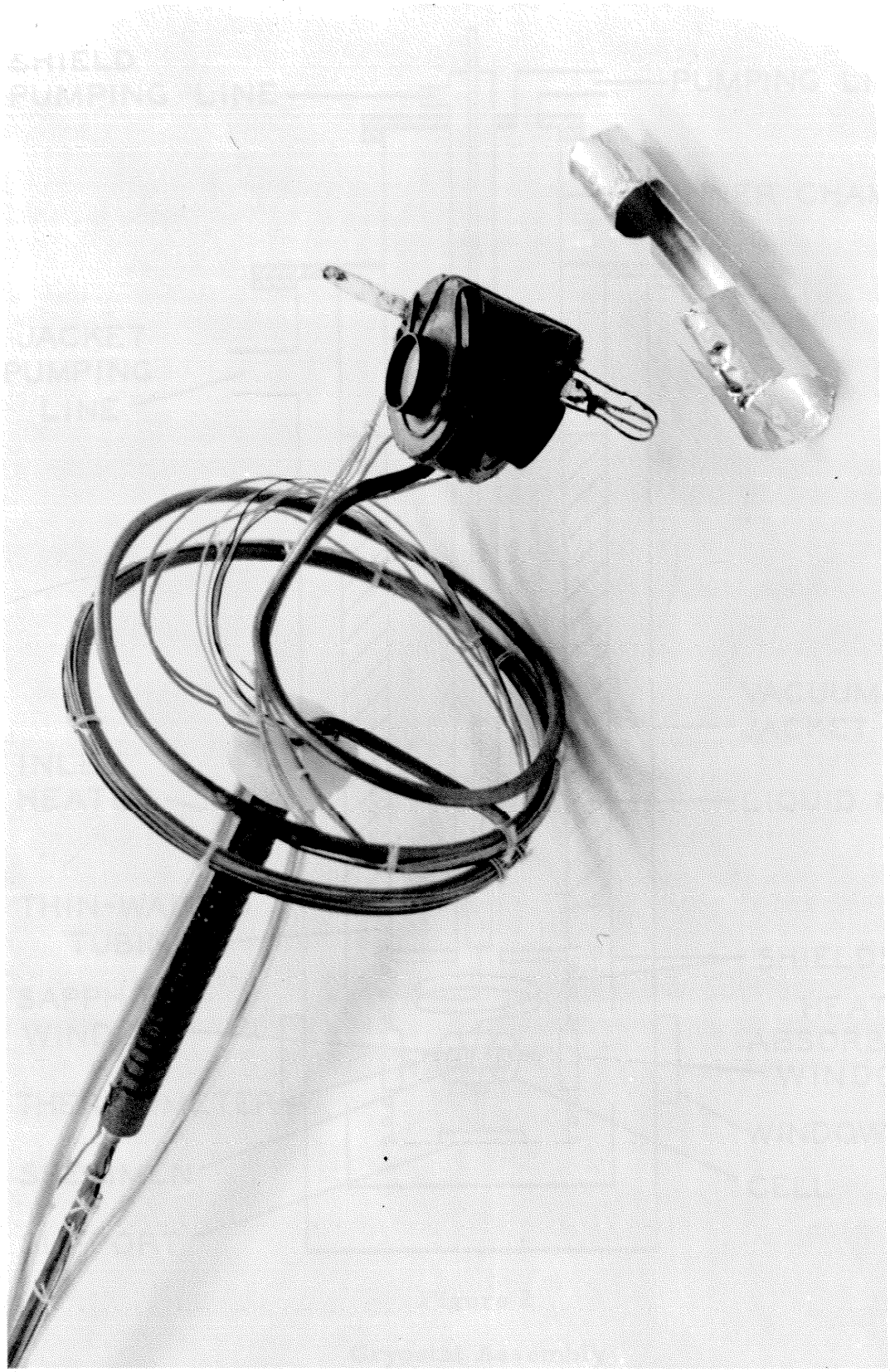

Figure 1
Prism Cell Assembly

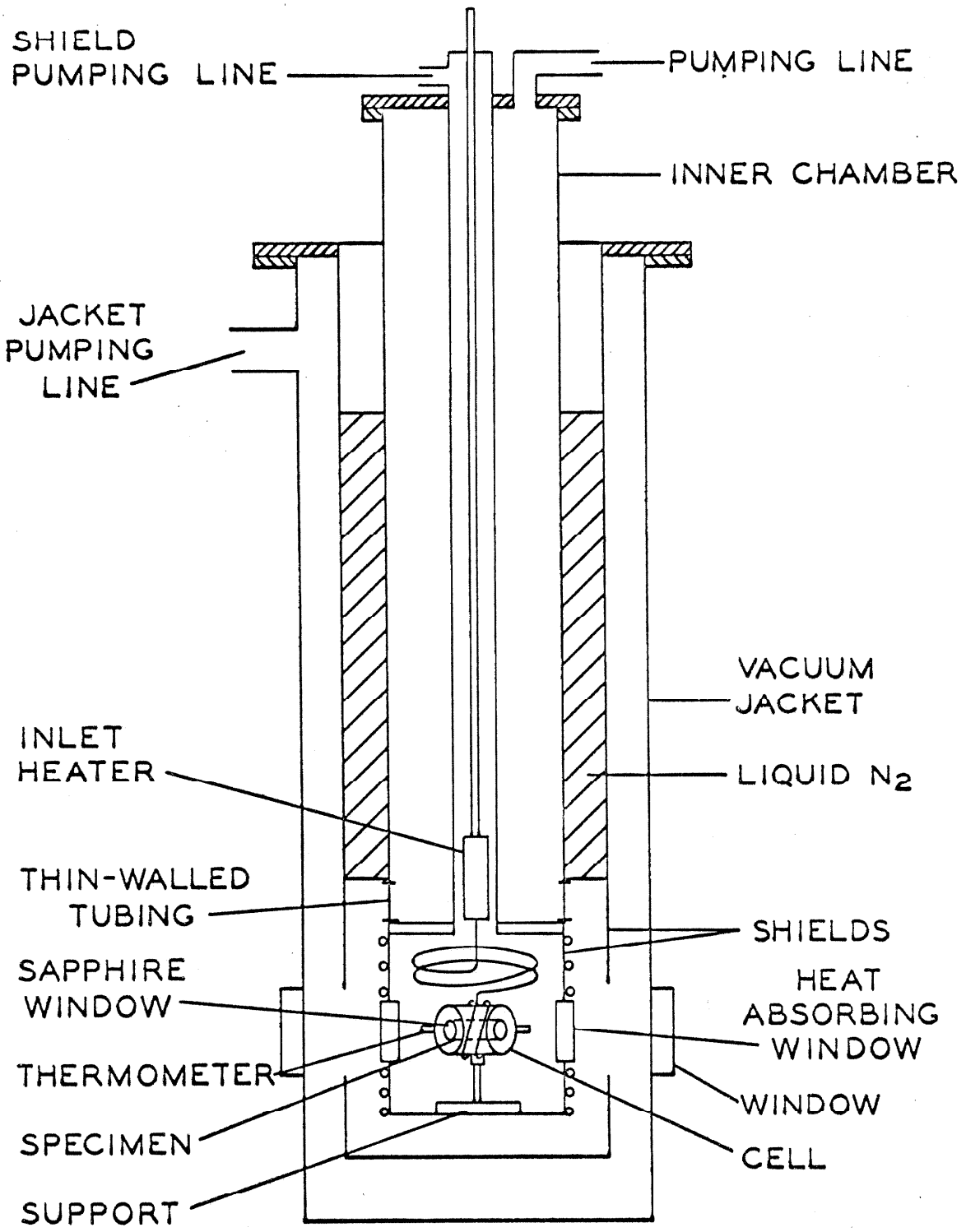

Figure 2

Cryostat Assembly

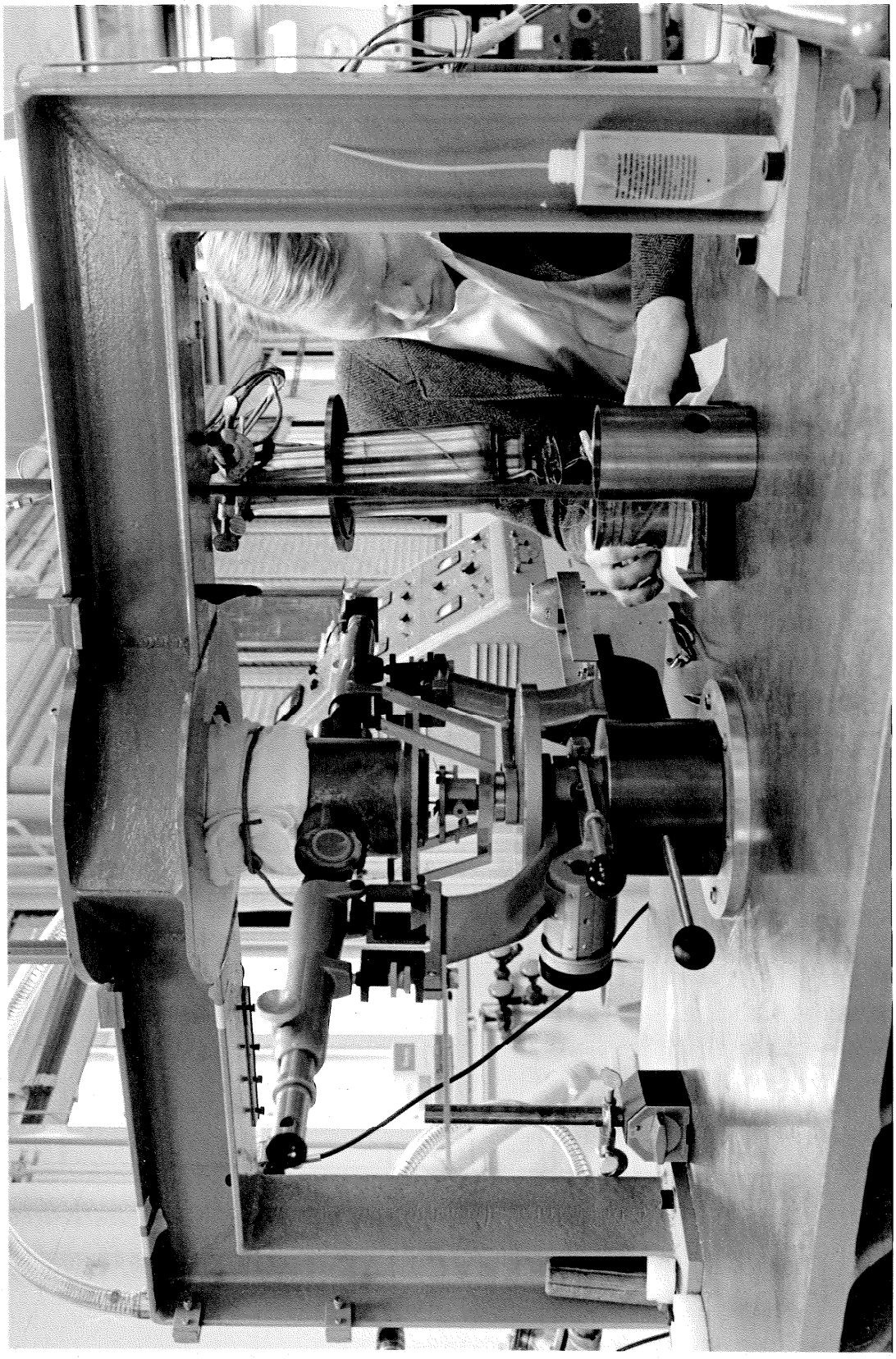

Figure 3
Spectrometer Assembly

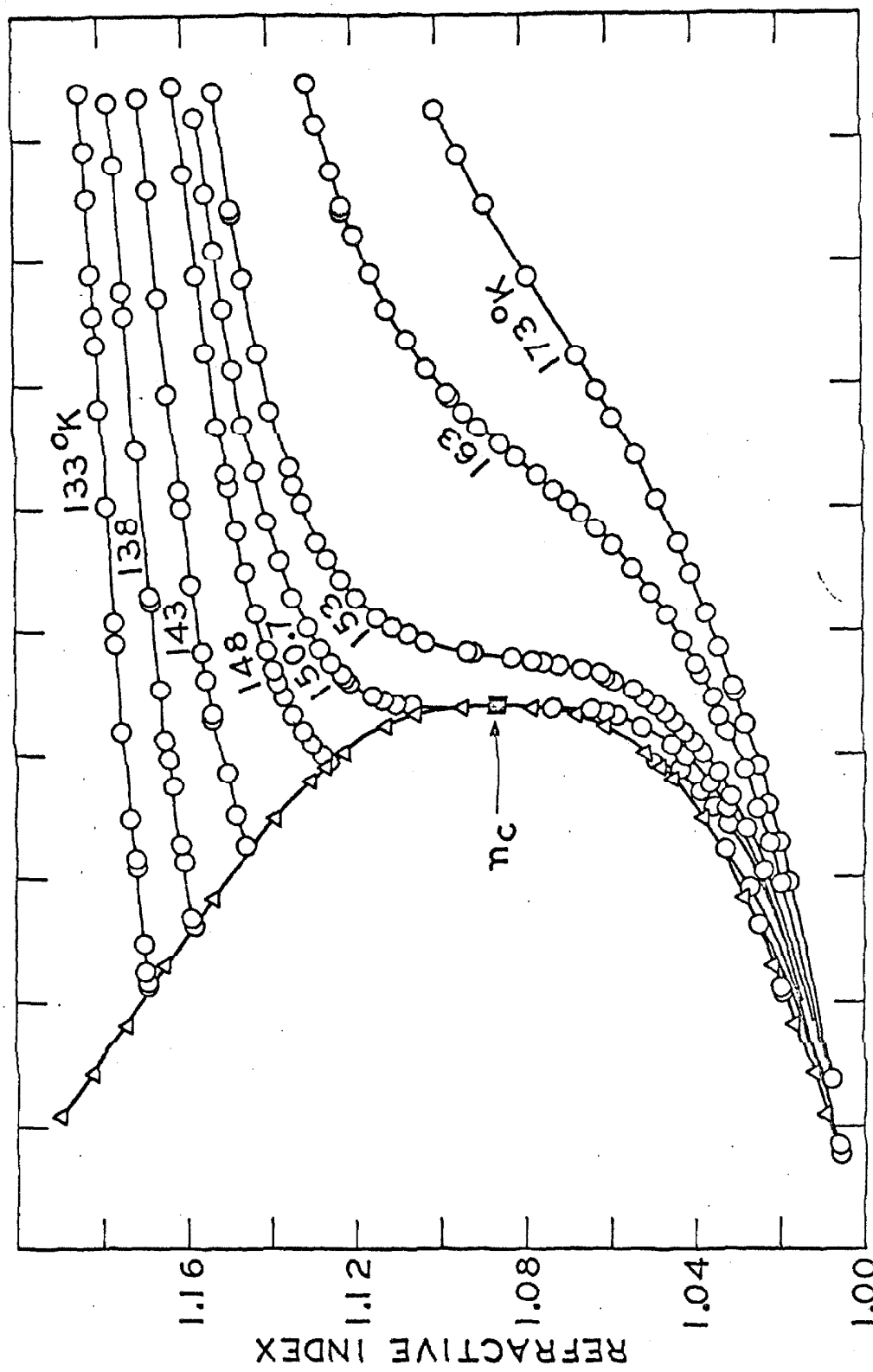

Figure 4

Experimental Refractive Index States

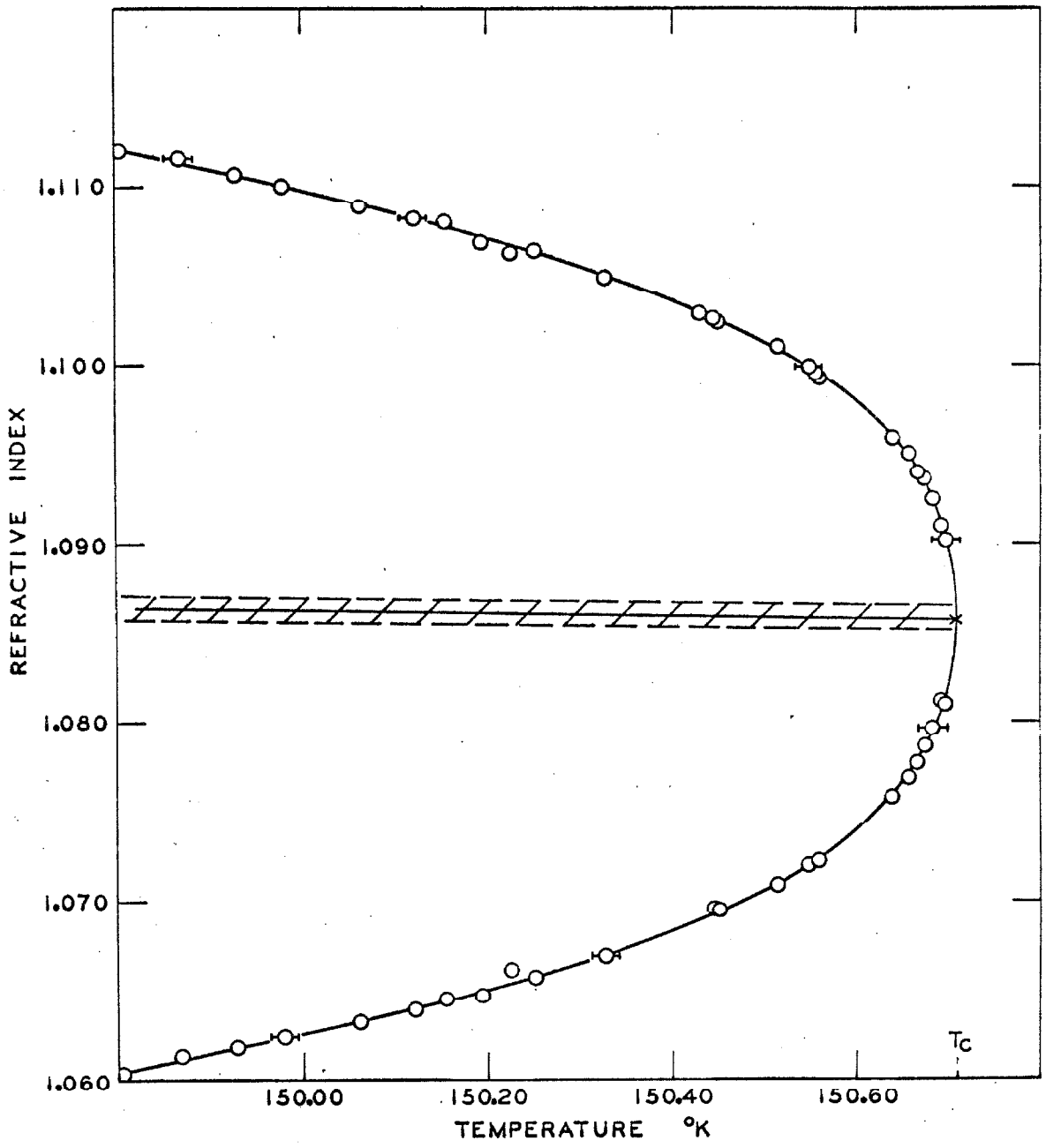

Figure 5

Refractive Index in the Critical Region

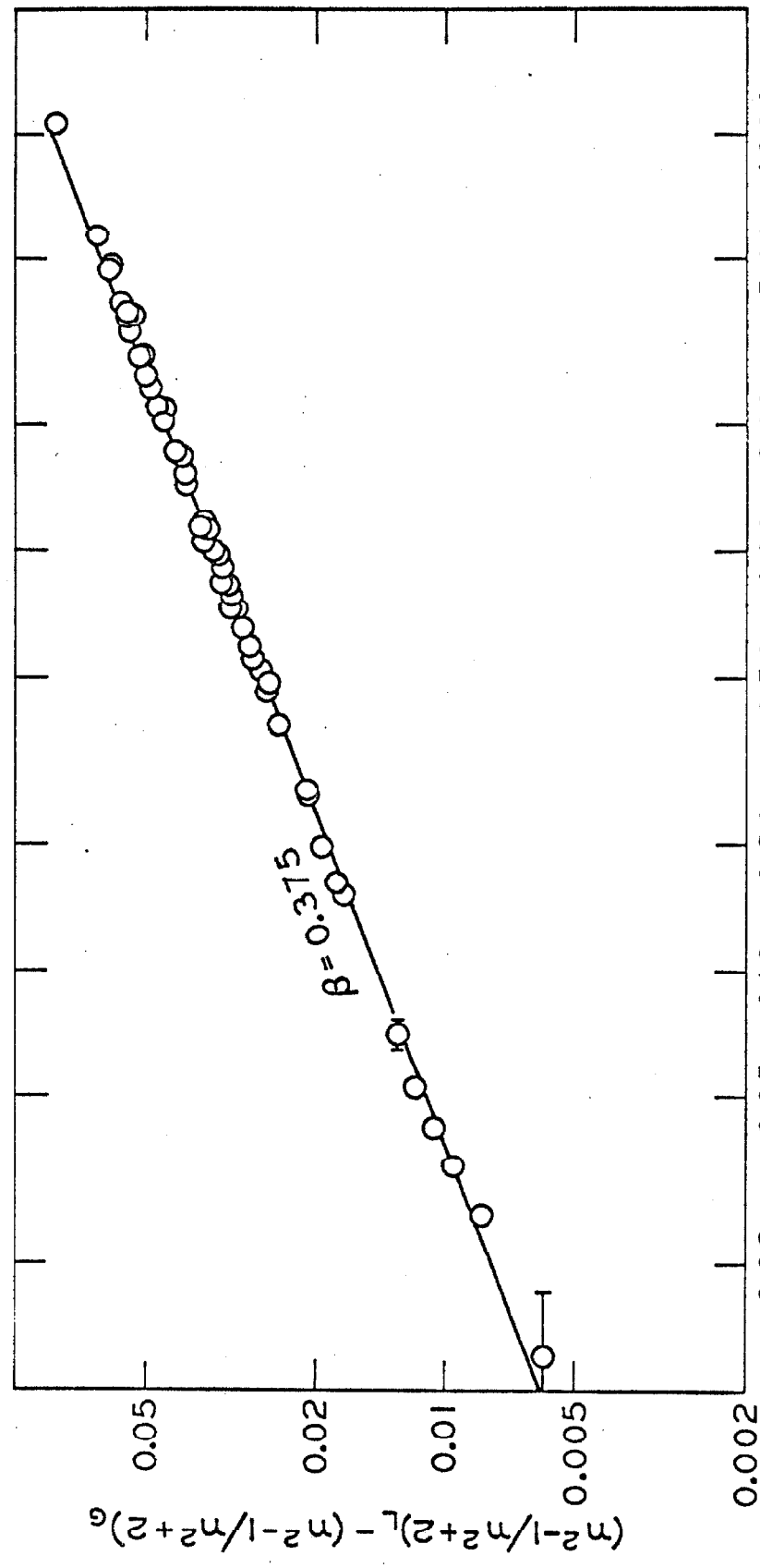

Figure 6

Critical Coefficient, $T_C = 150.709^{\circ}K$

Straight Line of Slope β

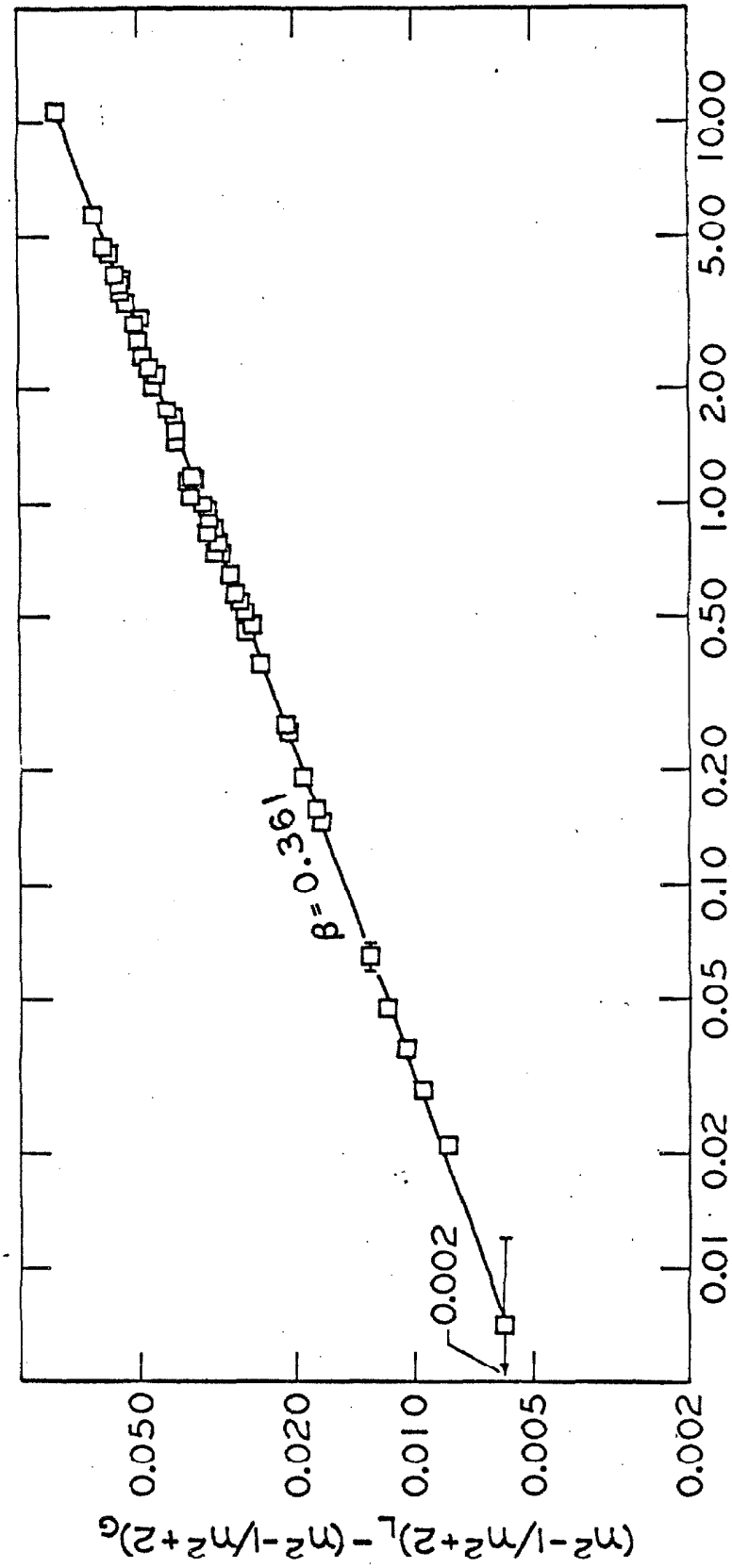

Figure 7

Critical Coefficient, $T_C = 150.704^{\circ}K$

Straight Line of Slope β

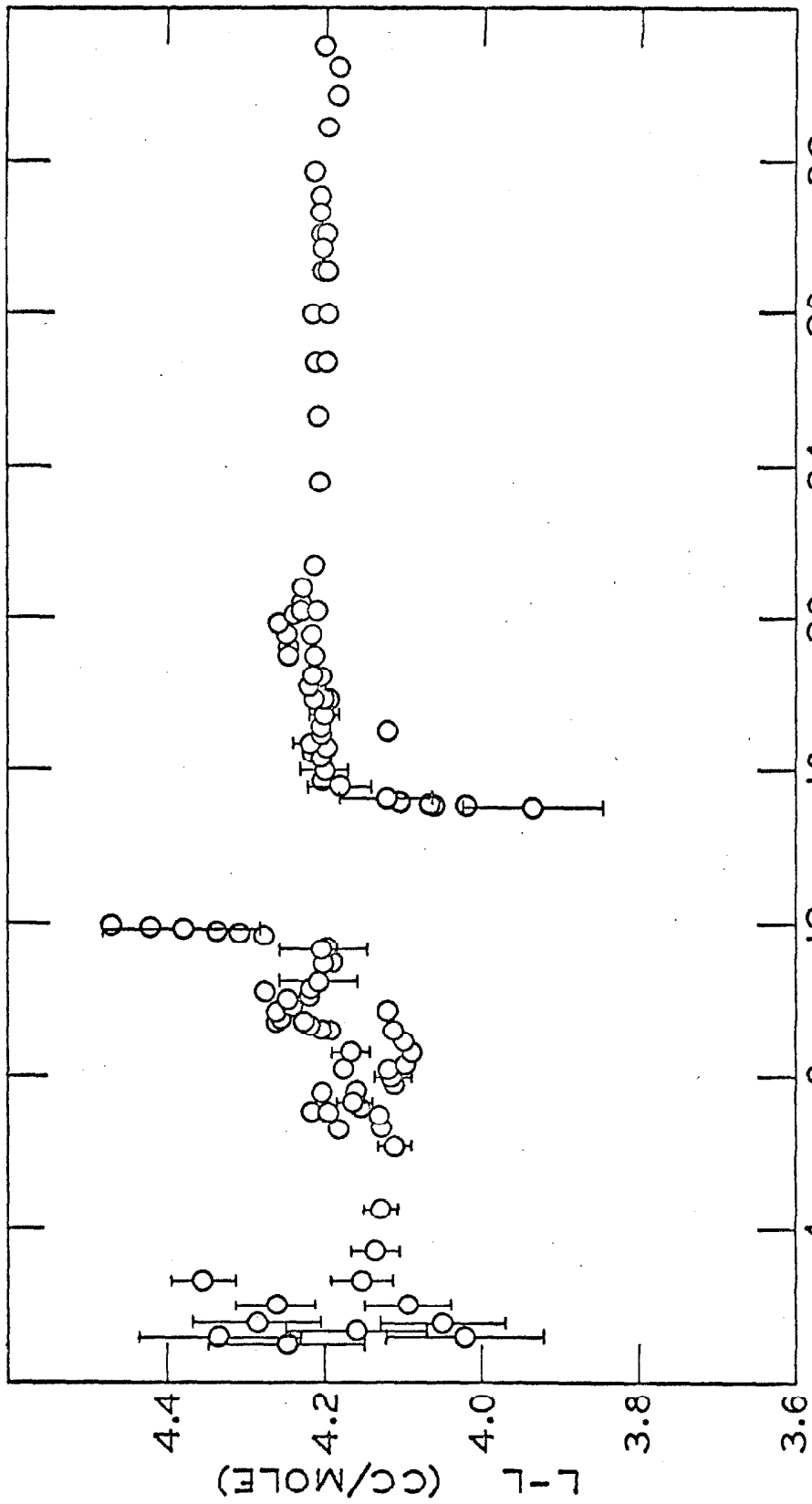

Figure 8

Lorentz-Lorenz Function for the Coexistence Curve

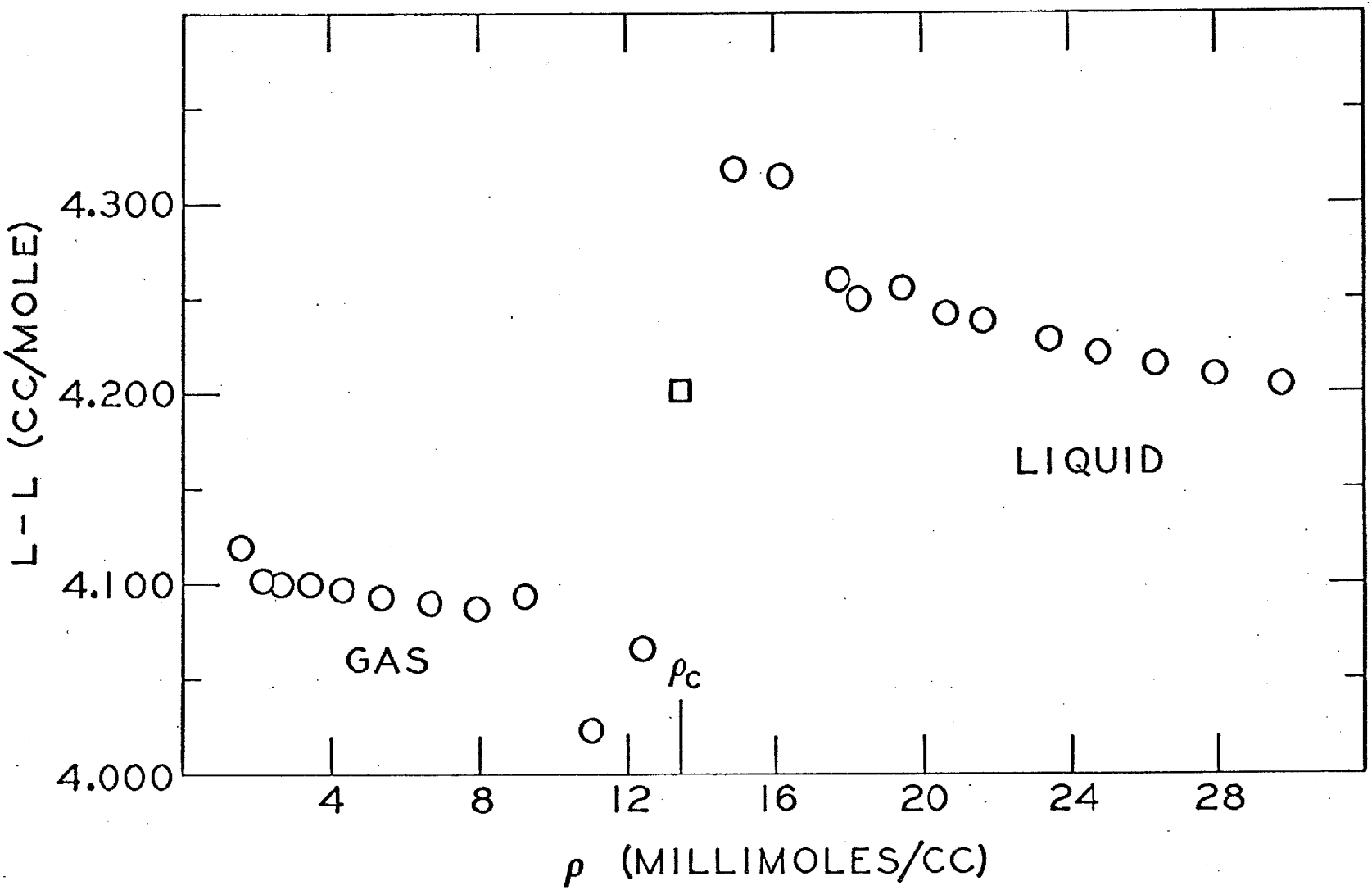

Figure 9

Lorentz-Lorenz Function for Densities Published by Levelt

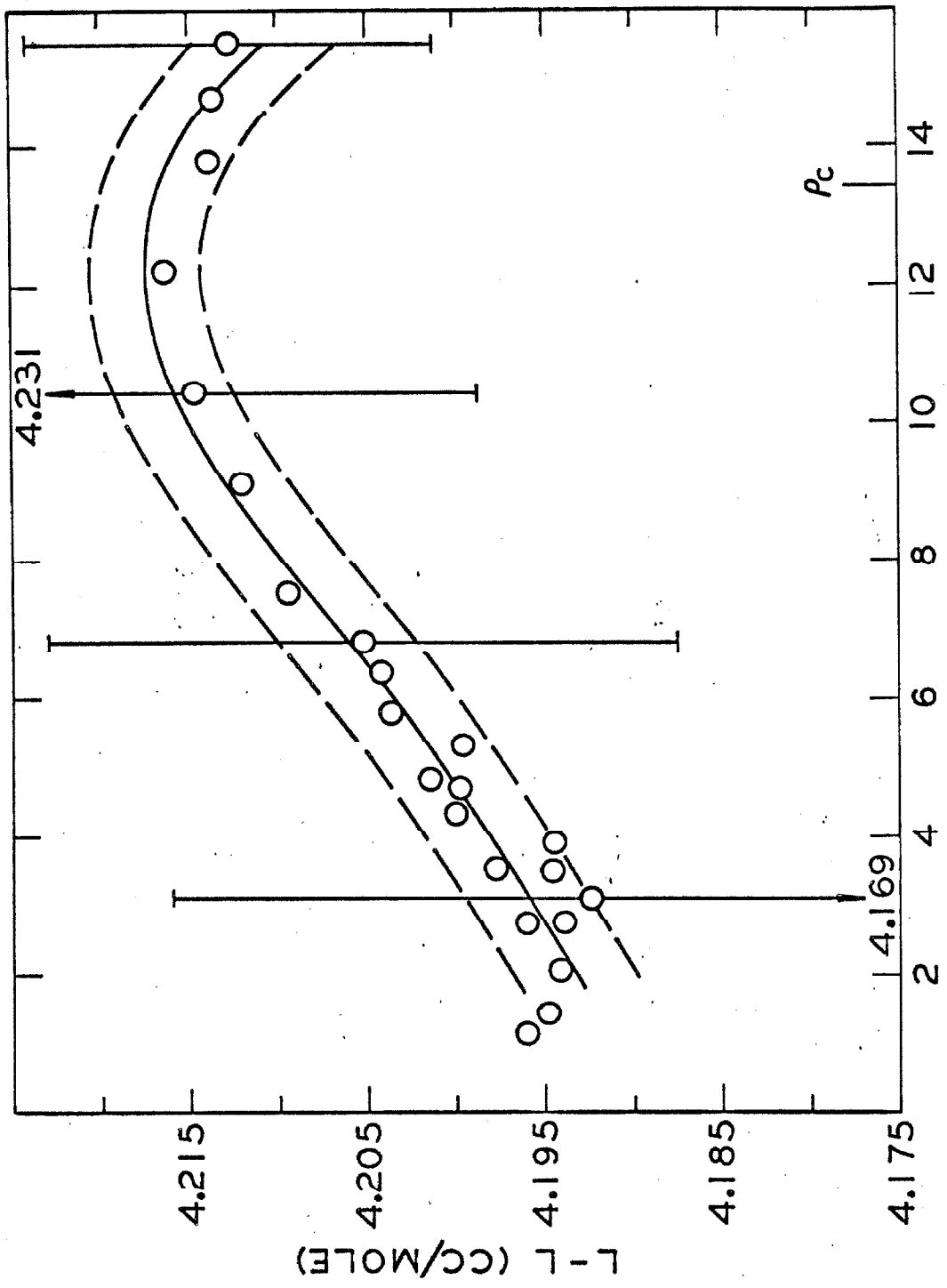

Figure 10

Lorentz-Lorenz Function for 173°K

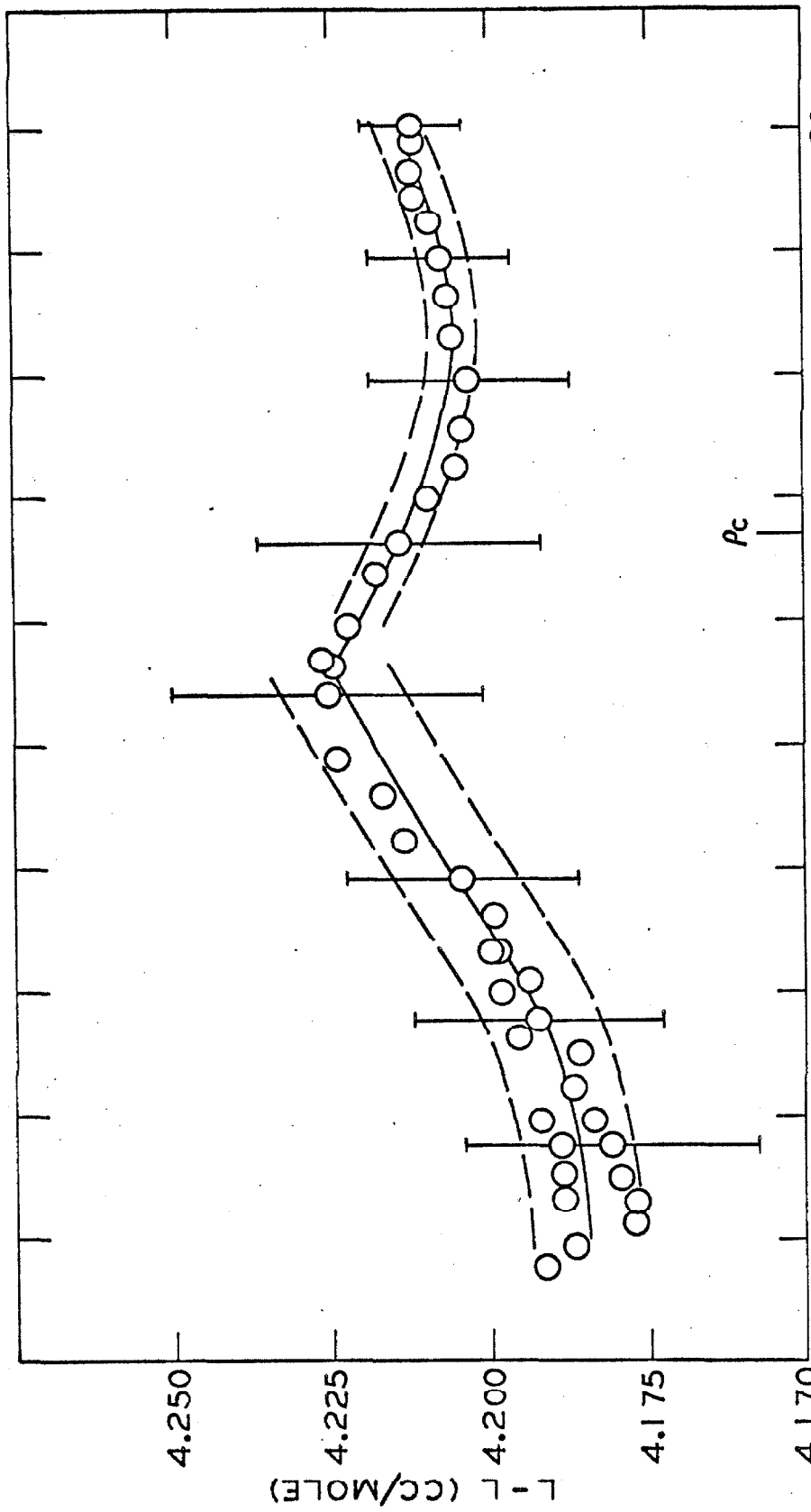

Figure 11

Lorentz-Lorenz Function for 163°K

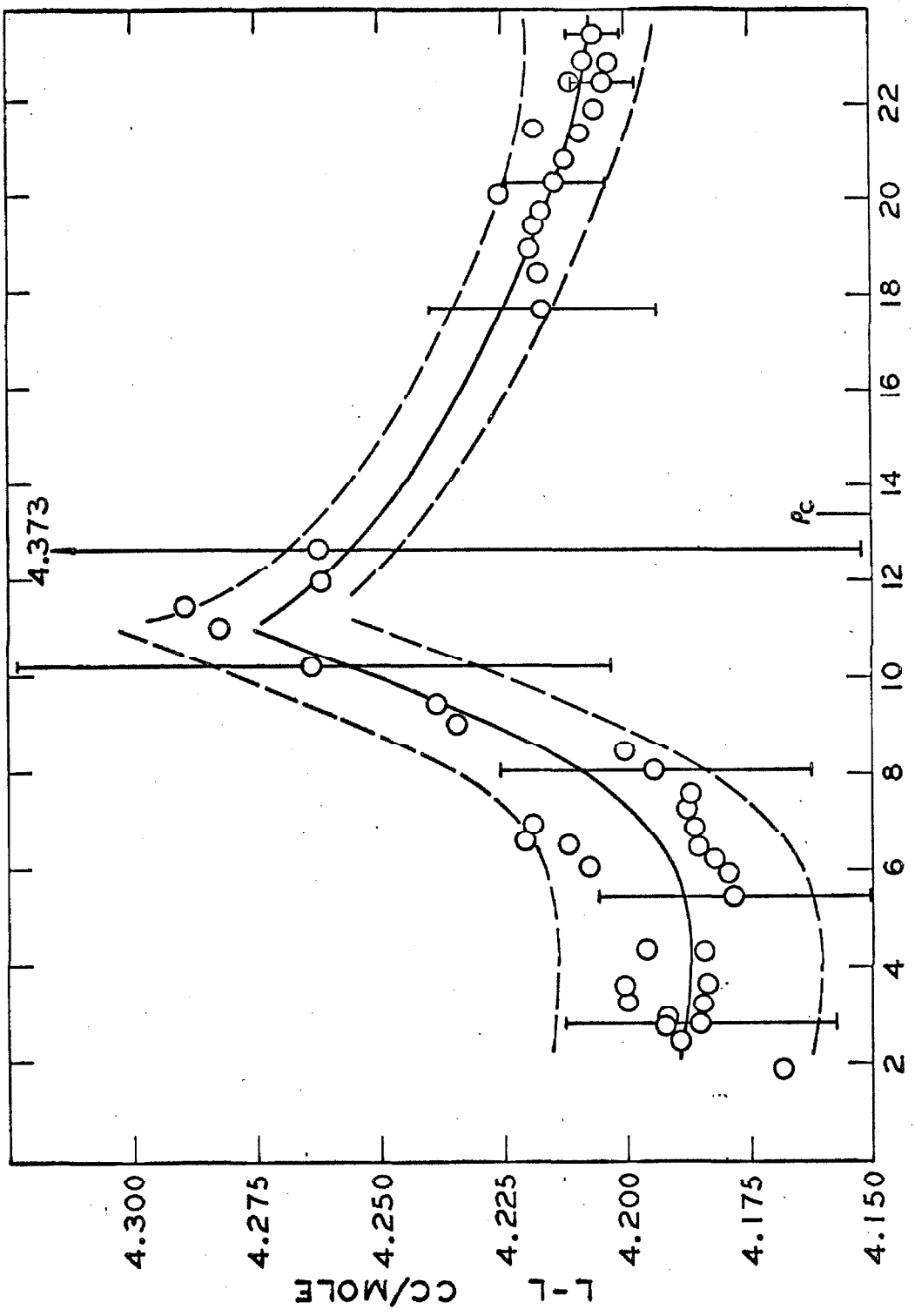

Figure 12
Lorentz-Lorenz Function for 153°K

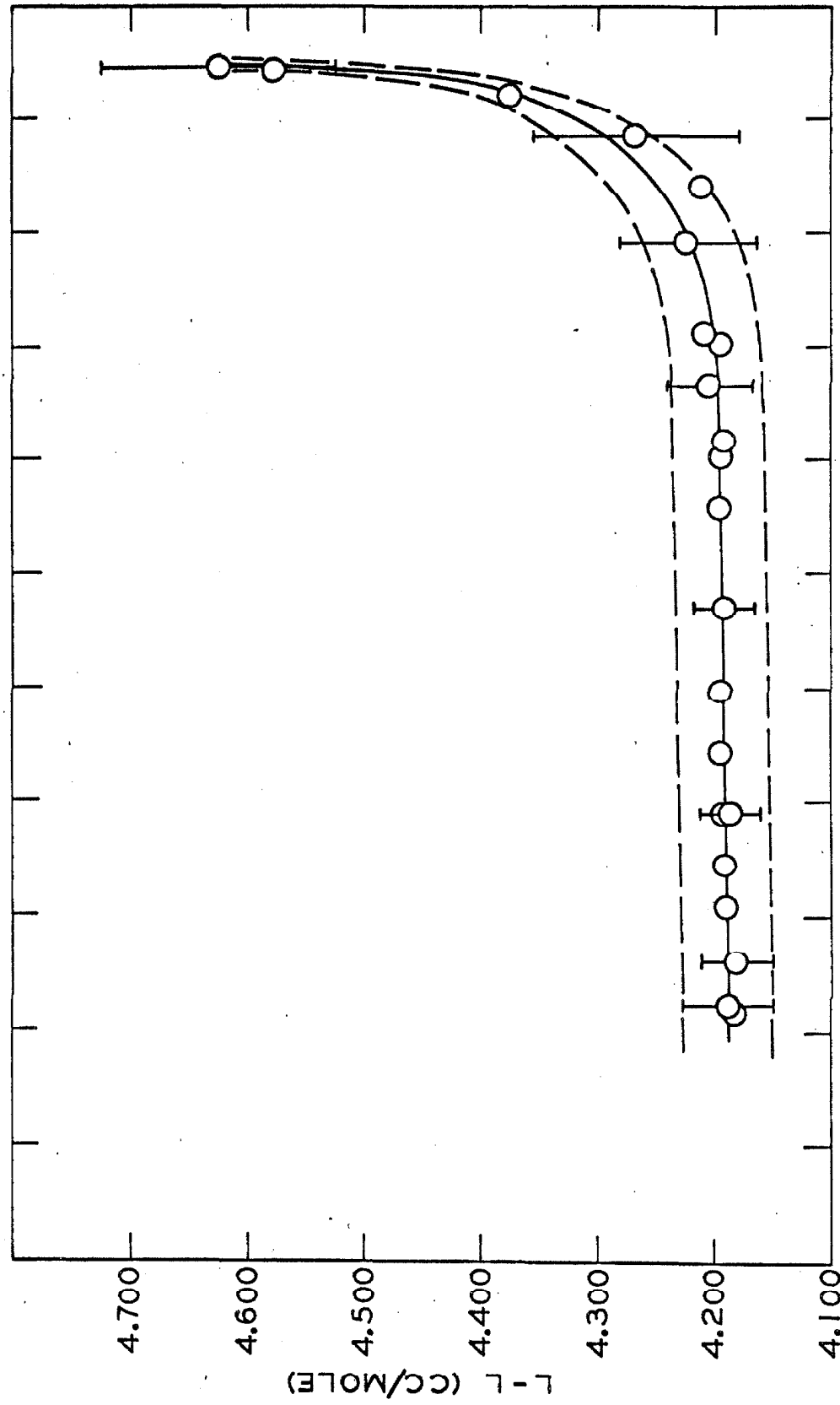

Figure 13

Lorentz-Lorenz Function for the Gas Phase at 150.7°K

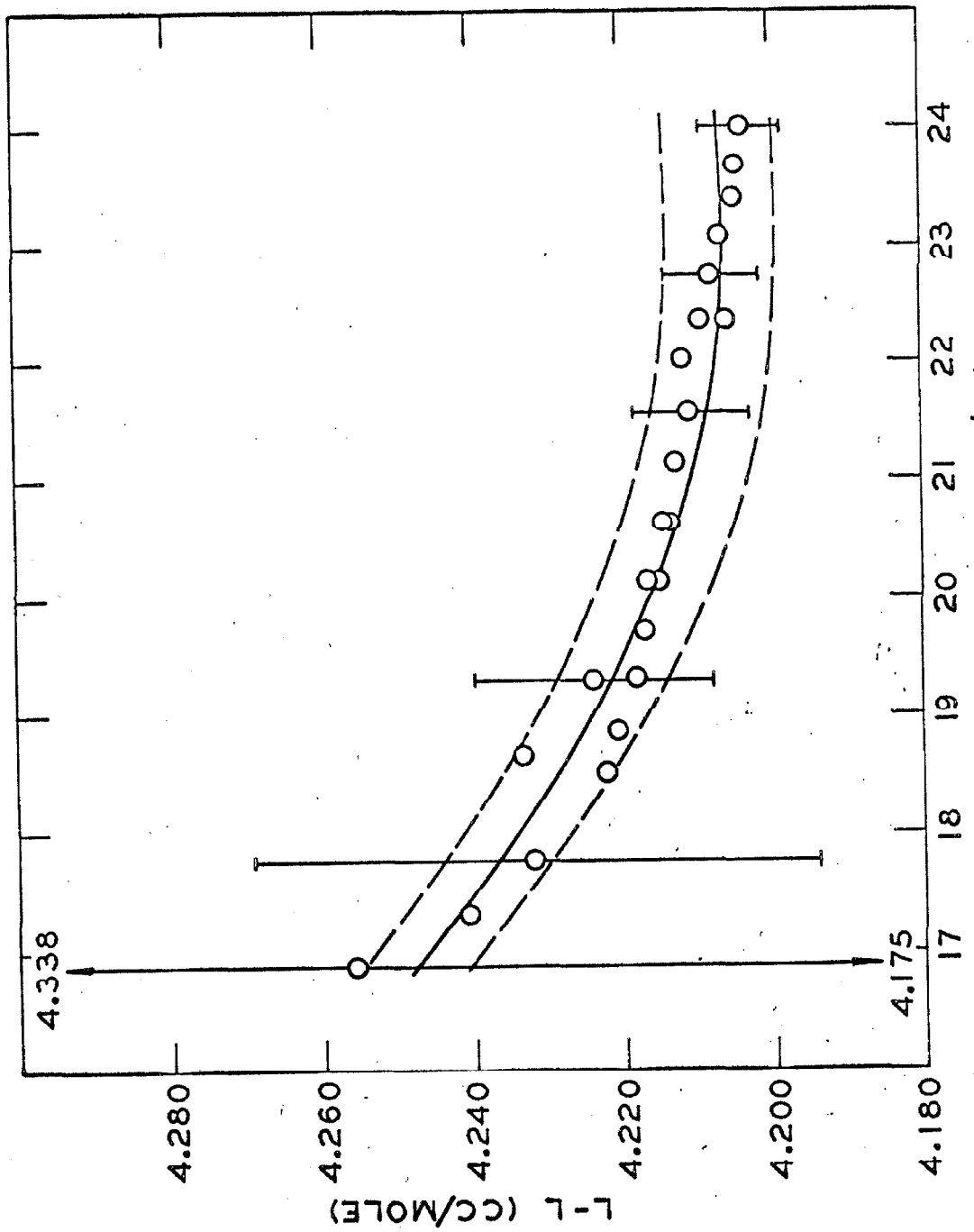

Figure 14
Lorentz-Lorenz Function for the Liquid Phase at 150.7°K

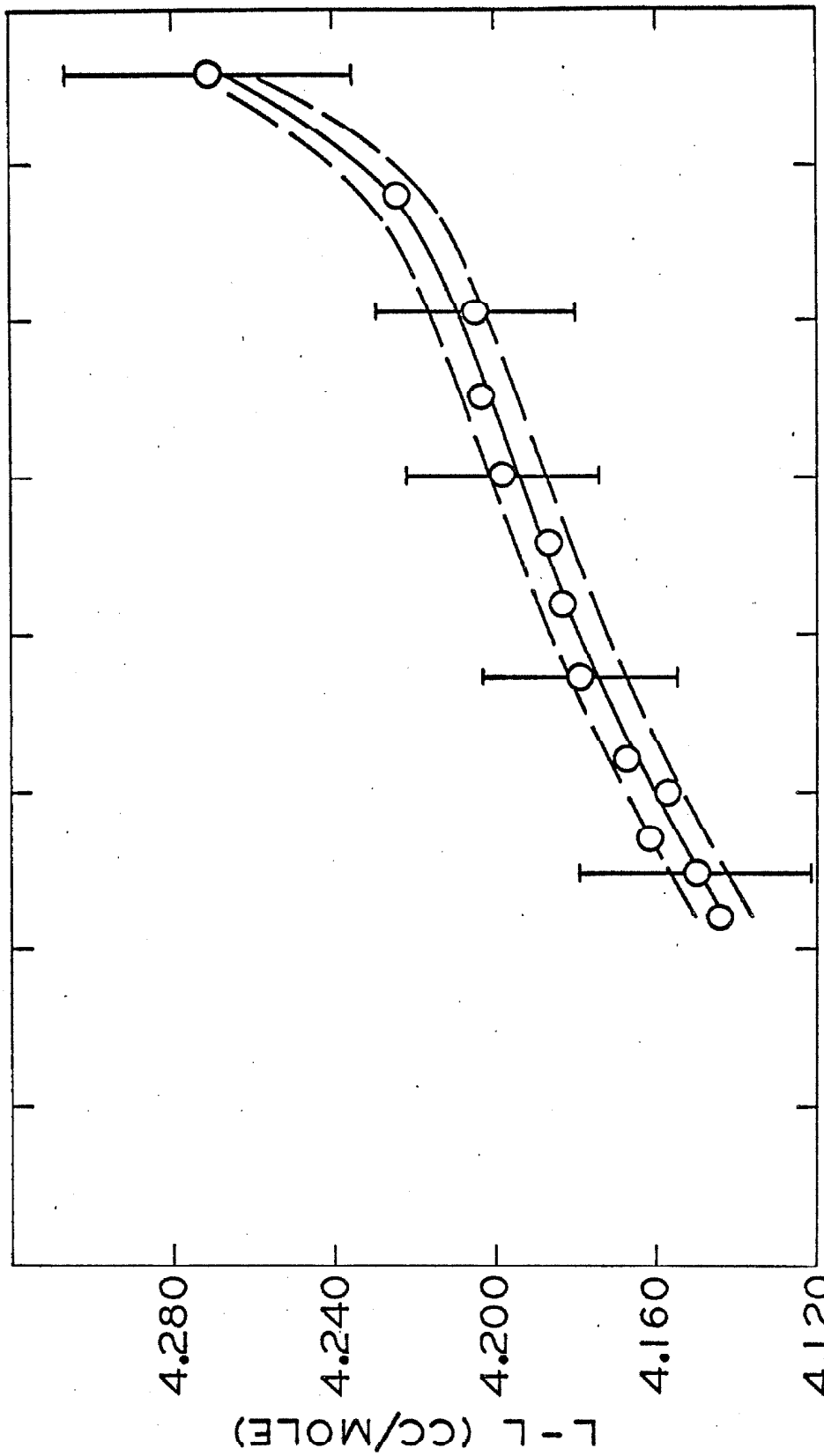

Figure 15

Lorentz-Lorenz Function for the Gas Phase at 148°K

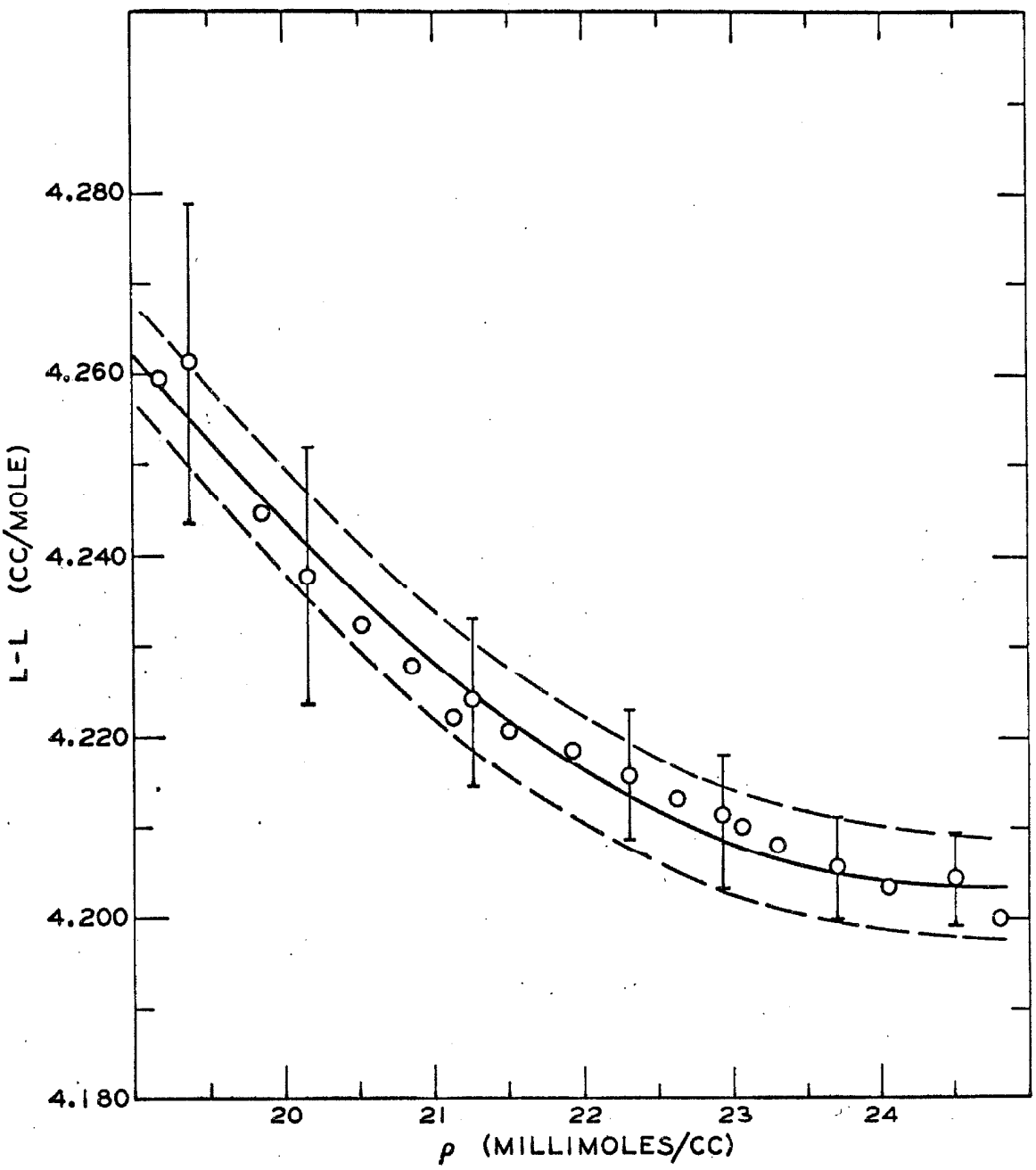

Figure 16

Lorentz-Lorenz Function for the Liquid Phase at 148°K

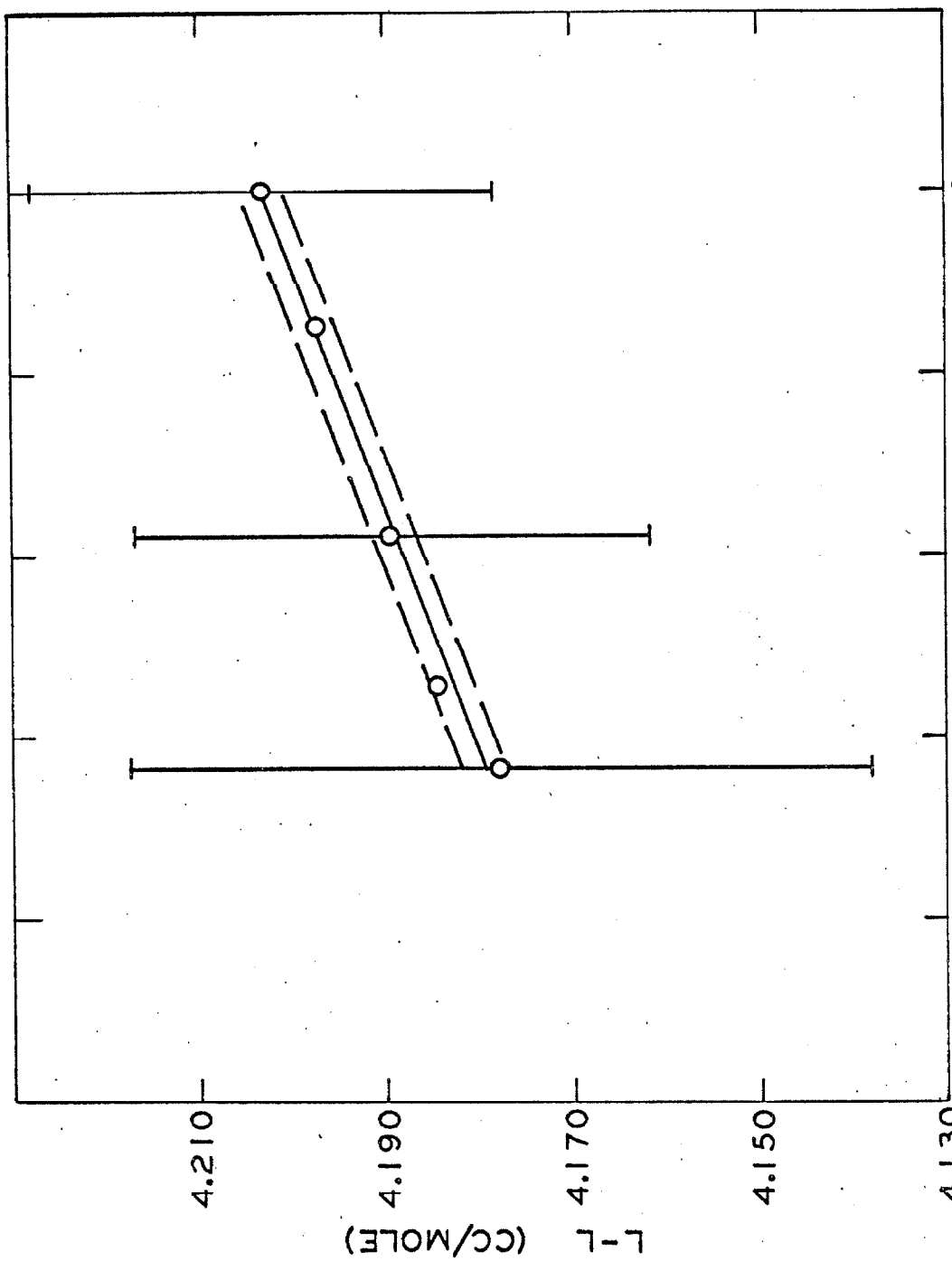

Figure 17
Lorentz-Lorenz Function for the Gas Phase at 143°K

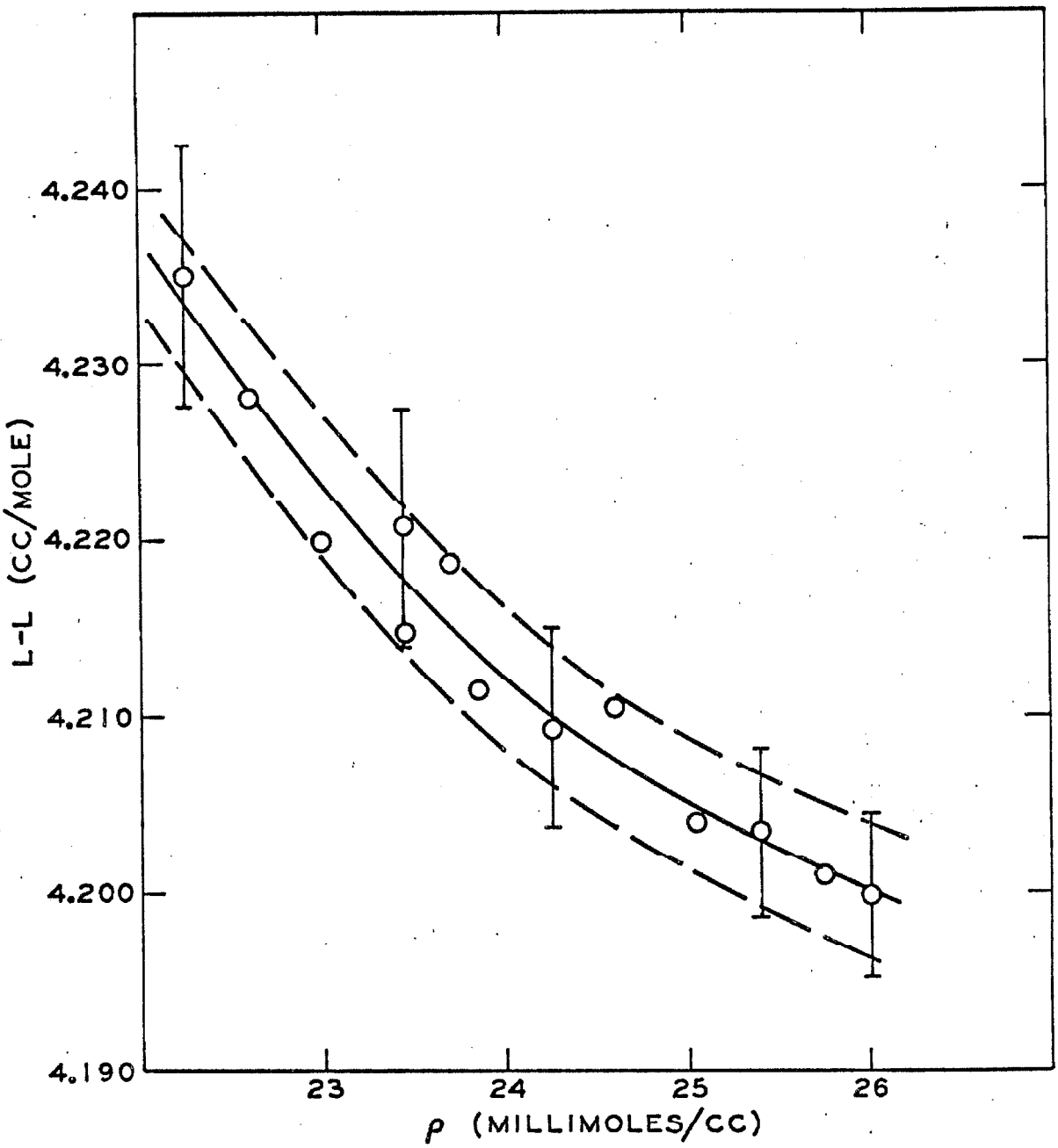

Figure 18

Lorentz-Lorenz Function for the Liquid Phase at 143°K

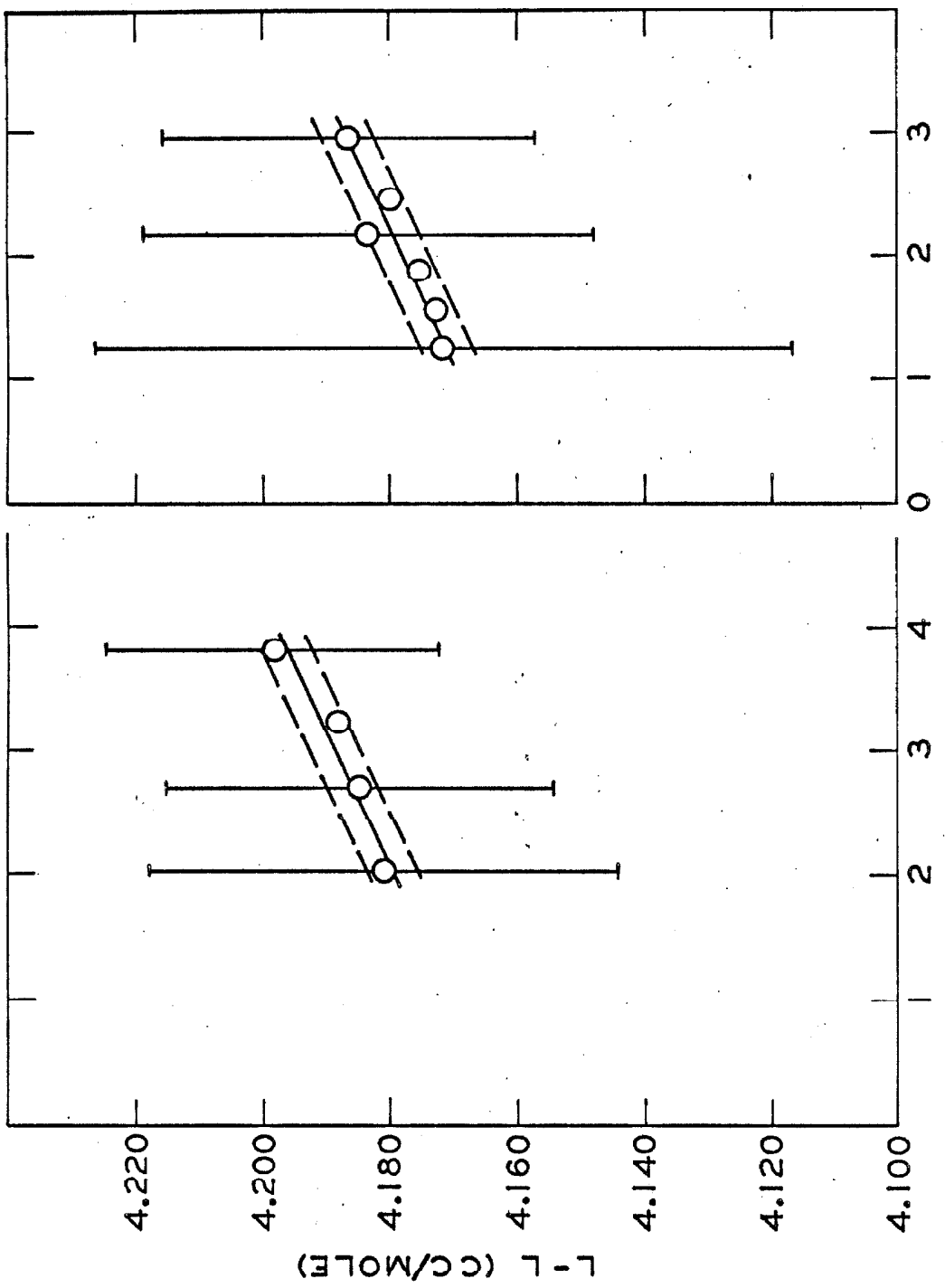

Figure 19

Lorentz-Lorenz Function for the Gas Phase at 138 and 133°K

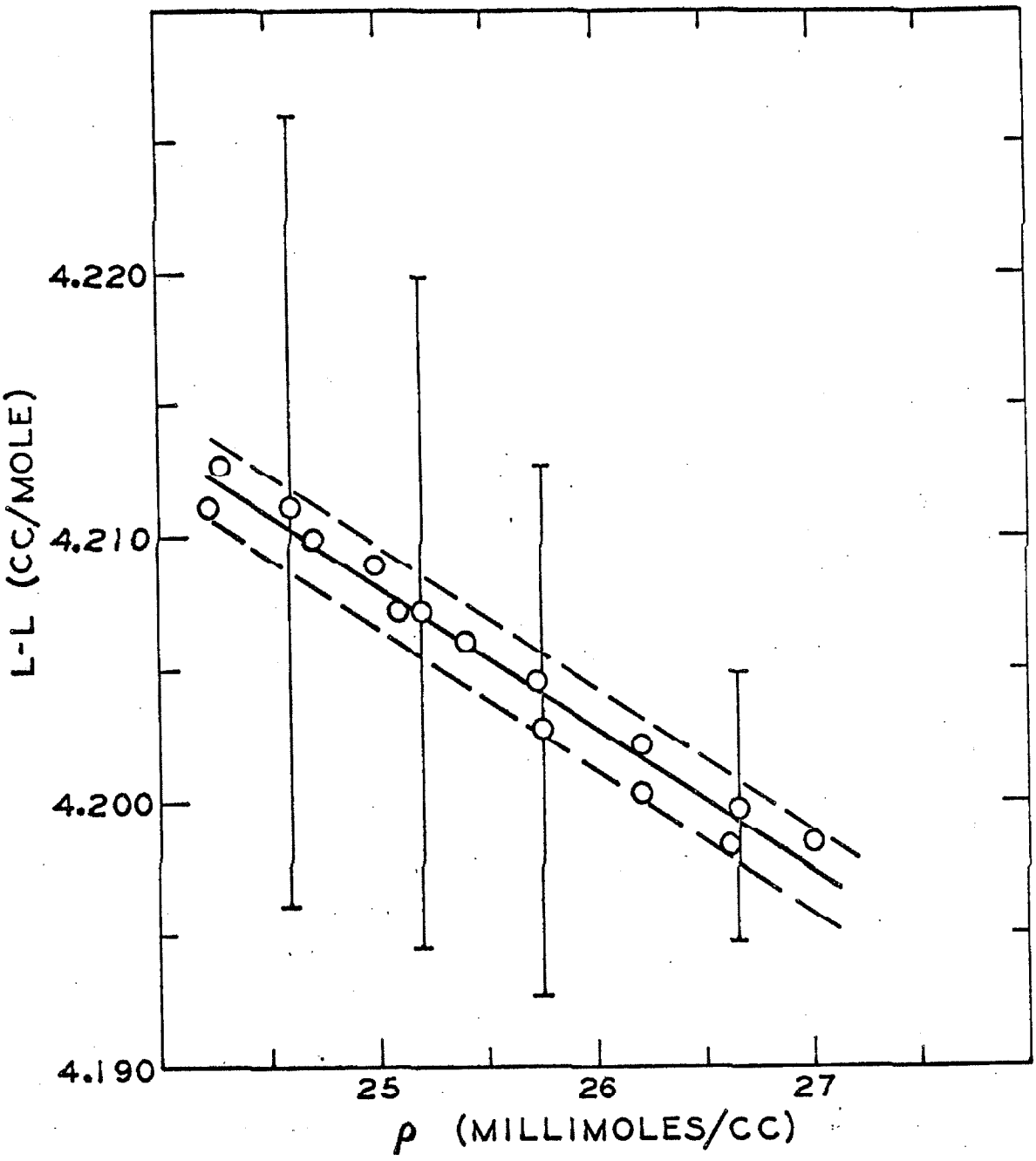

Figure 20

Lorentz-Lorenz Function for the Liquid Phase at 138°K

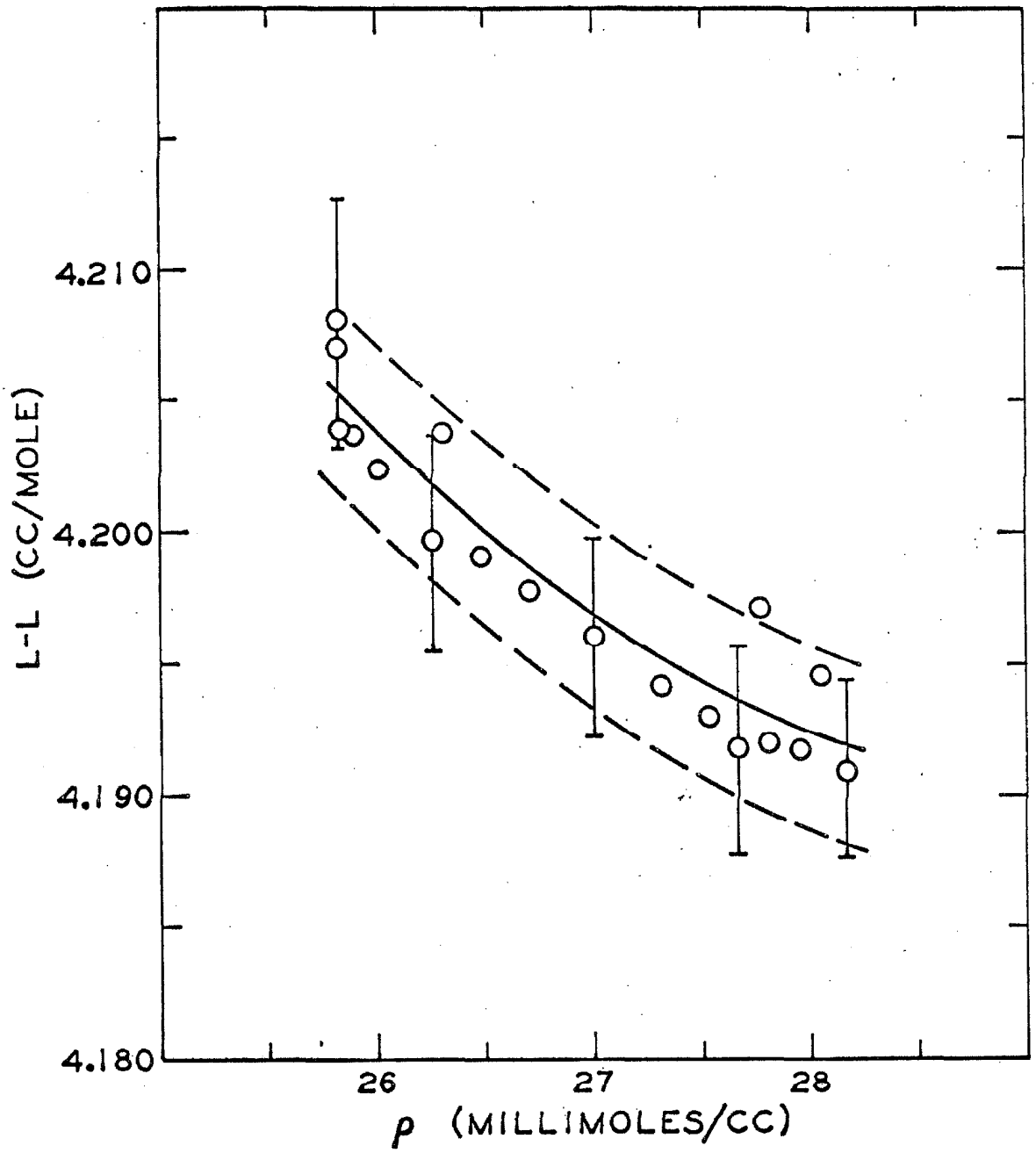

Figure 21

Lorentz-Lorenz Function for the Liquid Phase at 133°K

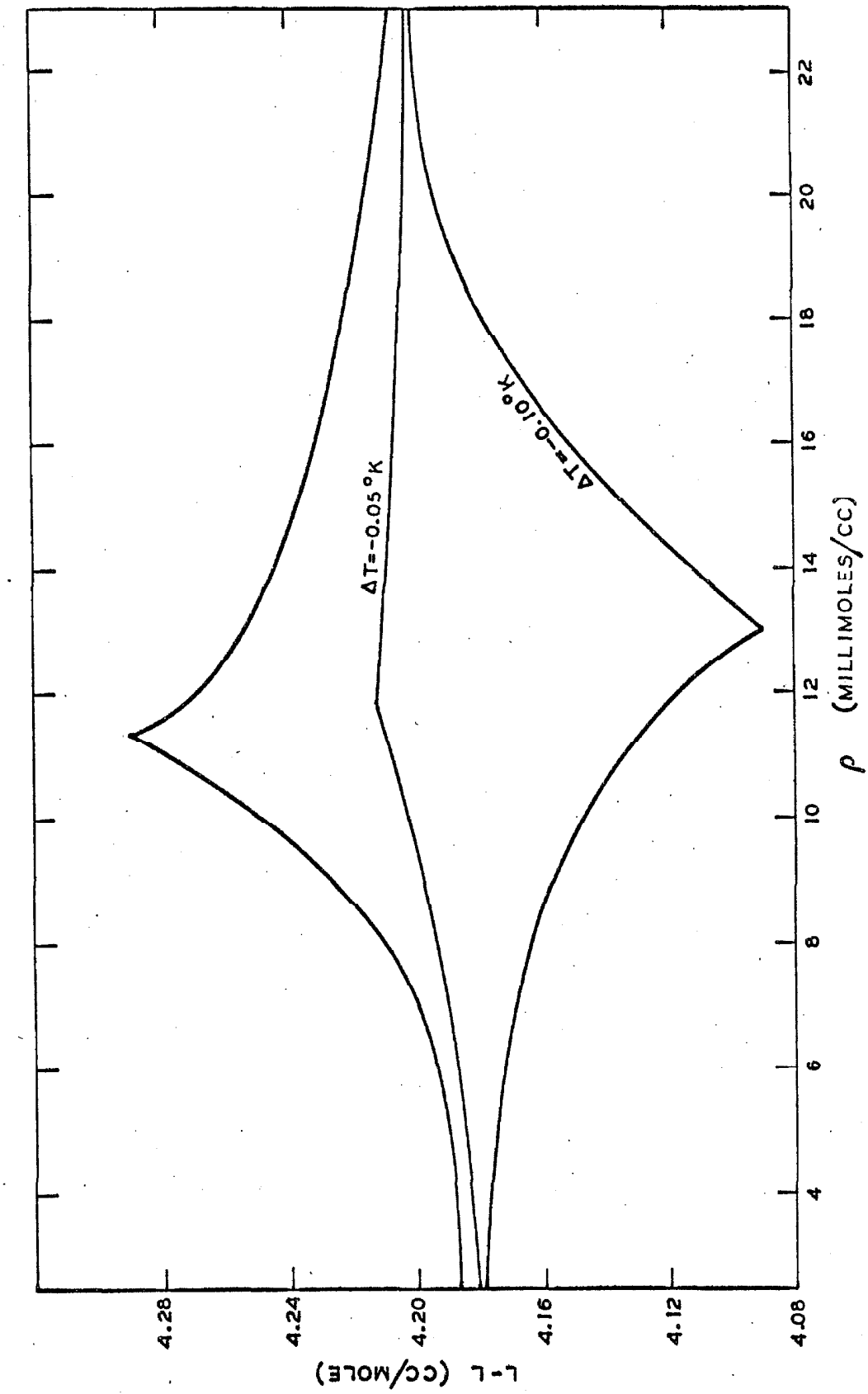

Figure 22

Variation of L - L Function with Temperature near the Critical Point

Table 1

Data for the Calculation of the Critical Coefficient

Temp ^{o}K	$T_c - T$ [a] ^{o}K	$\ell n T_c - T$	$\phi_L - \phi_G$ [b] $\times 10$	$\ell n \phi_L - \phi_G$
149.716	0.993	-0.0070	0.3435	-3.3712
149.979	0.730	-0.3147	0.3068	-3.4842
150.225	0.484	-0.7257	0.2591	-3.6532
149.805	0.904	-0.1009	0.3332	-3.4020
150.062	0.647	-0.4354	0.2946	-3.5249
150.194	0.515	-0.6636	0.2720	-3.6044
150.327	0.382	-0.9623	0.2450	-3.7093
150.450	0.259	-1.3509	0.2121	-3.8534
150.559	0.150	-1.8971	0.1747	-4.0473
149.733	0.976	-0.0243	0.3416	-3.3768
149.928	0.781	-0.2472	0.3151	-3.4573
150.121	0.588	-0.5310	0.2855	-3.5560
150.251	0.458	-0.7809	0.2623	-3.6407
150.513	0.196	-1.6296	0.1940	-3.9424
150.639	0.070	-2.6593	0.1296	-4.3461
150.667	0.042	-3.1701	0.1051	-4.5557
149.868	0.841	-0.1732	0.3241	-3.4292
150.155	0.554	-0.5906	0.2804	-3.5743
150.445	0.264	-1.3318	0.2127	-3.8505
150.548	0.161	-1.8263	0.1798	-4.0183

---

a $T_c = 150.709^{o}K$

b $\phi = n^2 - 1/n^2 + 2$

Table 1

Temp ^{o}K	$T_c - T$ ^{o}K	$\ell n T_c - T$	$\phi_L - \phi_G$ x 10	$\ell n \phi_L - \phi_G$
150.657	0.052	-2.9565	0.1173	-4.4455
150.683	0.026	-3.6496	0.08250	-4.7975
150.675	0.034	-3.3814	0.09604	-4.6456
150.697	0.012	-4.4228	0.05931	-5.1275
149.547	1.162	0.1501	0.3640	-3.3131
149.538	1.171	0.1579	0.3647	-3.3112
149.025	1.684	0.5212	0.4143	-3.1838
140.010	10.699	2.3702	0.8068	-2.5173
145.008	5.701	1.7406	0.6495	-2.7342
145.993	4.716	1.5510	0.6044	-2.8061
146.975	3.734	1.3175	0.5569	-2.8879
148.976	1.733	0.5499	0.4272	-3.1530
149.265	1.444	0.3674	0.4034	-3.2104
149.566	1.143	0.1337	0.3719	-3.2918
149.871	0.838	-0.1767	0.3352	-3.3957
149.976	0.733	-0.3106	0.3197	-3.4430
146.069	4.640	1.5347	0.6045	-2.8066
146.769	3.940	1.3712	0.5718	-2.8616
147.067	3.642	+1.2925	0.5563	-2.8890
147.367	3.342	1.2066	0.5428	-2.9137
147.770	2.939	1.0781	0.5158	-2.9646
148.068	2.641	0.9712	0.5004	-2.9949
148.269	2.440	0.8920	0.4850	-3.0261

Table 1

Temp ^{o}K	$T_c - T$ ^{o}K	$\ell n T_c - T$	$\phi_L - \phi_G$ x 10	$\ell n \phi_L - \phi_G$
148.476	2.233	0.8033	0.4696	-3.0585
148.668	2.041	0.7134	0.4567	-3.0862
149.180	1.529	0.4246	0.4023	-3.2132
149.662	1.047	0.0459	0.3693	-3.2988
147.745	2.964	1.0865	0.5081	-2.9796
148.512	2.197	0.7871	0.4554	-3.0891
146.961	3.748	1.3212	0.5518	-2.8971

Table 2

Fit of Data in Critical Region

Least Squares Fit of Data

$$\ell n(\phi_L - \phi_G) = \theta + \beta\, \ell n(T_c - T) + \theta_1 (T_c - T) + \theta_2 (T_c - T)^2$$

140 to 150.697°K		149 to 150.697°K	
Fit with: θ , β			
θ = -3.366		θ = -3.358	
β = 0.3752	σ_β = 0.00248	β = 0.3814	σ_β = 0.00402
σ_y = 0.0263		σ_y = 0.0281	
Fit with: θ, β, θ_1			
θ = -3.346		θ = -3.280	
β = 0.3853	σ_β = 0.00320	β = 0.4068	σ_β = 0.00587
θ_1 = -0.0105	σ_{θ_1} = 0.0025	θ_1 = -0.0876	σ_{θ_1} = 0.0176
σ_y = 0.0227		σ_y = 0.0203	
Fit with: $\theta, \beta, \theta_1, \theta_2$			
θ = -3.327		θ = -3.194	
β = 0.3925	σ_β = 0.00403	β = 0.4308	σ_2 = 0.00753
θ_1 = -0.0265	σ_{θ_1} = 0.00636	θ_1 = -0.277	σ_{θ_1} = 0.0489
θ_2 = 0.00148	σ_{θ_2} = 0.000549	θ_2 = 0.092	σ_{θ_2} = 0.0228
σ_y = 0.0214		σ_y = 0.016	

Table 3

Coefficients of the Equation

$$\ell n(\phi_L - \phi_G) = \theta + \beta \ell n(T_c - T) + \theta_1 (T_c - T) + \theta_2 (T_c - T)^2$$

	T_c+0.0[a]°K	+ 0.001	+ 0.002	+0.003	+0.004	+0.005	+0.006	+0.007	+0.008°K
θ	-3.327	-3.323	-3.318	-3.314	-3.310	-3.3067	-3.303	-3.300	-3.297
β	0.3925	0.3977	0.4027	0.4076	0.4123	0.4169	0.4213	0.4257	0.4299
θ_1	-0.0264	-0.0307	-0.0347	-0.0385	-0.0422	-0.0457	-0.0491	-0.0524	-0.0556
θ_2	0.00148	0.0017	0.00198	0.0022	0.0024	0.0026	0.0028	0.0039	0.0032
σ	0.02137	0.0231	0.0248	0.0265	0.0281	0.0297	0.0312	0.0327	0.0341
	T_c-0.0°K	-0.001	-0.002	-0.003	-0.004	-0.005	-0.006	-0.007	-0.008°K
θ	-3.327	-3.332	-3.337	-3.351	-3.353	-3.358	-3.357	-3.355	-3.386
β	0.3925	0.3870	0.3813	0.3725	0.3677	0.3609	0.3572	0.3531	0.3360
θ_1	-0.0264	-0.0220	-0.0172	-0.0057	-0.0038				0.0237
θ_2	0.00148	0.00121	0.0009						-0.0017
σ	0.0214	0.0197	0.0181	0.0170	0.0160	0.0161	0.0177	0.218	0.0259
Std. error of β									
	0.0040	0.0036	0.0033	0.0023	0.0022	0.0015	0.0016	0.0019	0.0042

a $T_c = 150.709$°K

Table 4

Refractive Index and Lorentz-Lorenz Function for Argon

Gas-Liquid Coexistence

Temp (^{o}K)	D_G (^{o})	n_G	ρ_G (moles/cc)	$(L-L)_G$ (cc/mole)	D_L (^{o})	n_L	ρ_L (moles/cc)	$(L-L)_L$ (cc/mole)
85.538					11.233	1.2312	0.03490	4.202 ± 0.10%
89.918					11.005	1.2266	0.03440	4.186 ± 0.10%
94.580					10.755	1.2216	0.03367	4.186 ± 0.10%
99.390					10.488	1.2162	0.03280	4.198 ± 0.11%
105.015					10.165	1.2096	0.03192	4.190 ± 0.11%
109.362					9.913	1.2046	0.03112	4.202 ± 0.12%
112.020	0.278	1.0060	0.000936	4.242 ± 2.5%	9.575	1.2015	0.03063	4.207 ± 0.12%
115.004	0.325	1.0068	0.001132	4.024 ± 2.4%	9.547	1.1972	0.03007	4.194 ± 0.12%
115.008	0.329	1.0070	0.001082	4.333 ± 2.4%	9.373	1.1973	0.03005	4.210 ± 0.12%
117.014	0.370	1.0079	0.001272	4.158 ± 2.2%	9.252	1.1948	0.02965	4.209 ± 0.12%
120.002	0.433	1.0091	0.001506	4.052 ± 2.0%	9.207	1.1902	0.029044	4.198 ± 0.04%
120.008	0.455	1.0097	0.001507	4.285 ± 2.0%	9.049	1.1906	0.029043	4.207 ± 0.04%

Table 4

Temp (°)	D_G (°)	n_G	ρ_G (moles/cc)	$(L-L)_G$ (cc/mole)	D_L (°)	n_L	ρ_L (moles/cc)	$(L-L)_L$ (cc/mole)
125.003	0.588	1.0122	0.001983	4.093 ± 1.4%	8.820	1.1824	0.027917	4.196 ± 0.05%
125.007	0.593	1.0127	0.001983	4.093 ± 1.4%	8.701	1.1834	0.027916	4.218 ± 0.05%
130.013	0.772	1.0162	0.002594	4.260 ± 1.4%	8.413	1.1741	0.026681	4.199 ± 0.05%
135.011	1.005	1.0211	0.003390	4.134 ± 0.82%	7.958	1.1648	0.025255	4.208 ± 0.06%
140.010	1.335	1.0279	0.004483	4.129 ± 0.51%	7.394	1.1534	0.023571	4.208 ± 0.07%
145.008	1.803	1.0378	0.006092	4.109 ± 0.49%	6.680	1.1387	0.021353	4.214 ± 0.10%
145.993	1.944	1.0415	0.006566	4.183 ± 0.49%	6.392	1.1354	0.020790	4.228 ± 0.12%
146.069	1.930	1.0412	0.006606	4.128 ± 0.50%	6.378	1.1351	0.020743	4.229 ± 0.12%
146.769	2.026	1.0433	0.006937	4.130 ± 0.50%	6.237	1.1321	0.020291	4.230 ± 0.14%
146.961	2.102	1.0449	0.007042	4.217 ± 0.50%	6.164	1.1306	0.020158	4.211 ± 0.14%
146.975	2.092	1.0447	0.007050	4.194 ± 0.50%	6.192	1.1312	0.020148	4.231 ± 0.14%
147.067	2.087	1.0446	0.007104	4.153 ± 0.50%	6.182	1.1310	0.020083	4.239 ± 0.14%
147.745	2.248	1.0480	0.007548	4.203 ± 0.53%	5.985	1.1269	0.019565	4.219 ± 0.16%
147.770	2.228	1.0476	0.007566	4.159 ± 0.53%	6.025	1.1277	0.019545	4.249 ± 0.16%
148.269	2.321	1.0495	0.007954	4.112 ± 0.55%	5.884	1.1248	0.019123	4.247 ± 0.18%

Table 4

Temp (°)	D_G (°)	n_G	ρ_G (moles/cc)	$(L-L)_G$ (cc/mole)	D_L (°)	n_L	ρ_L (moles/cc)	$(L-L)_L$ (cc/mole)
148.476	2.375	1.0507	0.008130	4.120 ± 0.56%	5.832	1.1236	0.018939	4.248 ± 0.18%
148.512	2.420	1.0516	0.00161	4.176 ± 0.56%	5.769	1.1223	0.018906	4.212 ± 0.18%
148.668	2.413	1.0515	0.008300	4.099 ± 0.56%	5.773	1.1224	0.018762	4.247 ± 0.19%
148.976	2.495	1.0532	0.008588	4.090 ± 0.59%	5.634	1.1195	0.018470	4.215 ± 0.22%
149.025	2.557	1.0545	0.008636	4.166 ± 0.60%	5.602	1.1188	0.018422	4.202 ± 0.23%
149.265	2.584	1.0551	0.008876	4.098 ± 0.68%	5.550	1.1177	0.018182	4.219 ± 0.26%
149.538	2.731	1.0582	0.009163	4.190 ± 0.75%	5.413	1.1148	0.017834	4.198 ± 0.30%
149.547	2.737	1.0584	0.009173	4.200 ± 0.75%	5.414	1.1149	0.017821	4.205 ± 0.30%
149.716	2.794	1.0596	0.009330	4.213 ± 0.76%	5.322	1.1129	0.017557	4.195 ± 0.35%
149.733	2.805	1.0598	0.009342	4.222 ± 0.81%	5.317	1.1128	0.017528	4.199 ± 0.35%
149.805	2.827	1.0603	0.009408	4.227 ± 0.83%	5.275	1.1120	0.017403	4.200 ± 0.37%
149.868	2.876	1.0613	0.009481	4.263 ± 0.84%	5.256	1.1116	0.017289	4.212 ± 0.39%
149.928	2.901	1.0618	0.009565	4.259 ± 0.86%	5.215	1.1107	0.017175	4.207 ± 0.41%
149.979	2.928	1.0624	0.009647	4.264 ± 0.86	5.183	1.1100	0.017075	4.206 ± 0.42%
150.062	2.966	1.0632	0.009802	4.249 ± 0.88	5.129	1.1089	0.016905	4.206 ± 0.46%

Table 4

Temp (°K)	D_G (°)	n_G	ρ_G (moles/cc)	$(L\text{-}L)_G$ (cc/mole)	D_L (°)	n_L	ρ_L (moles/cc)	$(L\text{-}L)_L$ (cc/mole)
150.121	3.000	1.0639	0.009928	4.241 ± 0.94%	5.097	1.1082	0.016780	4.211 ± 0.50%
150.155	3.025	1.0645	0.010007	4.247 ± 0.98%	5.088	1.1080	0.016705	4.222 ± 0.52%
150.194	3.037	1.0647	0.010102	4.220 ± 1.02%	5.036	1.1069	0.016618	4.202 ± 0.55%
150.225	3.102	1.0661	0.010182	4.276 ± 1.06%	5.006	1.1063	0.016547	4.197 ± 0.58%
150.251	3.084	1.0657	0.010252	4.222 ± 1.08%	5.010	1.1064	0.016487	4.216 ± 0.59%
150.327	3.139	1.0669	0.010472	4.208 ± 1.16%	4.938	1.1049	0.016306	4.204 ± 0.65%
150.445	3.265	1.0696	0.010900	4.203 ± 1.26%	4.832	1.1026	0.015973	4.200 ± 0.74%
150.450	3.264	1.0695	0.010910	4.193 ± 1.26%	4.819	1.1024	0.015954	4.197 ± 0.75%
150.513	3.329	1.0709	0.011121	4.195 ± 1.32%	4.755	1.1010	0.015716	4.203 ± 0.80%
150.548	3.380	1.0720	0.011269	4.204 ± 1.34%	4.700	1.0999	0.015584	4.194 ± 0.83%
150.559	3.390	1.0722	0.011315	4.198 ± 1.35%	4.674	1.0993	0.015543	4.180 ± 0.84%
150.639	3.562	1.0758	0.011652	4.277 ± 1.40%	4.510	1.0959	0.015241	4.120 ± 1.42#
150.657	3.613	1.0769	0.011728	4.310 ± 1.79%	4.473	1.0951	0.015173	4.104 ± 1.62%
150.667	3.650	1.0777	0.011771	4.338 ± 2.01%	4.420	1.0940	0.015136	4.068 ± 1.73%
150.675	3.696	1.0787	0.011804	4.381 ± 2.19%	4.401	1.0936	0.015105	4.059 ± 1.82%

Table 4

Temp (^{o}K)	D_G (^{o})	n_G	ρ_G (moles/cc)	$(L-L)_G$ (cc/mole)	D_L (^{o})	n_L	ρ_L (moles/cc)	$(L-L)_L$ (cc/mole)
150.683	3.745	1.0797	0.011838	4.423 ± 2.36%	4.352	1.0925	0.015075	4.020 ± 1.91%
150.697	3.805	1.0810	0.011897	4.472 ± 2.66%	4.244	1.0902	0.015022	3.936 ± 2.06%

Table 5

L-L Values Calculated for Levelt's Densities

Gas-Liquid Coexistence

$T_c - T$ (°K)	n^2-1/n^2+2	ρ(moles/cc)	L-L(cc/mole)
Gas			
0.0	0.0564	0.013412	4.202
0.056	0.0502	0.012348	4.066
0.385	0.0441	0.010961	4.023
1.200	0.0381	0.009296	4.093
2.674	0.0322	0.007887	4.086
4.725	0.0272	0.006641	4.090
8.057	0.0217	0.005297	4.093
11.697	0.0175	0.004266	4.097
15.879	0.0139	0.003385	4.099
20.750	0.0107	0.002608	4.101
24.813	0.0086	0.002099	4.102
30.533	0.0063	0.001533	4.120
Liquid			
0.0	0.0564	0.013412	4.202
0.096	0.0638	0.014770	4.319
0.446	0.0694	0.016090	4.315
1.190	0.0751	0.017632	4.260
1.612	0.0774	0.018200	4.250
2.836	0.0823	0.019334	4.256
4.544	0.0873	0.020585	4.243

Table 5

$T_c - T$	n^2-1/n^2+2	ρ(moles/cc)	L-L(cc/mole)
6.415	0.0917	0.021633	4.238
10.431	0.0990	0.023407	4.229
14.085	0.1043	0.024706	4.222
19.250	0.1107	0.026247	4.217
25.806	0.1175	0.027905	4.211
34.040	0.1249	0.029700	4.205

Table 6

Smoothed Values of Refractive Index

Gas-Liquid Coexistence

T(°K)	n_G	n_L
120	1.0096	1.1903
121	1.0101	1.1888
122	1.0107	1.1874
123	1.0113	1.1859
124	1.0119	1.1843
125	1.0126	1.1828
126	1.0133	1.1812
127	1.0140	1.1795
128	1.0147	1.1779
129	1.0155	1.1762
130	1.0164	1.1744
131	1.0172	1.1726
132	1.0182	1.1708
133	1.0191	1.1689
134	1.0202	1.1670
135	1.0213	1.1650
136	1.0224	1.1629
137	1.0237	1.1607
138	1.0250	1.1585
139	1.0264	1.1562
140	1.0280	1.1537
141	1.0296	1.1511

Table 6

$T(^{o}K)$	n_G	n_L
142	1.0315	1.1484
143	1.0335	1.1455
144	1.0357	1.1423
145	1.0382	1.1389
146	1.0410	1.1351
147	1.0444	1.1308
148	1.0486	1.1258
149	1.0540	1.1194
150	1.0624	1.1100
150.2	1.0650	1.1072
150.4	1.0685	1.1035
150.6	1.0741	1.0978

Table 7

Refractive Index and Lorentz-Lorenz Function

One Phase Isotherms

P(atm.)	D(°)	n	ρ(moles/cc)	L-L(cc/mole)
Run No. 14	173.149°K			
32.530	0.807	1.0173	0.002736	4.196 ± 0.67%
35.885	0.911	1.0195	0.003088	4.192 ± 0.62%
39.511	1.031	1.0221	0.003490	4.198 ± 0.57%
42.851	1.147	1.0245	0.003882	4.194 ± 0.53%
46.496	1.284	1.0274	0.004337	4.200 ± 0.50%
49.867	1.418	1.0303	0.004785	4.202 ± 0.47%
53.425	1.569	1.0335	0.005291	4.200 ± 0.45%
56.542	1.713	1.0366	0.005766	4.204 ± 0.44%
60.208	1.893	1.0404	0.006366	4.204 ± 0.42%
62.675	2.024	1.0432	0.006798	4.205 ± 0.42%
66.625	2.250	1.0480	0.007542	4.210 ± 0.41%
73.921	2.723	1.0581	0.009096	4.212 ± 0.40%
79.477	3.131	1.0667	0.010426	4.215 ± 0.40%
86.443	3.672	1.0782	0.012183	4.216 ± 0.38%
93.075	4.162	1.0885	0.013777	4.214 ± 0.34%
97.431	4.452	1.0946	0.014711	4.214 ± 0.31%
101.446	4.690	1.0997	0.015478	4.213 ± 0.29%
Run No. 21	173.083°K			
14.831	0.330	1.0071	0.001123	4.196 ± 1.43%
18.541	0.422	1.0090	0.001432	4.195 ± 1.15%

Table 7

P(atm.)	D(°)	n	ρ(moles/cc)	L-L(cc/mole)
25.600	0.607	1.0130	0.002061	4.194 ± 0.84%
32.510	0.806	1.0173	0.002736	4.194 ± 0.67%
39.518	1.031	1.0221	0.003494	4.194 ± 0.57%
49.088	1.387	1.0297	0.004683	4.200 ± 0.48%
Run No. 13	163.156°K			
25.873	0.672	1.0144	0.002291	4.177 ± 0.78%
28.821	0.768	1.0164	0.002616	4.177 ± 0.71%
32.136	0.883	1.0189	0.003004	4.179 ± 0.64%
36.072	1.031	1.0221	0.003504	4.181 ± 0.58%
38.990	1.151	1.0246	0.003905	4.184 ± 0.54%
42.699	1.317	1.0282	0.004462	4.187 ± 0.51%
46.000	1.480	1.0316	0.005011	4.186 ± 0.49%
48.880	1.641	1.0351	0.005542	4.193 ± 0.48%
52.015	1.834	1.0392	0.006187	4.194 ± 0.47%
53.945	1.969	1.0421	0.006626	4.200 ± 0.47%
56.315	2.148	1.0459	0.007221	4.200 ± 0.47%
58.433	2.329	1.0497	0.007813	4.204 ± 0.48%
60.471	2.527	1.0539	0.008448	4.214 ± 0.50%
62.554	2.750	1.0586	0.009175	4.217 ± 0.52%
64.041	2.930	1.0625	0.009747	4.224 ± 0.53%
67.503	3.414	1.0727	0.011261	4.248 ± 0.56%
68.852	3.592	1.0765	0.011905	4.223 ± 0.56%
70.535	3.840	1.0817	0.012722	4.218 ± 0.54%
71.642	4.000	1.0851	0.013251	4.214 ± 0.53%

Table 7

P(atm.)	D(°)	n	ρ(moles/cc)	L-L(cc/mole)
73.232	4.219	1.0897	0.013974	4.210 ± 0.50%
74.492	4.380	1.0931	0.014506	4.205 ± 0.47%
80.846	5.028	1.1068	0.016583	4.206 ± 0.34%
83.636	5.236	1.1111	0.017245	4.206 ± 0.30%
86.776	5.435	1.1153	0.017870	4.208 ± 0.27%
90.361	5.626	1.1193	0.018470	4.209 ± 0.24%
Run No. 20	163.095°K			
18.771	0.463	1.0099	0.001575	4.191 ± 1.06%
22.199	0.562	1.0120	0.001910	4.187 ± 0.90%
28.796	0.770	1.0165	0.002615	4.188 ± 0.70%
32.483	0.898	1.0192	0.003049	4.188 ± 0.63%
36.040	1.032	1.0221	0.003502	4.188 ± 0.58%
39.037	1.156	1.0247	0.003915	4.192 ± 0.54%
47.361	1.559	1.0333	0.005262	4.196 ± 0.48%
51.015	1.775	1.0379	0.005981	4.198 ± 0.47%
53.949	1.972	1.0421	0.006639	4.199 ± 0.47%
66.430	3.280	1.0699	0.010807	4.256 ± 0.56%
67.608	3.457	1.0736	0.011354	4.265 ± 0.56%
92.934	5.758	1.1221	0.018875	4.212 ± 0.23%
96.092	5.888	1.1248	0.019284	4.212 ± 0.21%
100.230	6.038	1.1280	0.019756	4.212 ± 0.20%
103.814	6.154	1.1304	0.020119	4.212 ± 0.19%
Run No. 12	153.163°K			
20.196	0.552	1.0118	0.001886	4.168 ± 0.92%

Table 7

P(atm.)	D(°)	n	ρ(moles/cc)	L-L(cc/mole)
27.423	0.815	1.0174	0.002769	4.185 ± 0.69%
30.598	0.947	1.0203	0.003217	4.184 ± 0.62%
33.476	1.080	1.0231	0.003666	4.183 ± 0.58
37.192	1.277	1.0273	0.004329	4.184 ± 0.55%
42.177	1.606	1.0343	0.005445	4.178 ± 0.53%
43.928	1.754	1.0375	0.005937	4.179 ± 0.55%
44.809	1.838	1.0393	0.006215	4.182 ± 0.56%
45.584	1.919	1.0410	0.006481	4.185 ± 0.57%
46.594	2.034	1.0434	0.006865	4.186 ± 0.60%
47.447	2.145	1.0458	0.007232	4.187 ± 0.63%
48.218	2.258	1.0482	0.007608	4.186 ± 0.68%
49.002	2.395	1.0511	0.008050	4.194 ± 0.75%
49.600	2.517	1.0537	0.008443	4.200 ± 0.82%
50.302	2.707	1.0577	0.008996	4.234 ± 0.94%
50.749	2.840	1.0606	0.009423	4.238 ± 1.09%
51.388	3.099	1.0660	0.010205	4.263 ± 1.40%
51.838	3.352	1.0714	0.010972	4.282 ± 1.78%
52.040	3.497	1.0745	0.011418	4.290 ± 2.02%
52.238	3.639	1.0775	0.011949	4.261 ± 2.32%
52.453	3.857	1.0821	0.012645	4.262 ± 2.61%
55.980	5.376	1.1141	0.017645	4.217 ± 0.54%
57.771	5.620	1.1192	0.018416	4.217 ± 0.41%
59.356	5.783	1.1226	0.018923	4.219 ± 0.35%
61.197	5.932	1.1257	0.019395	4.218 ± 0.30%
62.752	6.036	1.1279	0.019730	4.216 ± 0.26%

Table 7

P(atm.)	D(°)	n	ρ(moles/cc)	L-L(cc/mole)
66.195	6.226	1.1319	0.020337	4.214 ± 0.23%
69.418	6.369	1.1349	0.020796	4.212 ± 0.21%
74.560	6.556	1.1388	0.021392	4.209 ± 0.18%
79.562	6.703	1.1419	0.021867	4.206 ± 0.17%
86.284	6.872	1.1454	0.022401	4.204 ± 0.16%
92.199	6.998	1.1480	0.022802	4.203 ± 0.15%
Run No. 22	153.107°K			
24.416	0.701	1.0150	0.002384	4.188 ± 0.76%
27.363	0.814	1.0174	0.002763	4.192 ± 0.69%
28.552	0.862	1.0184	0.002926	4.192 ± 0.66%
30.830	0.962	1.0206	0.003254	4.199 ± 0.62%
33.598	1.091	1.0233	0.003690	4.200 ± 0.58%
37.161	1.280	1.0274	0.004328	4.195 ± 0.54%
44.258	1.800	1.0384	0.006052	4.208 ± 0.55%
45.576	1.935	1.0413	0.006494	4.212 ± 0.57%
46.750	2.076	1.0443	0.006949	4.219 ± 0.60%
74.706	6.583	1.1394	0.021433	4.218 ± 0.18%
86.211	6.888	1.1457	0.022417	4.211 ± 0.16%
92.570	7.022	1.1485	0.022845	4.208 ± 0.14%
103.050	7.209	1.1524	0.023439	4.206 ± 0.13%
Run No. 15	150.665°K			
22.078	0.635	1.0136	0.002163	4.183 ± 0.83%
25.422	0.761	1.0163	0.002591	4.181 ± 0.72%
28.888	0.908	1.0194	0.003082	4.190 ± 0.65%

Table 7

P(atm.)	D(°)	n	ρ(moles/cc)	L-L(cc/mole)
31.186	1.015	1.0217	0.003442	4.190 ± 0.61%
33.824	1.150	1.0246	0.003900	4.188 ± 0.57%
36.587	1.316	1.0281	0.004448	4.195 ± 0.55%
38.948	1.478	1.0316	0.004995	4.195 ± 0.55%
41.414	1.684	1.0360	0.005685	4.193 ± 0.57%
43.907	1.960	1.0419	0.006604	4.195 ± 0.64%
45.036	2.127	1.0454	0.007161	4.194 ± 0.71%
46.323	2.389	1.0510	0.008029	4.196 ± 0.97%
47.479	2.817	1.0601	0.009403	4.212 ± 1.62%
47.698	2.991	1.0638	0.009844	4.269 ± 1.89%
47.844	3.182	1.0678	0.010204	4.376 ± 2.10%
47.922	3.403	1.0725	0.010419	4.577 ± 2.21%
47.933	3.448	1.0734	0.010448	4.624 ± 2.22%
48.615	5.294	1.1124	0.017289	4.241 ± 1.36%
49.031	5.433	1.1153	0.017762	4.232 ± 0.83%
50.072	5.650	1.1198	0.018489	4.222 ± 0.56%
50.867	5.769	1.1223	0.018870	4.221 ± 0.48%
52.006	5.900	1.1251	0.019295	4.218 ± 0.38%
53.395	6.028	1.1278	0.019703	4.217 ± 0.31%
55.219	6.162	1.1306	0.020131	4.215 ± 0.28%
57.900	6.319	1.1338	0.020631	4.213 ± 0.24%
61.139	6.472	1.1370	0.021113	4.212 ± 0.21%
64.780	6.612	1.1400	0.021557	4.211 ± 0.19%
69.057	6.753	1.1429	0.021993	4.212 ± 0.17%
73.321	6.869	1.1453	0.022366	4.209 ± 0.16%

Table 7

P(atm.)	D(°)	n	ρ(moles/cc)	L-L(cc/mole)
78.218	6.986	1.1478	0.022738	4.208 ± 0.15%
83.623	7.101	1.1502	0.023100	4.207 ± 0.14%
88.956	7.200	1.1522	0.023417	4.205 ± 0.14%
94.093	7.289	1.1541	0.023694	4.205 ± 0.13%
100.714	7.393	1.1563	0.024018	4.204 ± 0.13%
Run No. 24	150.665			
22.637	0.656	1.0140	0.002231	4.189 ± 0.81%
31.219	1.016	1.0217	0.003448	4.187 ± 0.61%
33.789	1.150	1.0246	0.003894	4.192 ± 0.57%
44.756	2.083	1.0445	0.007010	4.196 ± 0.69%
45.831	2.281	1.0487	0.007654	4.204 ± 0.85%
46.425	2.424	1.0517	0.008116	4.210 ± 1.01%
47.162	2.675	1.0570	0.008911	4.224 ± 1.35%
50.387	5.716	1.1212	0.018651	4.233 ± 0.53%
52.008	5.909	1.1253	0.019295	4.224 ± 0.38%
55.220	6.165	1.1306	0.020132	4.217 ± 0.28%
57.976	6.325	1.1340	0.020644	4.214 ± 0.24%
73.407	6.865	1.1452	0.022373	4.206 ± 0.16%
Run No. B-3				
21.877	0.641	1.0137	0.002203	4.145 ± 0.82%
23.985	0.723	1.0155	0.002481	4.149 ± 0.75%
25.985	0.792	1.0169	0.002706	4.162 ± 0.71%
27.436	0.871	1.0186	0.002979	4.157 ± 0.67%
29.618	0.976	1.0209	0.003329	4.167 ± 0.62%

Table 7

P(atm.)	D (°)	n	ρ(moles/cc)	L-L(cc/mole)
31.844	1.096	1.0234	0.003723	4.179 ± 0.59%
34.266	1.240	1.0265	0.004208	4.183 ± 0.57%
35.904	1.352	1.0289	0.004580	4.187 ± 0.57%
37.585	1.486	1.0318	0.005016	4.198 ± 0.57%
39.212	1.636	1.0350	0.005513	4.203 ± 0.58%
40.653	1.798	1.0384	0.006049	4.204 ± 0.62%
42.183	2.039	1.0435	0.006802	4.234 ± 0.69%
43.235	2.294	1.0490	0.007577	4.270 ± 0.83%
43.774	5.988	1.1269	0.019372	4.261 ± 0.42%
44.945	6.118	1.1296	0.019854	4.245 ± 0.36%
45.914	6.205	1.1314	0.020156	4.238 ± 0.33%
47.385	6.314	1.1338	0.020525	4.232 ± 0.29%
49.036	6.416	1.1359	0.020863	4.228 ± 0.26%
51.418	6.538	1.1384	0.021263	4.224 ± 0.22%
53.158	6.613	1.1400	0.021512	4.220 ± 0.20%
56.554	6.743	1.1427	0.021927	4.218 ± 0.19%
60.179	6.859	1.1451	0.022301	4.216 ± 0.17%
63.834	6.958	1.1492	0.022626	4.212 ± 0.16%
67.766	7.056	1.1492	0.022936	4.211 ± 0.15%
73.152	7.170	1.1516	0.023710	4.208 ± 0.14%
79.841	7.296	1.1542	0.023710	4.205 ± 0.14%
86.620	7.408	1.1566	0.024068	4.203 ± 0.13%
95.826	7.548	1.1595	0.024495	4.204 ± 0.12%
103.606	7.643	1.1615	0.024815	4.200 ± 0.12%

Table 7

P(atm.)	D(°)	n	ρ(moles/cc)	L-L(cc/mole)
Run No. 19	148.123°K			
50.221	6.488	1.1374	0.021114	4.222 ± 0.24%
68.912	7.088	1.1499	0.023041	4.210 ± 0.15%
Run No. 18	143.170°K			
17.898	0.534	1.0114	0.001822	4.178 ± 0.95%
21.366	0.670	1.0144	0.002281	4.184 ± 0.80%
26.691	0.918	1.0196	0.003114	4.190 ± 0.66%
32.058	1.255	1.0268	0.004242	4.197 ± 0.59%
34.604	1.485	1.0317	0.005007	4.203 ± 0.60%
38.486	6.978	1.1476	0.022605	4.228 ± 0.17%
42.213	7.094	1.1500	0.023007	4.220 ± 0.16%
47.068	7.234	1.1529	0.023432	4.221 ± 0.15%
47.415	7.232	1.1529	0.023459	4.215 ± 0.15%
50.600	7.316	1.1546	0.023696	4.219 ± 0.15%
53.054	7.357	1.1555	0.023864	4.212 ± 0.14%
59.162	7.474	1.1579	0.024236	4.209 ± 0.14%
65.968	7.593	1.1604	0.024597	4.210 ± 0.13%
67.524	7.610	1.1608	0.024673	4.206 ± 0.12%
76.119	7.731	1.1633	0.025060	4.204 ± 0.12%
84.553	7.840	1.1656	0.025395	4.204 ± 0.11%
94.454	7.950	1.1678	0.025748	4.201 ± 0.11%
102.599	8.034	1.1696	0.026011	4.200 ± 0.11%
Run No. 9	138.173°K			
28.769	7.475	1.1580	0.024229	4.211 ± 0.41%

Table 7

P(atm.)	D(°)	n	ρ(moles/cc)	L-L(cc/mole)
34.362	7.596	1.1605	0.024601	4.211 ± 0.37%
43.502	7.752	1.1637	0.025104	4.207 ± 0.31%
57.310	7.947	1.1678	0.025717	4.204 ± 0.24%
70.978	8.105	1.1711	0.026215	4.202 ± 0.18%
85.178	8.245	1.1740	0.026659	4.200 ± 0.12%
96.696	8.347	1.1761	0.026978	4.198 ± 0.10%
Run No. 17	138.173°K			
18.536	0.596	1.0128	0.002030	4.180 ± 0.88%
22.787	0.793	1.0170	0.002695	4.185 ± 0.73%
25.554	0.948	1.0203	0.003217	4.188 ± 0.67%
28.057	1.122	1.0240	0.003795	4.198 ± 0.64%
29.321	7.491	1.1583	0.024269	4.213 ± 0.40%
35.823	7.622	1.1610	0.024689	4.210 ± 0.36%
41.102	7.716	1.1630	0.024982	4.209 ± 0.32%
45.022	7.776	1.1642	0.025179	4.207 ± 0.30%
49.667	7.845	1.1657	0.025395	4.206 ± 0.28%
57.870	7.950	1.1678	0.025739	4.203 ± 0.24%
70.886	8.100	1.1710	0.026212	4.200 ± 0.18%
83.059	8.222	1.1735	0.026596	4.198 ± 0.13%
102.230	8.385	1.1769	0.027120	4.194 ± 0.10%
Run No. 10	133.176°K			
23.376	7.985	1.1686	0.025813	4.208 ± 0.11%
34.486	8.133	1.1716	0.026290	4.204 ± 0.11%
83.064	8.590	1.1811	0.027724	4.197 ± 0.10%

Table 7

P(atm.)	D(°)	n	ρ(moles/cc)	L-L(cc/mole)
97.871	8.694	1.1833	0.028056	4.194 ± 0.09%
Run No. 16	133.176°K			
11.982	0.370	1.0079	0.001264	4.172 ± 1.31%
14.253	0.456	1.0098	0.001557	4.173 ± 1.10%
16.527	0.550	1.0118	0.001877	4.176 ± 0.94%
18.525	0.642	1.0138	0.002187	4.184 ± 0.84%
20.070	0.720	1.0154	0.002450	4.180 ± 0.78%
22.628	0.868	1.0186	0.002949	4.187 ± 0.70%
23.088	7.979	1.1684	0.025799	4.207 ± 0.11%
23.534	7.980	1.1685	0.025821	4.204 ± 0.11%
24.546	7.995	1.1688	0.025868	4.204 ± 0.11%
27.153	8.031	1.1695	0.025987	4.202 ± 0.11%
33.779	8.115	1.1713	0.026262	4.200 ± 0.11%
38.176	8.169	1.1724	0.026429	4.199 ± 0.11%
45.784	8.253	1.1741	0.026694	4.198 ± 0.10%
55.657	8.350	1.1762	0.027003	4.196 ± 0.10%
66.015	8.442	1.1781	0.027295	4.194 ± 0.10%
74.843	8.515	1.1796	0.027524	4.193 ± 0.10%
80.483	8.558	1.1805	0.027663	4.192 ± 0.10%
86.566	8.606	1.1814	0.027965	4.192 ± 0.10%
93.657	8.658	1.1825	0.027965	4.192 ± 0.09%
103.025	8.722	1.1838	0.028165	4.191 ± 0.09%

Table 8

Refractive Index

T°K	173.147	163.156	153.163	150.665	148.166	143.170	138.173	133.176
P(atm)								
10								
15	1.0072							1.0104
20	1.0097	1.0107	1.0117	1.0120	1.0136	1.0132	1.0141	1.0153
25	1.0126	1.0138	1.0154	1.0152	1.0162	1.0178	1.0196	1.1690
30	1.0157	1.0173	1.0197	1.0205	1.0216	1.0237	1.1586	1.1703
35	1.0189	1.0212	1.0248	1.0260	1.0274	1.1193	1.1607	1.1716
40	1.0225	1.0256	1.0310	1.0334	1.0369	1.1486	1.1626	1.1729
45	1.0262	1.0306	1.0398	1.0438	1.1295	1.1517	1.1653	1.1740
50	1.0304	1.0367	1.0586	1.1189	1.1370	1.1542	1.1658	1.1750
55	1.0350	1.0436	1.0982	1.1306	1.1418	1.1564	1.1671	1.1760
60	1.0402	1.0529	1.1235	1.1364	1.1451	1.1583	1.1684	1.1770
65	1.0461	1.0652	1.1349	1.1399	1.1477	1.1600	1.1696	1.1779
70	1.0526	1.0799	1.1367	1.1429	1.1501	1.1616	1.1708	1.1788

Table 8

$T^{o}K$	173.147	163.156	153.163	150.665	148.166	143.170	138.173	133.176
P(atm)								
75	1.0598	1.0947	1.1364	1.1460	1.1523	1.1630	1.1719	1.1796
80	1.0676	1.1056	1.1425	1.1490	1.1544	1.1644	1.1729	1.1805
85	1.0756	1.1130	1.1450	1.1513	1.1563	1.1657	1.1739	1.1813
90	1.0837	1.1191	1.1472	1.1527	1.1578	1.1668	1.1749	1.1821
95	1.0912	1.1239	1.1493	1.1537	1.1591	1.1680	1.1758	1.1828
100	1.0980	1.1276	1.1511	1.1558	1.1604	1.1690	1.1766	1.1835

APPENDIX A

DETERMINATION OF THE PRISM ANGLE

The prism angle A was determined indirectly from the angle of minimum deviation D for water. Many attempts to measure the angle A directly with a Gauss eyepiece were unsatisfactory. The reflection from the small (1/4" diameter) cell windows was too faint for reproducible results. Attempts were also made to determine the pressure and temperature dependence of the prism angle; no dependence was detected.

Special techniques had to be employed with the Gaertner L114 Spectrometer to achieve results for water with acceptable precision. The spectrometer has a graduated circle and vernier that gives readings to 0.33'. For measurements from 1 to 5^{o}, a micrometer tangent screw accurate to 0.02' can be used. In order to make use of the micrometer accuracy over a wider range, a special procedure was established.

After the telescope was moved until the illuminated slit was in the field of view, the micrometer screw was clamped to the base. The final adjustment was made with the micrometer. This reading was noted and was listed as V. Then looking through a microscope mounted above the graduated circle, the micrometer was advanced until an even degree was opposite 0 of the graduated circle vernier. The even degree and the new reading on the micrometer were noted as C and V_0 respectively. The difference V_0 - V was subtracted from C to find the original position of the telescope. This procedure increased the

reproductbility of the data by 3 to 4 times. Comparison checks show that the graduations on the micrometer tangent screw are compatible with the graduated circle.

The values for the angle of minimum deviation for water are given to illustrate the procedure. The spectrometer instrument zero refers to the spectrometer reading for the empty cell. This was measured before each set of data and in the case of water before and after the measurement.

Instrument Zero		Test No. 5
V	$= 0^{\circ}\ 46.13'$	variance, $\sigma^2 = 19 \times 10^{-41}$
V_0	$= 1^{\circ}\ 34.96'$	variance, $\sigma^2 = 64 \times 10^{-41}$
C	$= 105^{\circ}$	

Inst. Zero $= 104^{\circ}\ 11.17'$

Angle of minimum deviation for water

V	$= 0^{\circ}\ 47.11'$	$\sigma^2 = 19 \times 10^{-41}$
V_0	$= 1^{\circ}\ 33.16'$	$\sigma^2 = 64 \times 10^{-41}$ *
C	$= 121^{\circ}$	
$H_2O_{(20^{\circ})}$	$= 120^{\circ}\ 13.96'$	
D_{H_2O}	$= 16^{\circ}\ 2.79'$	$= 166 \times 10^{-41}$

From D_{H_2O} and the refractive index of H_2O at 20° it was possible to calculate the prism angle of the cell.

$n_{H_2O} = 1.33300 \pm 0.00002$ at 20.0 ± 0.2 C[35]

A $= 44^{\circ}\ 18.57' \pm 0.40'$

* Variance from a large sample is used as the population variance.

The error in A is for a 95% confidence level and includes the error in temperature.

Between Tests No. B-3 and 16, the spectrometer was modified for better mounting on the surface plate. This did not effect the scales or the telescopes except to improve the rotation in the horizontal plane.

APPENDIX B

CALIBRATION OF THE PRESSURE GAGE

All pressures reported in the experimental data were measured with a Texas Instrument Precision Pressure Gage No. 141. The gage indicates the degrees of rotation of a mirror attached to a Bourdon tube. The movement of the mirror is followed by an optical transducer mounted on a gear concentric with the Bourdon tube. The Bourdon tube is metal, and specific precautions must be taken to correct for hysteresis. The gage was calibrated between 240 psi to 1500 psi with a Hart Balance dead weight tester.

The same pressure balance system as described by Honeywell[24] was used in this calibration with the 700 - 1750 psi measuring cylinder. The balance has an accuracy of 1 in 10,000 and a reproducibility of 1 in 20,000. A pressure transducer model P3D made by Pace Engineering Co., North Hollywood was used between the oil of the pressure balance system and the argon sample system connected to the T.I. gage. This is a diaphram type transducer and is used with a 1 psi range diaphram. The transducer output displayed on a recorder showed a sensitivity and reproducibility to ± 0.05 psi.

The T.I. gage was connected directly into the argon sample system of the refractive index cell. A Bourdon tube with a maximum deflection of 100° at 5000 psi was used in the gage. To correct for hysteresis, the gage was pressurized three times to 1500 psi for two minutes and then rezeroed against vacuum. The chamber around the Bourdon tube is open to the atmosphere when metal tubes are used,

thus 0 degrees deflection is atmospheric pressure. Zero pressure was established at -0.280^{o} deflection under a mechanical pump vacuum (10^{-2} mm. H_g) when the barometric pressure is 736.8 mm. H_g (corrected).

The use of a 5000 psi metal tube for only 1500 psi should increase the stability and reproducibility, although increasing the proportionate error. For the calibration the data from Tests No. 7 to 11 were used along with Test No. A-1. In Tests No. 7 to 11 the dead weight tester and the T.I. gage were both connected to the system during refractive index measurements. For Test No. A-1 the refractive index cell was closed off. From the data no dependence on the different tests could be noted. The calibration data were used to compute the tube constant for the Bourdon tube - psi/degree deflection. This quantity - T. C. - was then used as a function of the degrees deflection for calibration purposes. A third order polynomial was used to fit the function T. C. = f(Deg). The gage has a sensitivity of 0.05 psi, but the use of a 95% confidence interval on the polynomial fit was felt to cover all of the reproducibilities and uncertainties in calibration; accounting for all three devices, the dead weight tester, the pressure transducer, and the T.I. gage. A 95% confidence interval is ± 0.06%, and this is used as the accuracy of all pressure measurements recorded.

$$T.C. = A_1 + A_2 Deg + A_3 Deg^2 + A_4 Deg^3$$

$$A_1 = 5.1426 \times 10^{1}$$

$$A_2 = -1.1012 \times 10^{-1}$$

$$A_3 = 4.2904 \times 10^{-3}$$

$$A_4 = -6.5810 \times 10^{-5}$$

$$\text{Variance} = 2.64 \times 10^{-4}$$

Table B

Texas Instruments Gage Calibration

P(psi)	Deg(°)	T.C.(psi/Deg)
Test No. 7		
285.340[a]	5.603	50.9263
*346.011	7.238	47.8048
*434.408	8.566	50.7131
*493.840	9.747	50.6658
*526.942	10.406	50.6383
574.276	11.348	50.6059
643.785	12.732	50.5734
*724.210	14.320	50.5734
856.534	16.967	50.4823
996.996	19.774	50.4196
1112.236	22.096	50.3927
*1179.696	25.277	46.4707
1473.764	29.343	50.2254
Test No. 8		
*317.447	6.232	50.9431
522.806	10.322	50.6497
607.555	12.000	50.6296
727.372	14.389	50.5505
955.907	18.948	50.4490
1282.125	25.490	50.2991
1417.629	28.200	50.2705
*403.274	7.947	50.7455
468.479	9.238	50.7121
Test No. 9		
408.566	8.044	50.7914
409.959	9.678	50.7293
625.073	12.353	50.6009
828.124	16.400	50.4954
1028.989	20.410	50.4158
1237.126	24.585	50.3204
1407.006	27.988	50.2718
Test No. 10		
329.090	6.470	50.8640
*492.004	9.713	50.6542
775.580	15.360	50.4935
1012.879	20.104	50.3820
*1382.330	23.962	50.2972
1423.456	28.336	50.2349

---

a Uncertainty P ± .01%

* Points omitted from polynomial fit at 95% confidence level

Table B

P(psi)	Deg(°)	T.C.(psi/Deg)	P(psi)	Deg(°)	T.C.(psi/Deg)
Test No. 11			Test No. A-1		
276.689	5.431	50.9463	*299.910	5.880	51.0050
356.555	7.014	50.8347	328.639	6.461	50.865
448.257	8.838	50.7193	350.510	6.894	50.8427
502.080	9.907	50.6793	*381.1534	7.503	50.8001
548.501	10.833	50.6325	425.444	8.382	50.7569
576.634	11.388	50.6352	459.504	9.056	50.7402
626.978	12.392	50.5954	499.440	9.853	50.6891
634.710	12.548	50.5826	*256.659	5.025	51.0763
644.791	12.747	50.5837	*281.874	5.540	50.8797
666.727	13.182	50.5786	*296.068	5.922	49.9945
*680.855	13.458	50.5912	*320.165	6.281	50.9735
699.313	13.830	50.5649	331.958	6.525	50.8493
717.521	14.193	50.5546	*332.300	6.535	50.8493
729.606	14.438	50.5337	348.290	6.843	50.8973
747.596	14.795	50.5303	359.9987	7.121	50.5545
766.390	15.172	50.5134	374.206	7.364	50.8156
*780.280	15.439	50.5396	258.421	5.051	51.1624
827.722	16.387	50.5109	274.766	5.380	51.0718
894.934	17.739	50.4501	303.666	5.958	50.9678
1089.661	21.633	50.3703	334.611	6.578	50.8683
*1254.468	24.941	50.2974	352.226	6.926	50.8556
*1491.624	29.683	50.2518	384.408	7.561	50.8505

Table B

P(psi)	Deg(°)	T.C.(psi/Deg)	P(psi)	Deg(°)	T.C.(psi Deg)
411.797	8.110	50.7765	1024.144	20.309	50.4281
429.278	8.451	50.7961	1050.564	20.843	50.4037
442.727	8.728	50.7249	*1059.251	21.310	49.7086
*459.711	9.050	50.7968	1097.4946	21.780	50.3900
482.945	9.528	50.6870	1129.117	22.411	50.3823
499.898	9.863	50.6841	1146.028	22.765	50.3417
533.157	10.525	50.6562	1173.514	23.313	50.3373
*561.613	11.081	50.6825	1201.437	23.870	50.3325
*582.418	11.515	50.5791	1225.040	24.334	50.3427
*609.334	12.032	50.6428	1248.402	24.813	50.3124
632.771	12.515	50.5610	1275.408	25.355	50.3020
671.320	13.277	50.5626	*1294.940	25.823	50.1468
692.517	13.709	50.5229	1325.134	26.352	50.2859
*719.726	14.223	50.6030	1354.181	26.930	50.2852
*744.998	14.768	50.4468	1375.988	27.363	50.2864
770.616	15.254	50.5189	1392.766	27.707	50.2677
794.693	15.738	50.4952	1424.540	28.336	50.2731
*819.324	16.219	50.5163	1445.648	28.764	50.2589
844.780	16.738	50.4708			
869.746	17.229	50.4815			
896.668	17.767	50.4682			
921.856	18.268	50.4629			
948.664	18.807	50.4421			
974.613	19.328	50.4249			
994.508	19.726	50.4161			

APPENDIX C

EXPERIMENTAL D VALUES OF ARGON

All of the experimental values of the angle of minimum deviation recorded in the investigation are listed in Tables C-1 and C-2. These experiments were carried out over approximately two years. Run 71 was recorded in August 1964 and one year later in August and September 1965 runs 3 to 15 were made. Then in the fall and winter of 1966 the remaining runs were completed. The two major equipment modifications took place in the intervals between the runs. Before run 3 the new cell was put into the cryostat. At this same time all the wiring and vacuum seals for the shield were also replaced. After run B-3, the new spectrometer mounting and the new cryostat support were set up.

Measurements for gas-liquid coexistence states are covered in runs 71, 3, 4, 6, B-2, and 26. Run 71 was made with the original cell designed by Smith[36], $A = 45.0^{\circ} \pm 0.002^{\circ}$, and all the remaining runs used the new cell, $A = 44.3094^{\circ} \pm 0.0067^{\circ}$.

For all the runs recorded the outside vacuum chamber was evacuated to a pressure between 1×10^{-5} and 1×10^{-4} mm. H_g. Then liquid nitrogen was placed in the reservoir, and the automatic level controller set to maintain the liquid nitrogen level at one inch. When the shield and the cell had cooled below the temperature to be studied, the shield was set up for automatic control. During the cooling period, the volume inside the shield was evacuated with only a mechanical pump to speed the cooling of the cell. The temperature and temperature

control of the shield were not effected by the vacuum in the shield chamber. The current to the shield heater was approximately 0.2 amps for all the temperatures studied. In order for this current to fall in the linear response range of the Leeds and Northrup Series 60 controller and Fincor power supply system, it was necessary to add a resistance in series with the shield heater. A 250Ω-160 watt adjustable resistor set at 100Ω was used. Typical control settings for the Series 60 controller used with the Speedomax H recorder are: Microvolt D. C. amplifier - 100μv; Proportional Band - 100%; Rate Time - 1 min.; Reset - 0.6 repeats/min. The control settings for the shield heater are not critical, and when properly set up the shield responds rapidly and stably.

When the shield temperature was established 2 or 3° below the temperature for the cell, the cell heater was connected to its control circuit. As indicated in the Experimental Details section, the set point for the platinum resistance thermometer attached to the cell was the Wenner potentiometer. The current to the cell heater varied from 0.01 to 0.02 a. A resistance in series with the heater was adjusted so that the current necessary to control corresponded to the mid-point of the controller output, 2.5 ma. A Speedomax G recorder was used with a Series 60 controller for the cell heater control, and typical control settings are: D. C. Microvolt amplifier - 100μv; Proportional Band - 100%; Rate Time - 1 min.; Reset - 1 repeats/min.; Recorder range - 2 mv. The cell control is sensitive to controller settings, and the best procedure is to establish the cell on control and check the stability before proceeding with the measurements. Once the proper setting is

found, the cell control is very stable with rapid response and temperature fluctuations less than 0.0001°K.

When the cell temperature was on automatic control the instrument zero for the spectrometer was determined. The details of the technique for the operation of the spectrometer are covered in Appendix A. Now argon was fed into the cell from the high pressure bomb until the gas liquid interface was at the center of the cell window. With the cell half filled with liquid it was possible to make measurements on both gas and liquid at the same time thus insuring equilibrium. No readings for the gas phase were recorded at the lower temperatures of run 71 because the angle of deviation was too small to be read. There are some other points where readings for the gas phase were not recorded because insufficient gas phase was available to give a distinct light image. The readings for the liquid phase in these cases were not included in further analysis.

The argon used in runs 3 to 6 was obtained from Linde who reported an impurity analysis of less than 20 ppm. The argon withdrawn from the supply cylinder was stored in a storage cylinder and reused. Care is taken to have all sample lines both vacuum and pressure tight. When the lines were tight, they were flushed repeatedly with argon before use.

Many of the points recorded in Table C-1 are not included in the final data presentation. These are indicated by * or †. Except near the critical temperature, the data indicated by * were questionable at the time they were recorded. Mostly the questions dealt with proper temperature control or recording. The exception is run B-2 which

seems to bear no relation to the other data recorded. At the time the results were recorded this discrepancy was attributed to sample contamination.

The many problems connected with the critical region are discussed in the section Experimental Details. Many results in this region are also discarded because of the reasons discussed. The vapor pressure measurements made in this region used the same pressure measuring system as in the one phase region. The gage was left connected to the system, and the gage reading was recorded at the same time as the angle of minimum deviation. A stable pressure gage reading for measurements near the critical temperature was used to help indicate equilibrium.

For operations in the region of the critical point additional considerations must be applied to the temperature control. When the shield chamber was pumped with a mechanical vacuum pump, the pressure was 2 to 6 x 10^{-3} mm. Hg. This provides sufficient gas for conduction cooling of the coiled inlet line above the cell. Near the critical point the small heat of vaporization allows liquid to boil in the cell and recondense in the line above. If the shield chamber is pumped with a diffusion pump to a pressure of 1 x 10^{-4} mm. Hg, sufficient heat flows down the inlet line to upset the cell temperature. This problem was over come on run 26 by using the heater on the inlet line and a vacuum of 2 to 6 x 10^{-3} mm. Hg. The thermocouple at the mid-point of the coil was used to monitor the temperature of the coil, and the inlet heater current was adjusted to give the same temperature in the coil as the cell. It was found that the same total current divided

between the inlet heater and the shield gave good control, about 3/4 of the current was put through the shield heater. It is convenient to have a series of adjustable resistances that can be switched in; this provides maximum flexibility to achieve the best control response.

In smoothing the data on the gas-liquid coexistence curve $\frac{n^2 - 1}{n^2 + 2}$ was fitted as a function of $T_C - T$, and points were excluded at a 95% confidence level. Points thus excluded are indicated by †. In the smoothing, all the data were fitted at one time, and even obviously bad points were included on the first fit.

For measurements on isotherms in the one phase region the experimental procedure was almost exactly the same. All the same heater currents and control settings apply. In this case it is necessary to measure the pressure. Before the instrument zero for the spectrometer was determined, the pressure gage was pressurized three times to its maximum pressure. Then the pressure gage was zeroed against vacuum, and at the same time the spectrometer zero was determined.

Argon was fed into the system as before, but in this case it was not necessary to carefully introduce a particular amount. This makes the measurements somewhat simpler. After the temperature and pressure were stable the angle of minumum deviation was determined. It should be noted that in this temperature measuring and control scheme, it was necessary to measure the potential drop in the standard resistor produced by the current to the resistance thermometer. It was also necessary to standardize the Wenner potentiometer since this instrument was continually connected into the control circuit.

Both of these operations were performed before each angle determination.

In the region of the critical temperature and near the gas-liquid coexistence pressure, care must be taken to insure true temperature and pressure equilibrium.

On all the isotherms an attempt was made to run exactly at the temperature reported by Levelt. This takes into account a correction obtained from her. This was not achieved because corrections had to be applied to the potentiometer readings. The cases where duplicate isotherms are separated by $0.05^{\circ}K$ result from potentiometer corrections. The data are reported in this form, and corrections were applied to Levelt's density values.

The two runs 7 and 8 gave values which could not be reproduced on reruns. It was also noted that these isotherms at low density crossed other isotherms, a highly unbelievable situation. These two runs were not included with the final data. For all isotherms two runs were performed to check reproducibility. Run 18 covers two runs on consecutive days.

In smoothing the data the L - L values are fitted as a function of ρ and points rejected at a 95% confidence level. These points are indicated by † in Table C-2.

The estimation of the relative error in D is $\pm 0.005^{\circ}$, and the relative error in P is $\pm 0.06\%$. The absolute uncertainty in T is $\pm 0.015^{\circ}K$, but the relative error in T should be less than $\simeq \pm 0.005^{\circ}K$. The values of n are computed from equation (9).

Table C-1

Experimental D Values of Argon

Coexisting Liquid-Vapor

T(°K)	P(atm.)	D_G(°)[a]	n_G	D_L(°)[a]	n_L
Test No. 71					
85.538[c]				11.233[b]	1.2312[d]
89.918				11.005	1.2266
94.580				10.755	1.2216
99.390				10.488	1.2162
105.015		0.192	1.0040[d]	10.165	1.2096
109.362		0.255	1.0054	9.913	1.2046
115.004		0.325	1.0068	9.547	1.1972
120.002		0.433	1.0091	9.207	1.1902
125.003		0.588	1.0122	8.820	1.1824
130.013		0.772	1.0162	8.413	1.1741
135.011		1.005	1.0211	7.958	1.1648
140.010		1.335	1.0279	7.394	1.1534
145.008		1.803	1.0378	6.680	1.1387
†150.008		2.897	1.0606	5.153	1.1073
Test No. 3					
*105.019[c]				10.003[e]	1.2103[d]
*107.007		0.213	1.0046	9.884	1.2078
*109.367		0.034	1.0007	9.720	1.2045

---

a Prism angle A = 45° ± .002°
b Uncertainty in D = ± 0.005° (2)
c Uncertainty T = ± 0.015°K
d Uncertainty n ± 0.0001
e Prism angle A = 44.3094 ± .0067°

Table C-1

T(°K)	P(atm.)	D_G(°)	n_G	D_L(°)	n_L
112.020		0.278	1.0060	9.575	1.2015
115.008		0.329	1.0070	9.373	1.1973
117.014		0.370	1.0079	9.252	1.1948
120.008		0.455	1.0097	9.049	1.1906
121.999				8.896	1.1874
125.007		0.593	1.0127	8.701	1.1834
*126.989		0.625	1.0134	8.520	1.1797
†130.017		0.792	1.0170	8.287	1.1748
*145.013		1.807	1.0386	6.564	1.1390
145.993		1.944	1.0415	6.392	1.1354
146.975		2.092	1.0447	6.191	1.1312
*147.973		2.282	1.0487	6.045	1.1281
148.976		2.495	1.0532	5.634	1.1195
149.265		2.584	1.0551	5.550	1.1177
†149.566		2.687	1.0573	5.420	1.1150
†149.871		2.811	1.0599	5.271	1.1119
†149.976		2.872	1.0612	5.222	1.1108
Test No. 4					
146.069		1.930	1.0412	6.378	1.1351
146.769		2.026	1.0433	6.237	1.1321
147.067		2.087	1.0446	6.182	1.1310
†147.367		2.150	1.0459	6.142	1.1302
147.770		2.228	1.0476	6.025	1.1277
†148.068		2.273	1.0485	5.952	1.1262
148.269		2.321	1.0495	5.884	1.1248

Table C-1

T(°K)	P(atm.)	D_G(°)	n_G	D_L(°)	n_L
148.476		2.375	1.0507	5.832	1.1236
148.668		2.413	1.0515	5.773	1.1224
†149.180		2.545	1.0543	5.500	1.1167*
†149.662		2.702	1.0576	5.415	1.1149
*150.068		2.874	1.0613	5.2142	1.1107
*150.267		2.991	1.0638	5.0903	1.1081
*150.475		3.088	1.0658	4.939	1.1049
*150.576		3.221	1.0686	4.836	1.1027
*150.683		3.342	1.0712	4.759	1.1011
*150.715		3.362	1.0716	4.683	1.0995
*150.761		3.468	1.0739	4.596	1.0977
Test No. 6					
*150.782		3.700	1.0788	4.401	1.0936
*150.794		3.838	1.0817	4.264	1.0907
*150.608		3.394	1.0723	4.710	1.1001
*150.627		3.431	1.0731	4.668	1.0992
*150.677		3.524	1.0750	4.569	1.0971
*150.730		3.674	1.0782	4.421	1.0940
*150.755		3.826	1.0814	4.267	1.0907
*150.762		3.992	1.0849	4.187	1.0890
*150.706		3.584	1.0763	4.507	1.0958
*150.718		3.621	1.0771	4.472	1.0951
*150.743		3.769	1.0802	4.299	1.0914

Table C-1

T(°K)	P(atm.)	D_G(°)	n_G	D_L(°)	n_L
Test No. B-2					
*117.055	10.034[f]	0.358		9.233	
*123.468	14.206	0.521		8.789	
*128.506	18.483	0.692		8.382	
*133.029	22.868	0.877		7.995	
*138.231	28.820	1.173		7.471	
*141.402	32.905	1.409		7.095	
*144.620	37.565	1.732		6.632	
*147.443	41.969	2.142		6.0860	
*149.266	45.076	2.547		5.564	
*150.712		3.350		4.703	
*150.757		3.449		4.615	
*150.807		3.578		4.494	
*150.819		3.605		4.454	
*150.844		3.708		4.361	
Test No. 26					
149.716	46.326	2.794	1.0596	5.322	1.1129
149.979	46.812	2.928	1.0624	5.183	1.1100
150.225	47.289	3.102	1.0661	5.006	1.1063
146.961	41.610	2.102	1.0449	6.164	1.1306
147.745	42.884	2.248	1.0480	5.985	1.1269
148.512	44.195	2.420	1.0516	5.769	1.1223
149.025	45.100	2.557	1.0545	5.602	1.1188
†149.444	46.001	2.733	1.0583	5.399	1.1146

---

f Uncertainty in P = ± 0.06%

Table C-1

$T(^{o}K)$	P(atm.)	$D_G(^{o})$	n_G	$D_L(^{o})$	n_L
149.805	46.455	2.827	1.0603	5.275	1.1120
150.062	46.940	2.966	1.0632	5.129	1.1089
150.194	47.172	3.037	1.0647	5.036	1.1069
150.327	47.414	3.139	1.0669	4.938	1.1049
150.450	47.670	3.264	1.0695	4.819	1.1024
150.429	47.666			4.841	1.1028
150.556	47.923			4.681	1.0995
150.599	47.919	3.390	1.0722	4.674	1.0993
149.538	46.076	2.731	1.0582	5.410	1.1148
149.733	46.414	2.805	1.0598	5.317	1.1128
149.928	46.772	2.901	1.0618	5.215	1.1107
150.121	47.123	3.000	1.0639	5.097	1.1082
150.251	47.365	3.084	1.0657	5.010	1.1064
150.513	47.870	3.329	1.0709	4.755	1.1010
150.639	48.092	3.562	1.0758	4.510	1.0959
150.667	48.154	3.650	1.0777	4.420	1.0940
150.697	48.204	3.805	1.0810	4.244	1.0902
149.547	45.999	2.737	1.0584	5.414	1.1149
149.868	46.573	2.876	1.0613	5.256	1.1116
150.155	47.102	3.025	1.0645	5.088	1.1080
150.445	47.632	3.265	1.0696	4.832	1.1026
150.548	48.827	3.380	1.0720	4.700	1.0999
150.657	48.030	3.613	1.0769	4.473	1.0951

Table C-1

T(°K)	P(atm.)	D_G(°)	n_G	D_L(°)	n_L
150.675	48.067	3.696	1.0787	4.401	1.0936
150.683	48.084	3.745	1.0797	4.352	1.0925
†150.692	48.108	3.813	1.0812	4.278	1.0910

Table C-2

Experimental D Values for Argon - Isotherms

P(atm.)	D(°)[a]	n
Test No. 14	173.149°K[e]	
†25.655[b]	0.622[c]	1.0133[d]
†28.952	0.700	1.0150
32.530	0.807	1.0173
35.885	0.911	1.0195
39.511	1.031	1.0221
42.851	1.147	1.0245
46.496	1.284	1.0274
49.867	1.418	1.0303
53.425	1.569	1.0335
56.542	1.713	1.0366
60.208	1.893	1.0404
62.675	2.024	1.0432
66.625	2.250	1.0480
†70.598	2.501	1.0534
73.921	2.723	1.0581
79.477	3.131	1.0667
86.443	3.672	1.0782
93.075	4.162	1.0885
97.431	4.452	1.0946
101.446	4.690	1.0997
Test No. 21	173.083°K	
14.831	0.330	1.0071
18.540	0.422	1.0090
25.600	0.607	1.0130
32.510	0.806	1.0173
39.518	1.031	1.0221
49.088	1.387	1.0296
†59.989	1.887	1.0403
†76.416	2.914	1.0621
25.873	0.672	1.0144
28.821	0.768	1.0164
32.135	0.883	1.0189
36.072	1.031	1.0220
38.990	1.151	1.0246
42.699	1.317	1.0282
46.000	1.480	1.0316

---

a Prism angle = 44.3094° ± .0067°
b Uncertainty P ± 0.06%
c Uncertainty D ± 0.005°
d Uncertainty n ± 0.0001
e Uncertainty T ± 0.015°K

Table C-2

P(atm.)	D(°)	n
48.880	1.641	1.0351
52.014	1.834	1.0392
53.945	1.969	1.0420
56.315	2.148	1.0458
58.433	2.329	1.0497
60.471	2.527	1.0539
62.554	2.750	1.0586
64.041	2.930	1.0625
†65.363	3.098	1.0660
†66.426	3.244	1.0691
67.503	3.414	1.0727
68.852	3.592	1.0765
70.535	3.840	1.0817
71.642	4.000	1.0851
73.232	4.219	1.0897
74.492	4.380	1.0931
†75.993	4.558	1.0969
†78.391	4.808	1.1021
80.846	5.028	1.1068
83.636	5.236	1.1111
86.776	5.435	1.1153
90.361	5.626	1.1193
†92.460	5.758	1.1221
Test No. 20	163.095°K	
†15.272	0.351	1.0075
18.770	0.463	1.0099
22.199	0.562	1.0120
†25.968	0.679	1.0145
28.796	0.770	1.0165
32.483	0.898	1.0192
36.040	1.032	1.0221
39.037	1.156	1.0247
47.361	1.559	1.0333
51.015	1.775	1.0379
53.949	1.972	1.0421
66.430	3.280	1.0699
†75.684	4.563	1.0970
†83.664	5.261	1.1117
92.934	5.758	1.1221
96.092	5.888	1.1248
100.230	6.038	1.1280
103.814	6.154	1.1304
†66.442	3.289	1.0701
67.608	3.457	1.0736
Test No. 12	153.163°K	
20.196	0.552	1.0118
27.423	0.815	1.0174

Table C-2

P(atm.)	D(°)	n	P(atm.)	D(°)	n
30.598	0.947	1.0203	†55.114	5.204	1.1105
33.476	1.080	1.0231	55.980	5.376	1.1141
37.192	1.277	1.0273	57.771	5.620	1.1192
†40.244	1.452	1.0310	59.356	5.783	1.1226
42.177	1.606	1.0343	61.197	5.932	1.1257
43.928	1.754	1.0375	62.752	6.036	1.1279
44.809	1.838	1.0392	66.195	6.226	1.1319
45.584	1.919	1.0410	69.418	6.369	1.1349
†45.932	1.973	1.0421	74.560	6.556	1.1388
46.594	2.034	1.0434	79.562	6.703	1.1419
47.447	2.145	1.0458	86.284	6.872	1.1454
48.218	2.258	1.0482	92.199	6.998	1.1480
49.002	2.395	1.0511			
49.600	2.517	1.0537	Test No. 22	153.107°K	
50.302	2.707	1.0577	24.416	0.701	1.0150
50.749	2.840	1.0606	27.363	0.814	1.0174
†50.995	2.879	1.0614	28.552	0.862	1.0184
51.388	3.099	1.0660	30.829	0.962	1.0206
51.838	3.352	1.0714	33.598	1.091	1.0233
52.040	3.497	1.0745	37.161	1.280	1.0274
52.238	3.639	1.0775	44.258	1.800	1.0384
52.453	3.857	1.0821	45.576	1.935	1.0413
†52.918	4.280	1.0910	46.750	2.076	1.0443
†53.852	4.820	1.1024	†48.804	2.398	1.0512
†54.418	5.026	1.1067	†50.947	2.726	1.0581

Table C-2

P(atm.)	D(°)	n	P(atm.)	D(°)	n
†52.958	4.582	1.0974	54.034	5.757	1.1221
†56.089	5.482	1.1163	57.267	6.047	1.1281
†67.850	6.333	1.1341	61.876	6.316	1.1338
74.706	6.583	1.1394	75.143	6.787	1.1436
86.211	6.888	1.1457	86.385	7.047	1.1490
92.570	7.022	1.1485	102.400	7.328	1.1549
103.050	7.209	1.1524			
Test No. 11	151.665°K		Test No. 15	150.665°K	
19.804	0.545	1.0117	22.078	0.635	1.0136
25.242	0.741	1.0158	25.422	0.761	1.0163
31.492	1.009	1.0216	28.888	0.908	1.0194
35.149	1.198	1.0256	31.186	1.015	1.0217
38.314	1.391	1.0297	33.824	1.150	1.0246
40.209	1.529	1.0327	36.587	1.316	1.0281
43.638	1.834	1.0392	38.948	1.478	1.0316
44.170	1.893	1.0404	41.414	1.684	1.0360
44.849	1.975	1.0422	43.907	1.960	1.0419
46.333	2.189	1.0467	45.036	2.127	1.0454
47.275	2.369	1.0506	46.323	2.389	1.0510
48.544	2.720	1.0580	†46.968	2.580	1.0550
49.783	3.983	1.0848	47.479	2.817	1.0601
50.619	5.034	1.1069	47.698	2.991	1.0638
51.837	5.418	1.1150	47.844	3.182	1.0678
53.123	5.634	1.1195	47.922	3.403	1.0725

Table C-2

P(atm.)	D(°)	n
47.933	3.448	1.0734
†48.352	5.172	1.1098
48.615	5.294	1.1124
49.031	5.433	1.1153
50.072	5.650	1.1198
50.867	5.769	1.1223
52.006	5.900	1.1251
53.395	6.028	1.1278
55.219	6.162	1.1306
57.900	6.319	1.1338
61.139	6.472	1.1370
64.780	6.612	1.1400
69.057	6.753	1.1429
73.321	6.869	1.1453
78.218	6.986	1.1478
83.623	7.101	1.1502
88.956	7.200	1.1522
94.093	7.289	1.1541
100.714	7.393	1.1562
Test No. 24	150.665°K	
22.636	0.656	1.0140
†25.386	0.758	1.0162
31.219	1.016	1.0217
33.789	1.150	1.0246
†38.950	1.494	1.0319
†43.885	1.978	1.0422
44.756	2.083	1.0445
45.831	2.281	1.0487
46.425	2.424	1.0517
47.162	2.675	1.0570
†48.234	4.978	1.1057
†48.936	5.440	1.1154
50.387	5.716	1.1212
52.007	5.909	1.1252
55.220	6.165	1.1306
57.976	6.325	1.1340
†61.154	6.639	1.1405
†65.933	6.816	1.1442
73.407	6.865	1.1452
Test No. 7	148.166°K	
*20.394	0.528	1.0113
*26.009	0.757	1.0162
*30.560	0.968	1.0207
*34.601	1.203	1.0257
*36.854	1.367	1.0292
*40.073	1.669	1.0357
*44.799	6.028	1.1278
*50.217	6.412	1.1358

Table C-2

P(atm.)	D(°)	n
*59.224	6.767	1.1432
*68.811	7.019	1.1485
*76.718	7.182	1.1519
*87.524	7.367	1.1557
*101.257	7.560	1.1597
Test No. B-3	148.166°K	
21.877	0.641	1.0137
23.985	0.723	1.0155
25.595	0.792	1.0169
27.436	0.871	1.0186
29.618	0.976	1.0209
31.844	1.096	1.0234
34.266	1.240	1.0265
35.904	1.352	1.0289
37.585	1.486	1.0318
39.212	1.636	1.0350
40.653	1.798	1.0384
42.183	2.039	1.0435
43.235	2.294	1.0490
†43.235	5.930	1.1257
43.774	5.988	1.1269
44.945	6.118	1.1296
45.914	6.205	1.1314
47.385	6.314	1.1337
49.036	6.416	1.1359
51.418	6.538	1.1384
53.158	6.613	1.1400
56.554	6.743	1.1427
60.179	6.859	1.1451
63.834	6.958	1.1472
67.766	7.056	1.1492
73.152	7.170	1.1516
79.841	7.296	1.1542
86.620	7.408	1.1566
95.826	7.548	1.1595
103.606	7.643	1.1615
Test No. 19	148.123°K	
†43.278	5.920	1.1255
50.221	6.488	1.1374
68.912	7.088	1.1499
Test No. 8	143.170°K	
*22.555	0.658	1.0141
*28.439	0.784	1.0168
*32.859	1.253	1.0268
*36.564	6.837	1.1447
*42.296	7.035	1.1488
*50.450	7.242	1.1531
*65.996	7.515	1.1588

Table C-2

P(atm.)	D(°)	n
*88.246	7.820	1.1651
*97.410	7.919	1.1672
Test No. 18	143.170°K	
†11.970	0.335	1.0072
17.897	0.534	1.0114
21.366	0.670	1.0144
26.690	0.918	1.0196
32.058	1.255	1.0268
34.603	1.485	1.0317
47.068	7.234	1.1529
50.600	7.316	1.1546
65.968	7.593	1.1604
†35.728	6.870	1.1454
38.486	6.978	1.1476
42.212	7.094	1.1500
47.415	7.232	1.1529
53.054	7.357	1.1555
59.162	7.474	1.1579
67.524	7.610	1.1608
76.119	7.731	1.1633
84.553	7.840	1.1656
94.454	7.950	1.1678
102.599	8.034	1.1696

P(atm.)	D(°)	n
Test No. 9	138.173°K	
28.769	7.475	1.1580
34.362	7.596	1.1605
43.502	7.752	1.1637
57.310	7.947	1.1678
70.978	8.105	1.1711
85.178	8.245	1.1740
96.696	8.347	1.1761
Test No. 17	138.173°K	
† 9.204	0.262	1.0056
†14.695	0.448	1.0096
18.536	0.596	1.0128
22.787	0.793	1.0170
25.554	0.948	1.0203
28.057	1.122	1.0240
29.321	7.491	1.1583
35.823	7.622	1.1610
41.102	7.716	1.1630
45.022	7.776	1.1642
49.667	7.845	1.1657
57.870	7.950	1.1678
70.886	8.100	1.1710
83.059	8.222	1.1735
102.230	8.385	1.1769

Table C-2

P(atm.)	D(°)	n	P(atm.)	D(°)	n
Test No. 10	133.176°K		66.014	8.442	1.1781
23.376	7.985	1.1686	74.843	8.515	1.1796
34.486	8.133	1.1716	80.483	8.558	1.1805
†53.766	8.343	1.1760	86.566	8.606	1.1814
†69.938	8.319	1.1755	93.657	8.658	1.1825
83.064	8.590	1.1811	103.025	8.722	1.1838
97.871	8.694	1.1833			
Test No. 16	133.176°K				
† 8.450	0.250	1.0054			
11.982	0.370	1.0079			
14.253	0.456	1.0098			
16.526	0.550	1.0118			
18.525	0.642	1.0138			
20.070	0.720	1.0154			
22.628	0.868	1.0186			
†23.088	0.890	1.0190			
23.088	7.979	1.1684			
23.533	7.980	1.1685			
24.546	7.995	1.1688			
27.153	8.031	1.1695			
33.779	8.115	1.1713			
38.176	8.169	1.1724			
45.784	8.253	1.1741			
55.657	8.350	1.1762			

PROPOSITION I.

It is proposed that the refractive index n obeys the law of rectilinear diameters. This leads directly to the use of n with the principle of corresponding states and the equation for the critical coefficient.

The rectilinear diameter was first used by Cailletet and Mathias[1]. The idea was developed for densities in the gas-liquid coexistence region; here the density values form a curve similar to a parabola when plotted against temperature. The rectilinear diameter $(\rho_L + \rho_G)\frac{1}{2}$ should be a straight line when plotted against temperature and should intersect the parabola at the critical temperature, giving the critical density. When the critical temperature is known, the rectilinear diameter can be extrapolated to T_C to find the critical density.

Mathias used the rectilinear diameter extensively and later investigators at the laboratory in Leiden also worked with it. Mathias used an equation of the form[2]:

$$\frac{1}{2}(\rho_G + \rho_L) / \rho_C = 1 + a(1 - T_r) \qquad (1)$$

where a is a characteristic of the material.

Partinton[3] gave a very complete resume of the work that has been done with the rectilinear diameter. He discussed the deviations from the straight line principle for various materials. At present no theoretical justification for the rectilinear diameter has been developed, but Guggenheim[4] showed that the rectilinear diameter is obtained if

the principle of corresponding states is used to describe the liquid and vapor densities along the coexistence curve. This gives only an empirical justification for the rectilinear diameter.

This proposition uses the experimental refractive index measurements for argon in the thesis of Teague[5]. The justification is obtained by comparison to the density measurements of Levelt[6]. Her experimental values extend over 30° up to $0.05^{\circ}K$ of the critical temperature, and the rectilinear diameter is straight over the range. It was noted in her work that the rectilinear diameter is not sensitive to small uncertainties in temperature.

The rectilinear diameter is used to predict values in regions other than the critical region. Mathias[2] used it to predict low density gas values. The rectilinear diameter was obtained in a region where values for both phases were available. Then measurements in one phase and the extrapolation of the rectilinear diameter were used to predict values in the other phase.

If it is assumed that the Lorentz-Lorenz function in valid for argon, equation (2), then n is directly related to ρ.

$$\frac{n^2 - 1}{n^2 + 2} = \left(\frac{4}{3}\pi a\right)\rho = C_\rho \qquad (2)$$

Here a is the molar polarizability. For low density gases where n is approximately equal to 1, the relation reduces to

$$\frac{(n-1)(n+1)}{n^2+2} = C_\rho \simeq n - 1 = \frac{3}{2} C_\rho. \qquad (3)$$

Then to this approximation, n - 1 is directly proportional to ρ. It has been shown that the rare gas elements obey the principle of corres-

ponding states very well[7]. A statement of this rule is

$$\rho r = G(T_r, P_r). \tag{4}$$

Here the reduced variable is defined as the value at the state of the system divided by the value at the critical state. If (4) applies to the rare gas elements, then

$$\frac{n-1}{n_C-1} = G(T_r, P_r). \tag{5}$$

This is written as a true reduced property

$$\frac{n}{n_C} = G(T_r, P_r)\, L + M \tag{6}$$

where L and M are constants determined by n_C. This equation is valid if the molar polarizability C in equation (2) is a constant, independent of state.

Along the vapor pressure curve the density is a function of temperature alone. Guggenheim[4] showed that equation (7) is valid for the argon system.

$$\rho_G/\rho_C = 1 + \frac{3}{4}\left(1 - \frac{T}{T_C}\right) - \frac{7}{4}\left(1 - \frac{T}{T_C}\right)^{1/3}$$

$$\rho_L/\rho_C = 1 + \frac{3}{4}\left(1 - \frac{T}{T_C}\right) + \frac{7}{4}\left(1 - \frac{T}{T_C}\right)^{1/3} \tag{7}$$

He used this to show that the rectilinear diameter followed directly:

$$\frac{\rho_G + \rho_L}{2\rho_C} = 1 + \frac{3}{4}\left(1 - \frac{T}{T_C}\right) \tag{8}$$

or

$$\frac{\rho_G + \rho_L}{2} = N + Q(T_C - T) \tag{9}$$

and similarly, it follows that:

$$\frac{n_G + n_L}{2} = N' - Q'(T_C - T) \tag{10}$$

The basic assumptions for this relation are the validity of the Lorentz-Lorenz relation and that n is approximately equal to 1. It will be shown later that if the starting assumption is the law of rectilinear diameters, the equation (7) is the direct result.

The refractive index data of Teague[5] were used to find the rectilinear diameter equation for n and $\frac{n^2 - 1}{n^2 + 2}$ and these are compared to the equation given by Levelt[6] for ρ. The equations are given in Table I. The equations for n fit the data from 105 to 150.7°K, and Levelt's equation for ρ is for 120°K to 150.86°K. If the standard deviation is used to indicate the linearity, then the equations for n are more linear than for ρ. This is the condition used to justify the law of rectilinear diameters, and therefore, the law is as valid for n as for ρ.

With the validity of the rectilinear diameter established, it is possible to find the temperature dependence of states on the gas-liquid coexistence curve. The behavior of the coexistence curve near the critical point can be described by the equation (11)[8]

$$(\rho_L - \rho_G) \sim (T_G - T)^{\beta} \tag{11}$$

The van der Waals equation of state gives a value of $\beta = \frac{1}{2}$, but approximations from statistical mechanics give β = 0.303 to 0.312. The The measurements of Teague[5] give a value of β = 0.361 at T_C = 150.704°K.

If the rectilinear diameter equation (9) is assumed valid then it can be combined directly with equation (11) to yield the functional relation (7) given by Guggenheim.

For application of this approach to the refractive index, the Lorentz-Lorenz relation (2) is again used. Substitution of (2) into (11) gives

$$(n_L - n_G) = \frac{R}{(n_L + n_G)} (T_C - T)^{\beta} \qquad (12)$$

It was shown by the rectilinear diameter analysis that the term $(n_L - n_G)$ is not constant, but it only changes by 0.046% per degree. The assumption that this is constant is compatible with the other approximations.

Following the example for the density, equation (12) is combined with equation (10) to provide the functional form for n on the gas-liquid coexistence curve.

$$n_L = N' + Q'(T_C - T) + S(T_C - T)^{\beta} \qquad (13)$$

The equations given in Table I for n and $\frac{n^2 - 1}{n^2 + 2}$ were obtained by an independent fit of the data so that the constants are not uniform. The standard deviation of the fit is used as justification for this approach. The equation for n fitted these data much better than Guggenheim fitted his equation (7) to the density, 1%.

The coefficients for $\frac{n^2 - 1}{n^2 + 2}$ can be compared to the coefficients for the Guggenheim equation when the molar polarizability is known. From Teague[5] the average value of C for coexisting gas-liquid states

is 4.188 cc/mole. From the 7th equation in Table I the value of the first coefficient in Guggenheim's equation for ρ_L calculated from the refractive index data is 0.82. This is not the same as 0.75, but the agreement is not too bad considering that different critical parameters were used. The important part of the proposal is not the coefficients but the functional form of the equation. The standard deviation of the data fit for any of the refractive index equations is better than the density equation. This generally indicates the great difficulty in making density measurements.

NOMENCLATURE

G - arbitrary function

n - refractive index

P - pressure

T - temperature

C, L, M, N, Q, R, S - constants

α - molar polarizability

β - critical coefficient

ρ - density

Subscripts

C - critical state

G - gas

L - liquid

r - reduced property

REFERENCES

1. Caillett and E. Mathias, Comptes Rendus 102, 1202 (Academie des Sciences, Paris, 1886).
2. E. Mathias, H. Kamerlingh Onnes, and C. A. Crommelin, Communications from the Physical Laboratory, University of Leiden, No. 131a, (1912).
3. J. R. Partington, Treatise on Physical Chemistry, Vol. 1, 639 (Longman and Green, London, 1949).
4. E. A. Guggenheim, Journal of Chemical Physics 13, 253 (1945).
5. R. K. Teague, doctoral thesis, California Institute of Technology, 1968.
6. J. M. H. Levelt, doctoral thesis, Amsterdam, 1958.
7. J. S. Rowlinson, Liquids and Liquid Mixtures, 271 (Academic Press Inc., New York, 1959).
8. J. S. Rowlinson, Critical Phenomena, 9 (National Bureau of Standards Miscellaneous Publications 273, Washington, D. C., 1966).

TABLE I.

1. $\frac{\rho_G + \rho_L}{2} = 300.4 - 1.3\,(t - 122.29)$ [6]

ρ in amogats

t in $^{\circ}C$ $\qquad t_c = 122.29^{\circ}C$

$\sigma = 0.58$ amogats

2. $\left(\frac{n^2-1}{n^2+2}\right)_G + \left(\frac{n^2-1}{n^2+2}\right)_L \frac{1}{2} = 0.056295 + 0.000258\,(T_C - T)$

$\sigma = 0.00013$

T in $^{\circ}K$ $\qquad T_C = 150.704^{\circ}K$

3. $\frac{n_G + n_L}{2} = 1.0859 + 0.00046\,(T_C - T)$

$\sigma = 0.00042$

T in $^{\circ}K$ $\qquad T_C = 150.704^{\circ}K$

4. $n_G = 1.08603 + 0.000563\,(T_C - T) - 0.0272\,(T_C - T)^{0.361}$

$\sigma = 0.00050$

5. $n_L = 1.08565 + 0.000338\,(T_C - T) + 0.0274\,(T_C - T)^{0.361}$

$\sigma = 0.00048$

6. $\left(\frac{n^2-1}{n^2+2}\right)_G = 0.05651 + 0.000356\,(T_C - T) - 0.0177\,(T_C - T)^{0.361}$

$\sigma = 0.00023$

7. $\left(\frac{n^2-1}{n^2+2}\right)_L = 0.05623 + 0.000174\,(T_C - T) + 0.0176\,(T_C - T)^{0.361}$

$\sigma = 0.00020$

PROPOSITION II

It is proposed that an analytical procedure using extraction with concentrated nitric acid and an absorption measurement be used for the analysis of copper in catalyst and other samples. While there are more than one hundred colorimetric analysis for copper, this one has distinct advantages for analysis of copper in copper-impregnated catalysts. A study of related literature indicated that this procedure has not been used before[1].

In this procedure the copper is extracted by concentrated nitric acid in a Soxhlet extraction apparatus. The use of this apparatus is necessary since any insoluble catalyst carrier particles will interfere with the absorption measurement. In a copper catalyst the copper is usually in the form of CuO. Hot nitric acid is necessary to get the copper into solution as $Cu(NO_3)_2$.

The copper extracted from a weighed catalyst sample is washed with concentrated nitric acid directly into a volumetric flask. If an alumina is the catalyst support then some of the alumina will dissolve as the nitrate. In concentrated nitric acid excess aluminum nitrate sometimes precipitates out of the solution. If 10% distilled water is added to the concentrated nitric acid solution in the volumetric flask, aluminum nitrate precipitation is prevented. Since the absorption is dependent on the nitric acid concentration, the distilled water must be measured exactly.

A typical determination would use 1 g. of catalyst which is 5% by weight CuO. The final solution will consist of 90 ml. of concentra-

ted nitric acid and 10 ml. of distilled water. This concentration will prevent precipitation of aluminum nitrate[2]. The final concentration of $Cu(NO_3)_2$ is approximately 6.29×10^{-3} moles per liter, and this provides accurate measurements with a cell of 1 cm. length. For determinations with smaller concentrations, a cell of longer length can be used.

The alumina support and many other materials do not interfere with the analysis. It has been experimentally determined that Beer's law[3] is obeyed for this system.

$$\ell n(I_o/I) = \varepsilon\, c\, \ell \qquad (1)$$

The copper nitrate solution has its maximum absorbance at .970 microns wave length. The maximum is used so that slight variations in wave length will not effect the results. The precaution is necessary since ε varies with wavelength.

The advantages of this method are the direct, simple steps in the analysis. The analysis can be performed with simple apparatus and an inexpensive Bousch and Lomb Spectronic 20. This analysis is necessary for copper impregnated alumina catalyst since the copper is preferentially absorbed by the alumina from the impregnating solution. This type of analysis could also be extended to copper analysis of ore samples.

NOMENCLATURE

c - molar concentration

ϵ - extinction coefficient

I - intensity of light

I_0 - intensity of incident light

ℓ - path length of absorbing medium wave length

REFERENCES

1. Kodama, K., Methods of Quantitave Inorganic Analysis, Interscience Publishers, New York (1963) p. 176.

2. W. F. Linke, Solubilities, 189 (American Chemical Society, Washington, D. C., 1958).

3. Eggers, D. E. Jr., N. W. Gregory, G. O. Halsey, and B. S. Roinovitch, Physical Chemistry, John Wiley and Sons, Inc., New York, (1964), p. 672.

PROPOSITION III

It is proposed that a Jamin interferometer designed for refractive measurements can be used to follow the rate of reaction in a gaseous system. In the Jamin interferometer a sample of refractive index n is introduced into one of the interfering beams[1]. The other beam passes through a similar cell which has been evacuated. The increase in the optical path due to the sample is (n - 1) times the length of the cell, l. This introduces $(n - 1)l/\lambda$ more waves into the path of the sample beam. Then Δm is the number of fringes by which the system is displaced

$$\Delta m = (n - 1)l/\lambda \qquad (1)$$

The refractive index is determined by counting the number of fringes displaced.

Edwards and Woodbury[2] modify the Jamin interferometer so that the number of fringes are recorded electrically. They use a Bausch and Lomb eyepiece camera viewing head so that the fringes can be observed visually although this is not necessary. A cylindrical lens is used in the eyepiece of the interferometer telescope to achieve magnification perpendicular to the fringe pattern only. The fringe pattern then falls on a slit set to distinguish a fraction of a fringe. A photomultiplier tube is placed behind the slit, and the output of the tube varies with the movement of the fringe. The photomultiplier tube and an electric counting system or recorder can be chosen to suit the particular system under investigation. It is reasonable that a system response time of .01 seconds can be achieved.

The proposed method would follow changes in composition with time by a observing the rate of movement of the fringes. The rapid response time could follow a fast reaction. The refractive index is related to the composition by the Lorentz-Lorenz relation [3].

$$\frac{n^2 - 1}{n^2 + 2} = \frac{4}{3} \pi \sum N_k \alpha_k \tag{2}$$

In this equation N_k is the number of molecules of component k per unit volume; α_k is the polarizability per molecule of component k. Then for a mixture for components 1 and 2 the equation is

$$\frac{n^2 - 1}{n^2 + 2} = \frac{4}{3} \pi N_0 \rho (X_1 \alpha_1 + X_2 \alpha_2) \tag{3}$$

The use of this relation assumes that the Lorentz-Lorenz relation is valid. In order for this relation to be useful, it must also be assumed that α_k is the same in the mixture as in the pure state. This is more correct for low density gases. In this region n is close to 1. Then equation (3) can be rewritten as

$$n - 1 = 2 \pi N_0 \rho (X_1 \alpha_1 + X_2 \alpha_2) \tag{4}$$

Then from equation (1) we see that

$$\frac{d(n - 1)}{dt} = \frac{\lambda}{l} \frac{d(\Delta m)}{dt} \tag{5}$$

Using these equations the rate of movement of the fringes can be converted into the change in composition. Taking as an example one of the reactions studied by Nebeker[4], $Cl_2 + I_2 \rightarrow 2ICl$. In this particularly simple reaction using equations (5) and (2)

$$\frac{\lambda}{l} \frac{d(\Delta m)}{dt} = 2 \pi \frac{d}{dt} N_{ICl} \left(-\frac{1}{2} \alpha_{Cl_2} - \frac{1}{2} \alpha_{I_2} + \alpha_{ICl} \right). \tag{6}$$

This approach to the measurements of reaction rates is similar to the use of a spectrometer to measure absorption[5]. This system would be used in measuring the rate of reaction of dilute gases. If the reactants are introducted simultaneously into the reaction cell, a certain mixing time is necessary during which no measurements can be made. This mixing time can be determined experimentally. The values for the polarizability of the pure components and the mixtures can be obtained at low temperatures where no reaction takes place. The optical polarizabilities of dilute gases are independent of temperature even for molecules with a permanent dipole such as ICl[6].

This system has several advantages. The reaction is followed directly, and no sampling is required. The length of the cell can be varied to change Δm to suit the particular reaction. The measurements can be made very accurately since Δm is a relatively large number. This system can also be used to study rapid reactions since the system response is very fast. This method could not be used when the difference in polarizability between the reactants and the product is very small.

NOMENCLATURE

a_k - polarizability per molecule of component k

l - length of cell

λ - wave length of light

Δm - the number of fringes displaced

N_k - the number of molecules of component k per unit volume

N_o - Avogadro's number

n - refractive index

ρ - molar density

t - time

x_k - mole fraction of component k

REFERENCES

1. Jenkins, F. A., and H. E. White, Fundamentals of Optics, McGraw-Hill Book Co., Inc., (1950) Q. 24.

2. Edwards, M. H., and N. C. Woodbury, Can. J. of Physics, 39, 1833, (1961).

3. Bottcher, C. J. F., Theory of Electric Polarization, Elsevies Publishing Co., New York, (1952), pp. 229-291.

4. E. B. Nebeker, doctoral thesis, California Institute of Technology, 1965.

5. W. F. Sheehan, Physical Chemistry, 576 (Allyn and Bacon, Inc., New York, 1961).

6. N. Davidson, Statistical Mechanics, 411 (McGraw-Hill Book Co., Inc., New York, 1962).

PROPOSITION IV.

It is proposed that experimental measurements of the temperature dependence for monolayers of ferromagnetic metals be used to test Onsager's solution to the two dimensional Ising magnet. Verification of the Ising model for magnets and the lattice gas will indicate the usefulness of this approach for the real three dimensional system. This model has been frequently discussed[1, 2, 3, 4], and it is almost a classic problem. In the Ising model only nearest neighbors are considered. In the magnet the interaction energy between the unpaired electrons of nearest neighbor molecules is of two kinds; parallel spins and anti-parallel spins. In the lattice gas the nearest neighbor lattice sites are either occupied or unoccupied.

It has been known for some time that the temperature dependence of the spontaneous magnetization is the same type of curve as presented by the coexisting gas-liquid densities. The functional form of these relations is

$$\frac{M(T)}{M(0)}_{H=0} \sim \frac{D}{T_C}(T_C - T)^{\beta} \qquad (1)$$

$$\frac{\rho_L - \rho_G}{2\rho_C} \sim \frac{D'}{T}(T_C - T)^{\beta} \qquad (2)$$

Here M(T) is the spontaneous magnetization at T and M(0) is the value at T = 0. The spontaneous magnetization is the magnetization at zero field, H = 0. T_C is the Curie temperature in the equation for M. In the density equation T_C is the gas-liquid critical temperature.

The classical theories of van der Waals for the fluid[5] and

Weiss[6] for the ferromagnet give a value of $\beta = 1/2$. Experimental measurements for both fluids[7] and magnets[4] give a value of $\beta \simeq 0.33$. Using the Ising model, statistical mechanics also gives an equation of this form. At present the only solution of the problem in closed form is the Onsager[8] solution for the two dimensional case. For the two dimensional magnet or the two dimensional lattice gas the solution of Onsager gives a value of $\beta = 1/8$.

There have been series solutions for the three dimensional case but not a solution in closed form. There have been many measurements on the three dimensional system but few for a two dimensional system. There are no published measurements on the temperature dependence of a two dimensional magnet near its Curie temperature. It would appear that an experimental test of the two dimensional closed solution would indicate the validity of the three dimensional approximate solution.

A monolayer of iron, nickel, or gadolinium on a silica substrate would be a two dimensional magnet. Gadolinium would be particularly convenient since it has a Curie temperature of 12°C. These monolayers can be formed by vacuum deposition on the substrate. Professor Humphrey at California Institute of Technology has prepared films of permalloy (80% Ni - 20% Fe) 8 Å in thickness and made measurements of magnetic properties. These films have approximately 3 atomic layers, and it is felt that a true monolayer is needed to test the theory accurately. Some measurements on nickel films as thin as 20 Å have been made[9]. These measurements determined the Curie temperature as the temperature where the spontaneous magnetization disappeared.

They used equation (1) with $\beta = 1/2$ and found that it did not fit the data near the Curie Temperature. The measurements did not extend very close to the Curie temperature, 6^{o}, and the temperature control was not very accurate.

There are two means of measurements that could be used with two dimensional magnets. The first is the magnetic torque balance. This is a common technique, and the measurements on nickel films[9] used this method. Humphrey[10] has constructed and operated an automatic torque balance with a sensitivity capable of measuring the magnetization of 1 cm. diameter films of less than one atomic layer thickness. This device could be adapted with suitable temperature control to make measurements near the Curie temperatures. The other experimental technique would be to determine the magnetic moment indirectly from resonance[11]. Thin films and powdered samples of ferromagnetic metals have been used in these measurements. The ferromagnetic resonance spectrum obtained from paramagnetic resonance instruments is broad and difficult to interpret. Nevertheless, the greater simplicity of the temperature control makes this a valuable method.

Although the measurement is experimentally difficult, it does provide a means of checking the two dimensional solution of the Ising model. From this the extension of the theoretical approach to the three dimensional system can be evaluated.

REFERENCES

1. T. L. Hill, Statistical Mechanics, 286 (McGraw-Hill Book Co., Inc., New York, 1956).
2. N. Davidson, Statistical Mechanics, 428 (McGraw-Hill Book Co., Inc., New York, 1962).
3. M. E. Fisher, Critical Phenomena, 21 (National Bureau of Standards Miscellaneous Publications 273, Washington, D. C., 1966).
4. G. B. Benedek, Critical Phenomena, 42 (National Bureau of Standards Miscellaneous Publications 273, Washington, D. C., 1966).
5. J. S. Rowlinson, Liquids and Liquid Mixtures, 79 (Academic Press Inc., New York, 1959).
6. J. O. Hirschfelder, C. F. Curtiss, and R. B. Bird, Molecular Theory of Gases and Liquids, 877 (John Wiley and Sons, Inc., New York, 1954).
7. A. M. Weinberger and W. G. Schneider, Canadian Journal of Chemistry 30, 424 (1952).
8. L. Onsager, Physical Review 65, 117 (1944).
9. B. R. Livesay and E. J. Scheibner, Journal of Applied Physics 36, 3240 (1965).
10. F. B. Humphrey and A. R. Johnston, Review of Scientific Instruments 34, 348 (1963).
11. M. Bersohn and J. C. Baird, An Introduction to Electron Paramagnetic Resonance, 149 (W. A. Benjamin, Inc., New York, 1966).

PROPOSITION V.

It is proposed that dielectric constant measurements can be used to determine the properties of the opalescence that occurs at the gas-liquid critical point of a one component system. In the description of fluid properties using the radial distribution function, problems arise at the critical point. From the theory of density fluctuations and the virial equation of state the value of $g(r) - 1$ becomes very large in the critical region; $g(r)$ is the radial distribution function. The general theories show a divergence in the $\int g(r)\, dr$ as the critical temperature is approached since the compressibility becomes infinite here[3]. If it can be shown that the higher derivatives of $(\partial V / \partial P)$ are not zero at the critical point, then the fluctuations and light scattering from the fluctuations are not infinite at the critical point[2].

In the first correction term for the expanded Lorentz-Lorenz or Clausius-Mossotti functions the integral $\int_0^\infty \frac{g(r)\, dr}{r^4}$ appears, and if the $g(r)$ is large for critical opalescence, then this integral should show an anomaly. The Ornstein-Zernike Approach[3], which predicts infinite scattering at the critical point, says that near the critical point $g(r) - 1$ varies as $\frac{e^{-Kr}}{r}$. This function was used by Larsen[4] to estimate the correction to the Lorentz-Lorenz function in the critical region. Their calculation shows a change of 0.1% in this function as T approaches T_C. The simple, incorrect, theory using the van der Waals equation of state shows that $g(r) - 1$ is proportional to $r^{-3/2}$ [2], and for the more

complicated approaches the dependence is r^{-1}. None of these functions will give a large enough value for the integral to make a significant change in $L - L > 0.1\%$. This is in contrast to the preliminary finding of B. L. Smith, Sussex. He has made some density measurements concurrent with refractive index measurements, and he finds changes of 1.0% or greater at the critical point.

There have been many studies of the critical region both from light scattering[5] and refractive index measurements[6]. Neither of these methods can be used to make measurements of the heavy opalescence at exactly the critical point. Light scattering can not be used because of multiple scattering due to the large clusters. Refractive index measurements can not be made since the sample is essentially opaque.

There have been similar measurements of the dielectric constant for the liquid-liquid consolute point of the nitrobenzene - iso-octane system[7]. This is a polar-nonpolar system, and although similar it is not the same as a gas-liquid critical point. Quinn and Smyth determined the time dependence of the concentration fluctuations from dispersion measurements. The maximum dispersion occurs in the region of 500 to 2000 Kc. Relaxation times for a gas-liquid critical system were determined by Schneider[8] for xenon. He found the maximum dispersion for sound absorption occurred between 250 and 1250 Kc.

A basic aspect of the proposed measurements is that they be carried out in a closed cell of fixed volume. This cell must also have windows so that the critical opalescence can be observed. In this

apparatus the critical density, the density for which the meniscus disappears at the mid-point of the cell, can be determined at the same time as the dielectric constant. The amount of opalescence can be observed in this cell. The problem of superheating of the two phase system can also be checked.

Some preliminary measurements for the ethane system were made. For this, an inexpensive air capacitor was mounted in a fixed volume cell. The cell was horizontal, approximately 1 inches high, 3 inches wide, and 1 inch deep. Two glass windows 1 1/2 inches thick were sealed on each side with O-rings. With a valve just above the cell it was possible to close the system to keep the volume constant. The entire cell was mounted in a water bath.

The cell was filled until the total density was approximately the critical density. Then three states were studied, (1) liquid in equilibrium with the vapor below the critical temperature, (2) fluid ethane with heavy opalescence, and (3) homogeneous fluid at the critical density but above the critical temperature. It was found that superheating occurred frequently, and the critical opalescence could only be approached from above.

The capacitance measurements were made with a Wayne-Kerr Bridge which is one accurate to ± 1%. The range of frequencies was from 50 to 1000 Kc. This bridge does have the advantage that all the capacitance of the leads can be included in the instrument null, and therefore, only the capacitance of the capacitor itself is measured. The temperature of the water bath could be measured to only ± 0.05°C, but the stability was much greater than this.

The capacitance in vacuum was determined to be 22.80 picofarads. The values of the dielectric constant measured are

$T(^{\circ}C)$	ϵ	ρ(moles/cc.)[9]	$\frac{\epsilon - 1}{\epsilon + 2} \frac{1}{\rho}$ (cc./mole)
31.40	1.270	0.007481	11.037
32.58 (Critical Opalescence)	1.232	0.007056	10.171
32.91	1.232	0.007056	10.171

$T_C = 32.35^{\circ}C$ $\rho_C = 0.007056$ moles/cc.

The most important thing to remember when looking at these results is that they are inaccurate. First the critical temperature as determined from the disappearance of the meniscus occurred at $32.55^{\circ}C$ instead of $32.35^{\circ}C$. Next the density at $31.40^{\circ}C$ was obtained by linear interpolation in a region that is definitely not linear. The significantly new information obtained is that the dielectric constant ϵ is the same for the homogeneous gas phase and the critical opalescence. This is within the accuracy of the measurement, $\pm$ 1%. For the point at $32.58^{\circ}C$ heavy opalescence occurred. No frequency dependence was recorded for any of the temperatures studied. This does not agree with other dispersion measurements for related phenomena, but no dielectric constant measurements for a simple system have been performed in the critical region. These measurements are definitely in disagreement with Smith's preliminary findings. His measurements of the refractive index are outside the region of opalescence, and he finds exceptionally large values for the Lorentz-Lorenz function in this region.

Much more accurate measurement of the dielectric constant can be made. Orcutt and Cole[10] report measurements accurate to 1 ppm., and measurements of this accuracy should certainly give a definite answer for the dielectric properties of critical opalescence. The closed cell feature of this proposal means that the density can be specified and maintained exactly. The use of dielectric constant measurements provides a means of working through the entire region of critical opalescence. This is a feature that neither light scattering nor refractive index measurements can achieve.

REFERENCES

1. M. E. Fisher, Critical Phenomena, 108 (National Bureau of Standards Miscellaneous Publication 273, Washington, D. C., 1965).
2. J. O. Hirschfelder, C. F. Curtiss, and R. B. Bird, Molecular Theory of Gases and Liquids, 128 (John Wiley and Sons, Inc., New York, 1954).
3. J. S. Rowlinson, Liquids and Liquid Mixtures, 106 (Academic Press Inc., New York, 1959).
4. S. Y. Larsen, R. D. Mountain, and R. Z. Wanzig, Journal of Chemical Physics 42, 2187 (1965).
5. A. L. Babb and H. G. Drickamer, Journal of Chemical Physics 18, 650 (1950).
6. E. H. Schmidt and K. Traube, Progress in International Research on Thermodynamic and Transport Properties, A. S. M. E., 193 (Academic Press Inc., New York, 1962).
7. R. G. Quinn and C. P. Smyth, Journal of Chemical Physics 39, 3285 (1963).
8. A. G. Chynoweth and W. G. Schneider, Journal of Chemical Physics 20, 1777 (1952).
9. F. Din, Thermodynamic Functions of Gases, Vol. 3, 194 (Butterworth, London, 1961).
10. R. H. Orcutt and R. H. Cole, Journal of Chemical Physics 46, 687 (1967).